LANDSAT APPLICATION OF REMOTE SENSING TO SHORELINE-FORM ANALYSIS

Final Report For Period 3 April 1975 To 3 January 1978

Prepared By: ROBERT DOLAN
Principal Investigator

BRUCE HAYDEN
JEFFREY HEYWOOD
Investigators

DEPARTMENT OF ENVIRONMENTAL SCIENCES
UNIVERSITY OF VIRGINIA
CHARLOTTESVILLE, VIRGINIA 22903

Prepared For: NASA-GODDARD SPACE FLIGHT CENTER
GREENBELT, MARYLAND 20771

NASA Technical Officer:
HAROLD OSEROFF
CODE 902, NGSFC

CONTRACT NO. NAS5-20999
INVESTIGATION NO. 21240

1 MARCH 1978

TECHNICAL REPORT STANDARD TITLE PAGE

1. Report No.	2. Government Accession No.	3. Recipient's Catalog No

4. Title and Subtitle	5. Report Date
Landsat Application of Remote Sensing to Shoreline Form Analysis	March, 1978
	6. Performing Organization Code
7. Author(s) Robert Dolan, P.I.; Bruce Hayden Jeffrey Heywood, Investigators	8. Performing Organization Report No.
9. Performing Organization Name and Address Department of Environmental Sciences University of Virginia Charlottesville, Virginia	10 Work Unit No.
	11. Contract or Grant No. NAS5-20999
	13. Type of Report and Period Covered Final Report 4/3/75 to 1/3/78
12. Sponsoring Agency Name and Address NASA-Goddard Space Flight Center Greenbelt, Maryland 20771 Harold Oseroff, Technical Monitor	14. Sponsoring Agency Code

15. Supplementary Notes

16. Abstract

The relationship between coastal orientation and historical shoreline change for Assateague Island, Cape Hatteras, and Cape Lookout National Seashores was studied using data from Landsat imagery and low-altitude aerial photography. Significantly high correlations were found for most of the six barrier island sections that were examined. However, relationships were not consistent from island to island. We concluded that coastal vulnerability to storm damage can not be assessed based on coastal orientation alone. However, when orientation data are combined with erosion data for individual barrier islands, the relationship could be used as a basis for barrier island classification.

A new method was developed to obtain large amounts of historical data on surface coastal processes from aerial photography, which we call the Orthogonal Grid Address System (OGAS). Data on shoreline change and overwash penetration that we have gathered on over 400 km of the mid-Atlantic coast are being used by various federal and state agencies for planning purposes.

17. Key Words (Selected by Author(s))	18. Distribution Statement
Aerial Photography, Barrier Island, Coastal Orientation, Coastal Processes, Landsat, Overwash Penetration, Shoreline Erosion	

19. Security Classif. (of this report)	20. Security Classif. (of this page)	21. No. of Pages	22. Price*
Unclassified	Unclassified	118	

*For sale by the Clearinghouse for Federal Scientific and Technical Information, Springfield, Virginia 22151.

PREFACE

Objective

The objective of this investigation was to explore the feasibility of applying remote sensing to the analysis of shoreline form and shoreline processes. Through the use of Landsat imagery, high-altitude aerial photography, and low-altitude aerial photography, we studied longshore variations in coastal orientation, measured historical shoreline erosion, and studied associated environmental changes. We studied the relationships among these dynamic features (both quantitatively and qualitatively). Our study site included the mid-Atlantic coast from Beach Haven, New Jersey, to Cape Lookout, North Carolina, with special emphasis on Assateague Island, Cape Hatteras, and Cape Lookout National Seashores.

Scope of Work

Much of our effort was spent in establishing a data base for patterns and trends of historical shoreline change and storm-surge or overwash penetration from aerial photography. This included more than 400 kilometers of coastline. Data were collected at 100-meter intervals along the coast for up to seven different dates of photography, extending as far back in time as 1930, and as recent as 1976. In order to collect this data accurately and efficiently, we developed a new method of data collection we have called the Orthogonal Grid Address System (OGAS).

We also developed a method for measuring the orientation of relatively straight coastal segments using Landsat imagery. Computer programs were written to process and assist in the analysis of the OGAS and orientation data through tabular and graphical output.

We conducted field trips to Assateague Island, Cape Hatteras, and Cape Lookout to collect data on beach features to correlate with data on shoreline change and coastal orientation. This investigation included assessment of the relative merits of Landsat, and high and low-altitude aerial photography for measuring change in subaerial land area at the southern end of Assateague Island.

We have studied the ecological response to barrier island processes, assessed the vulnerability of segments of the coast to storm damage based on historical erosion and overwash data, and the feasibility of assessing coastal vulnerability based on coastal orientation.

Finally, we are developing a model for barrier island migration, based on our shoreline erosion and overwash penetration data; a paper on this subject is now in preparation. In addition, we have written numerous publications and given a number of presentations during the past two years to present our work to the public sector.

CONCLUSIONS

Significantly high correlations were found to exist (negative and positive) between coastal orientation and three different expressions of historical shoreline change for most of the six barrier island sections we studied; however, the correlations were not consistent from island to island. Therefore, we conclude that it is not possible to predict areas of vulnerability to storm damage on a sedimentary coast based solely upon orientation of coastal segments. We conclude that the relationship between historical shoreline change and coastal orientation can serve as a basis for classification of barrier islands with respect to island dynamics. Additional research aimed at designing a model for barrier island migration is needed.

In the absence of sophisticated imagery interpretation equipment, low-altitude aerial photography remains the best source of data for analysis of surface processes in the coastal zone. The resolution of Landsat imagery is inadequate to detect change in shoreline or storm-surge penetration to the degree of accuracy required in a coastal monitoring program.

SUMMARY OF RECOMMENDATIONS

As part of a coastal zone monitoring program, the Federal Government should initiate annual low-altitude flights over all sedimentary coastlines of the United States, for the purpose of obtaining remote sensing data. This should include color infra-red photography at a scale from 1:15,000 to 1:24,000 with 60% overlap. The flight should take place at the same time each year in late summer during high tide of the monthly spring tide. One agency should be responsible for collecting and storing the data and imagery and making it available for use by the general public. EROS Data Center or NOAA are logical choices.

The resolution of Landsat imagery must be increased if the imagery is to be of use in measuring coastal dynamics without the aid of sophisticated equipment.

Finally, research into the process/response relationships on barrier islands should be continued toward the end of developing predictive models in ecological response, barrier island migration, and coastal vulnerability to storm damage.

ACKNOWLEDGMENTS

Numerous people have contributed to the research effort of this project over the past three years. Specifically, we want to thank: Linwood Vincent of the Waterways Experiment Station, Vicksburg, Mississippi, for contributing many good ideas during the initial phase of our work; Kathy Schroeder, Michael Schroeder, and Ruth Kampuries, for gathering historical erosion and overwash penetration data; Clark Hewitt, for his assistance with photography and for gathering coastal orientation data; Jeffrey Michel, for gathering field data and assisting in its interpretation, and for assisting with the index of aerial photography; John Ponton, for his assistance in computer programming; and Vicki Womack for her assistance with graphics and mapping.

We wish to acknowledge the continuous support of Paul Alfonsi and the Chesapeake Bay Ecological Program Office at NASA-Wallops. Without their close cooperation in monitoring our study site and in providing photo-interpretation equipment and expertise, we would not have been able to accomplish many of the objectives of our research. We also wish to acknowledge the cooperation of our many colleagues in NASA and the National Park Service.

Finally, we wish to express our deepest appreciation to Wilma Le Van, who has done a magnificent job in typing all of our manuscripts for publication, and our quarterly and final reports for this project.

TABLE OF CONTENTS

LIST OF ILLUSTRATIONS

LIST OF TABLES

LIST OF GRAPHS

INTRODUCTION

This is the final report for the work performed at the University of Virginia between 3 April 1975 and 3 January 1978 under Landsat Follow-On Investigation No. 21240, Contract No. NAS5-20999, under Marine Resources Applications. During this time period, we developed a method for measuring historical shoreline erosion and storm-surge penetration using low-altitude aerial photography, and collected the most complete set of such data now in existence for more than 400 kilometers of the mid-Atlantic coast from New Jersey to North Carolina. We also developed a simple method for measuring coastal orientation using Landsat imagery in order to study the relationships among coastal erosion, coastal orientation, and beach features which were measured in the field. Results of our analyses are presented in this report. We have also assessed the relative merits of low-altitude aerial photography, high-altitude aerial photography, and Landsat imagery in a coastal zone monitoring system.

BACKGROUND

Some of the most dynamic landforms in the United States are the mid-Atlantic and Gulf coast barrier islands. The geological substrate is composed primarily of sand, and the shorelines are under constant stress from ocean currents, wind and waves, sea level rise, and occasional storm surge. Barrier island configuration is, therefore, undergoing continuous change. The most apparent manifestation of this is in shoreline erosion (landward migration), or shoreline accretion (seaward migration). The most dynamic evidence of the ability of coastal processes to alter the landscape is the creation of inlets and sedimentation overwash fans caused by storm waves and surge.

Sand beaches and barrier islands are seldom long and straight over extensive reaches, as described at one time by Professor R.J. Russell (1958), but rather sinuous when viewed in plan. These longshore variations in shoreline form occur as organized patterns with features or curvatures ranging in size from beach cusps to very large shoreline meanders.

Since the 1960's there has been a rapid increase of interest among coastal investigators in longshore variations in inshore processes and their relationship to rhythmic and crescentic beach morphology, shoreline erosion, and overwash processes (Bruun 1954, Hom-ma and Sonu 1962, Dolan and Ferm 1968, Dolan 1971, Komar 1971, Bowen and Inman 1971, Sonu

1972, Dolan, Vincent, and Hayden 1974, Guza and Inman 1975, and Vincent and Dolan 1976). Dolan and Ferm (1968) indicated that rhythmic longshore variations in the sandy shorelines occurred in a hierarchical pattern, the elements of which were often superimposed. The elements included (1) small cusps, or cusplets, only a meter across, (2) beach cusps which were up to tens of meters in length, (3) giant beach cusps, or shoreline sand waves, from 100 to 3,000 meters in length, (4) secondary capes 25 to 50 kilometers apart, and (5) capes 100 to 200 kilometers apart. Of the wide range of rhythmic and crescentic shoreline forms, the larger coastal landforms classified by Dolan (1971) as shoreline sand waves and secondary capes are the most significant in determining where the rapid environmental changes occur along sand beaches and barrier islands. We refer to these landforms as mesoscale, that is - measured in terms of kilometers.

Efforts are underway to formulate the physical processes responsible for the longshore variations; however, research is needed to characterize the beach features, their distribution in both time and space, and their relationship to erosional trends and overwash processes. These phenomena are of economic and environmental importance in coastal regions.

In view of these considerations, we undertook this project for a number of reasons. We wanted to quantify the relationship between coastal erosion and coastal orientation using

correlation statistics. This would require us to create a substantial data base on historical shoreline change, and to develop methods for collecting, processing and interpreting the data. It would require us to develop similar methods for handling coastal orientation data.

Since remote sensing was obviously the best data base for both purposes, this provided an ideal opportunity to test the usefulness of Landsat imagery and various kinds of aerial photography for incorporation into a coastal zone monitoring system. We also obtained field measurements to find relationships among coastal erosion, coastal orientation and beach features such as width, slope, and sand-grain size. Finally, the project would lead to a data base that could serve long into the future for our basic research, which seeks a better understanding of process/response relationships in the coastal zone.

All of these objectives have been met and will be reviewed in this Final Report. However, although the project officially ended on 3 January 1978, the value of the work will be realized for many years into the future as analysis of the data produced during the project continues. We expect to publish numerous papers dealing with the geomorphology of barrier islands as a result of the foundation work of the past three years.

MEASURING HISTORICAL SHORELINE CHANGE WITH LOW ALTITUDE AERIAL PHOTOGRAPHY AND AN ORTHOGONAL GRID ADDRESS SYSTEM (OGAS)

A useful method for collecting large amounts of land-use and land-cover data efficiently and accurately is based on an orthogonal grid-address system (OGAS). This is a method for gathering data that locates natural and cultural features, or any point or area on land, with reference to horizontal (x) and vertical (Y) co-ordinates on a rectangular (orthogonal) grid. The grid is used in conjunction with any planar projection of the landscape, such as a vertical aerial photograph, or U.S.G.S. topographic map, and is fixed in place with reference to selected permanent control points on the land. The system allows for computer storage and manipulation of data for rapid reference and facilitated analysis. We have developed such a grid-address system to be used with low-altitude aerial photography and U.S.G.S. topographic maps to measure coastal erosion and overwash on the mid-Atlantic barrier island coasts, from southern New Jersey to Cape Lookout, North Carolina, (Figure 1).

Each section of the coast to be studied was divided into segments of 3.5 kilometers measured along the coast and outlined by a rectangular frame which defined a base map. Figures 2 to 6 show the locations of our base maps for south New Jersey, Fenwick Island, Assateague Island, Cape Hatteras National Seashore, and Cape Lookout National Seashore respectively.

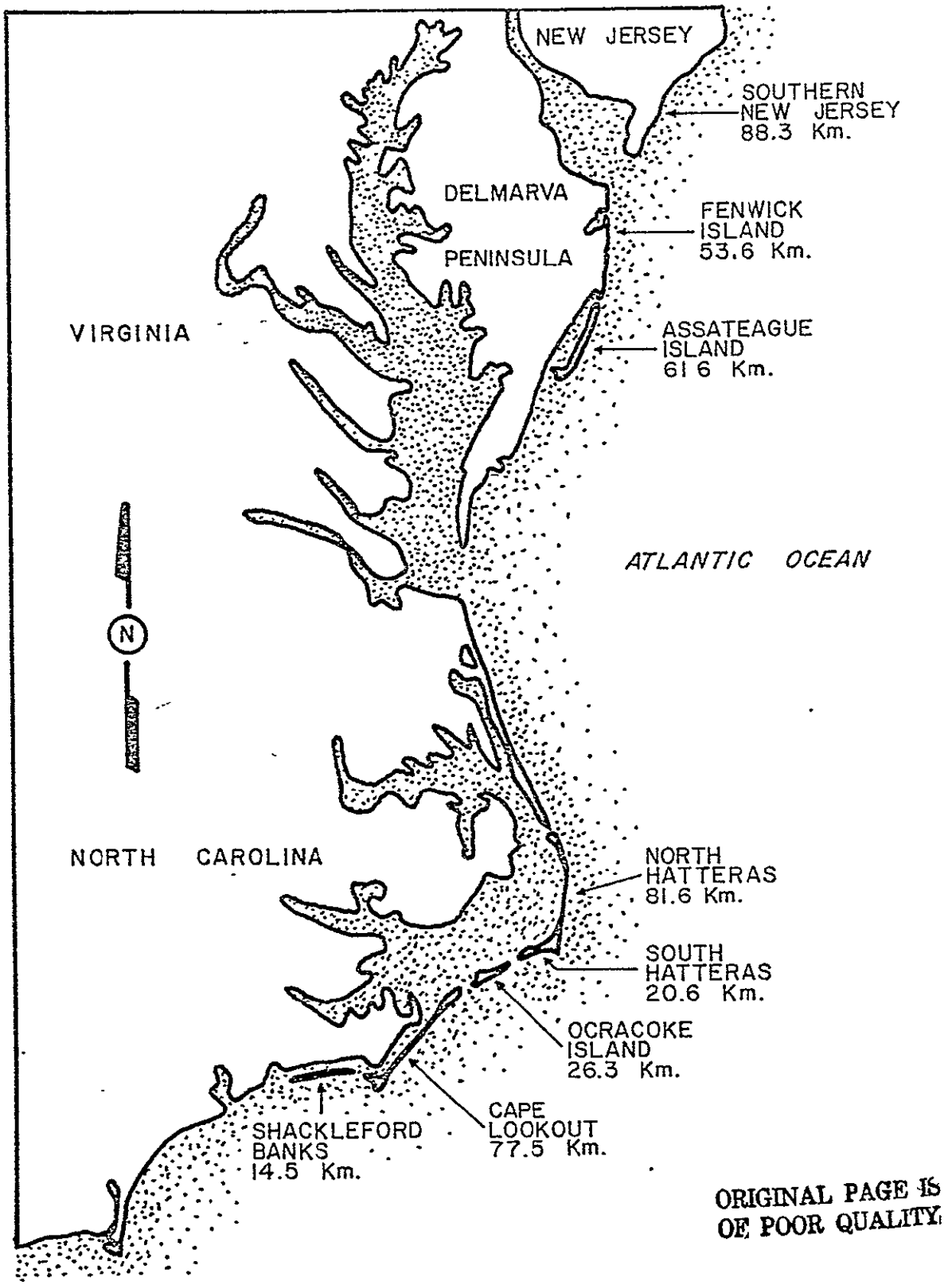

FIGURE 1: Overwash And Shoreline Erosion Studies Have Been Performed On Over 400 Kilometers Of Mid-Atlantic Coast From New Jersey To North Carolina.

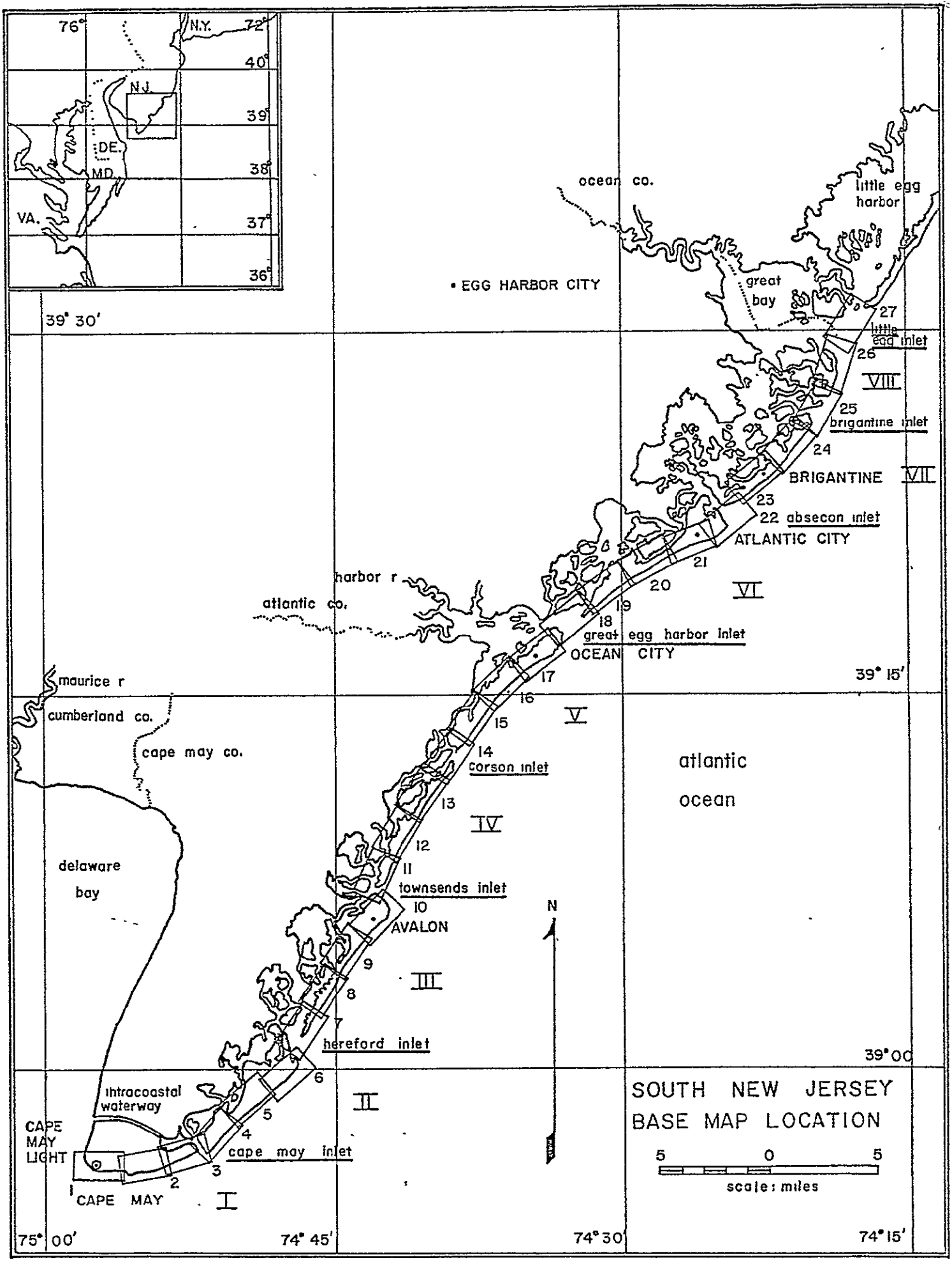

FIGURE 2: Base Maps For Southern New Jersey.

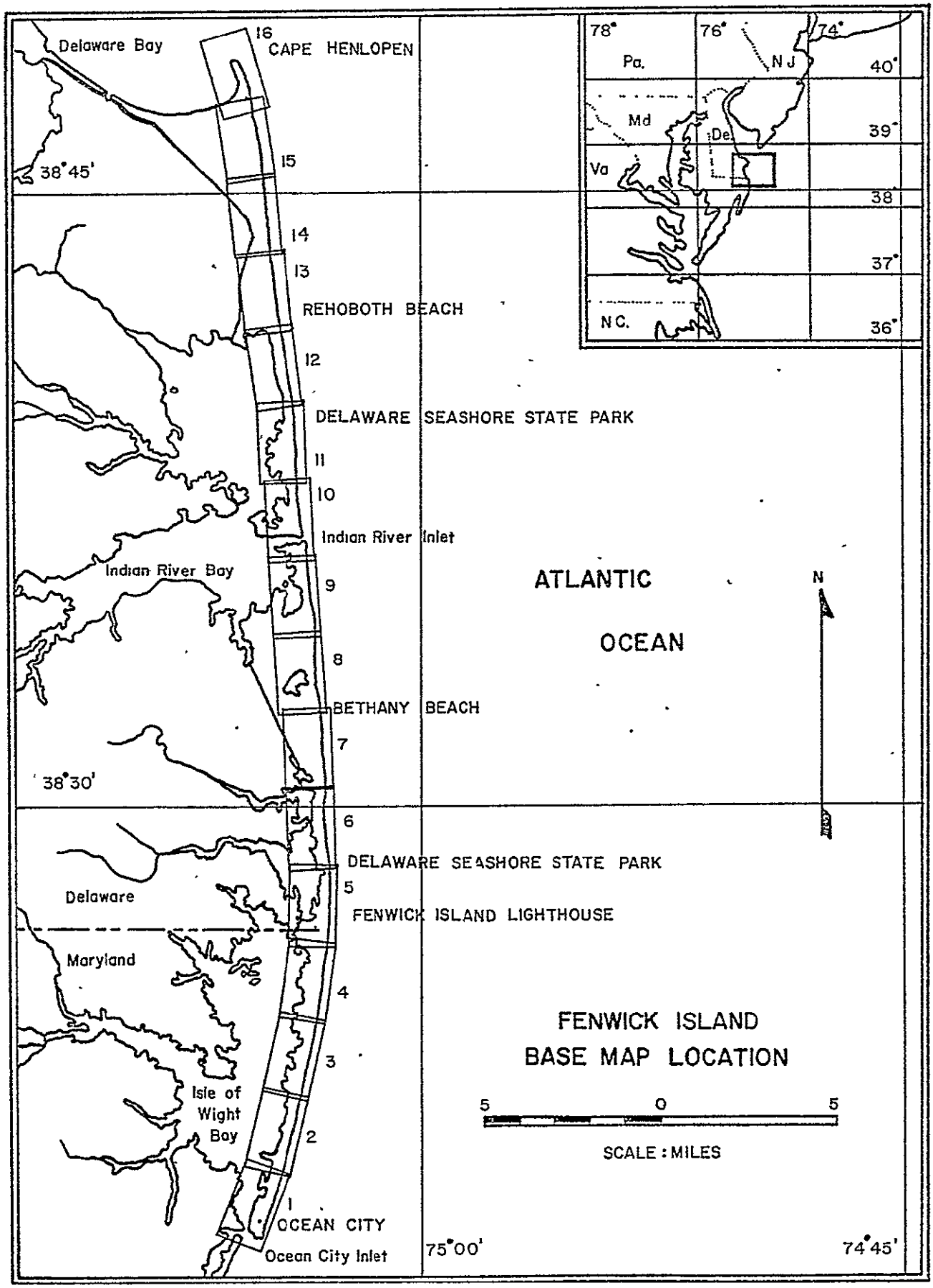

FIGURE 3: Base Maps For Fenwick Island.

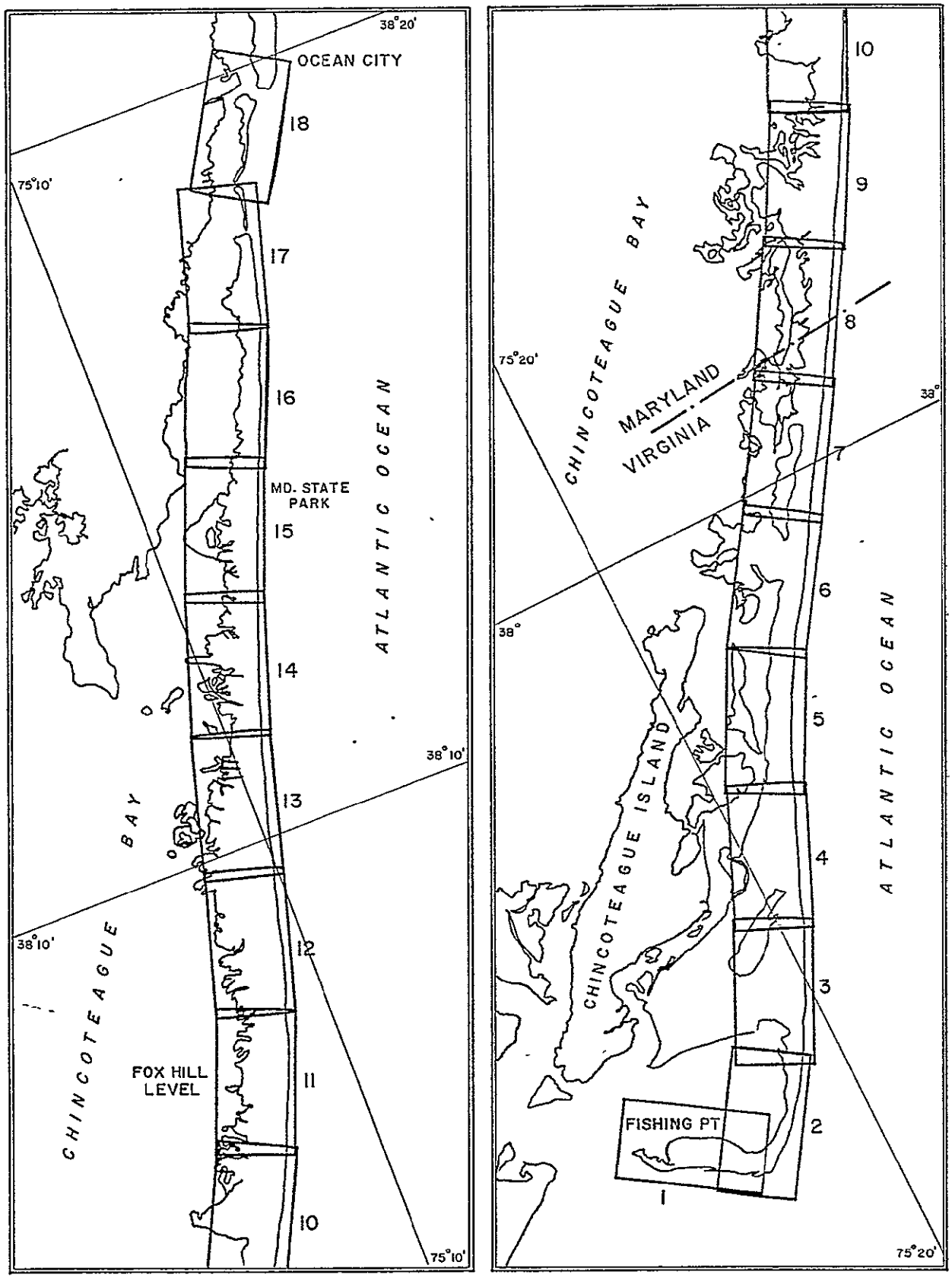

FIGURE 4: Base Maps For Assateague Island.

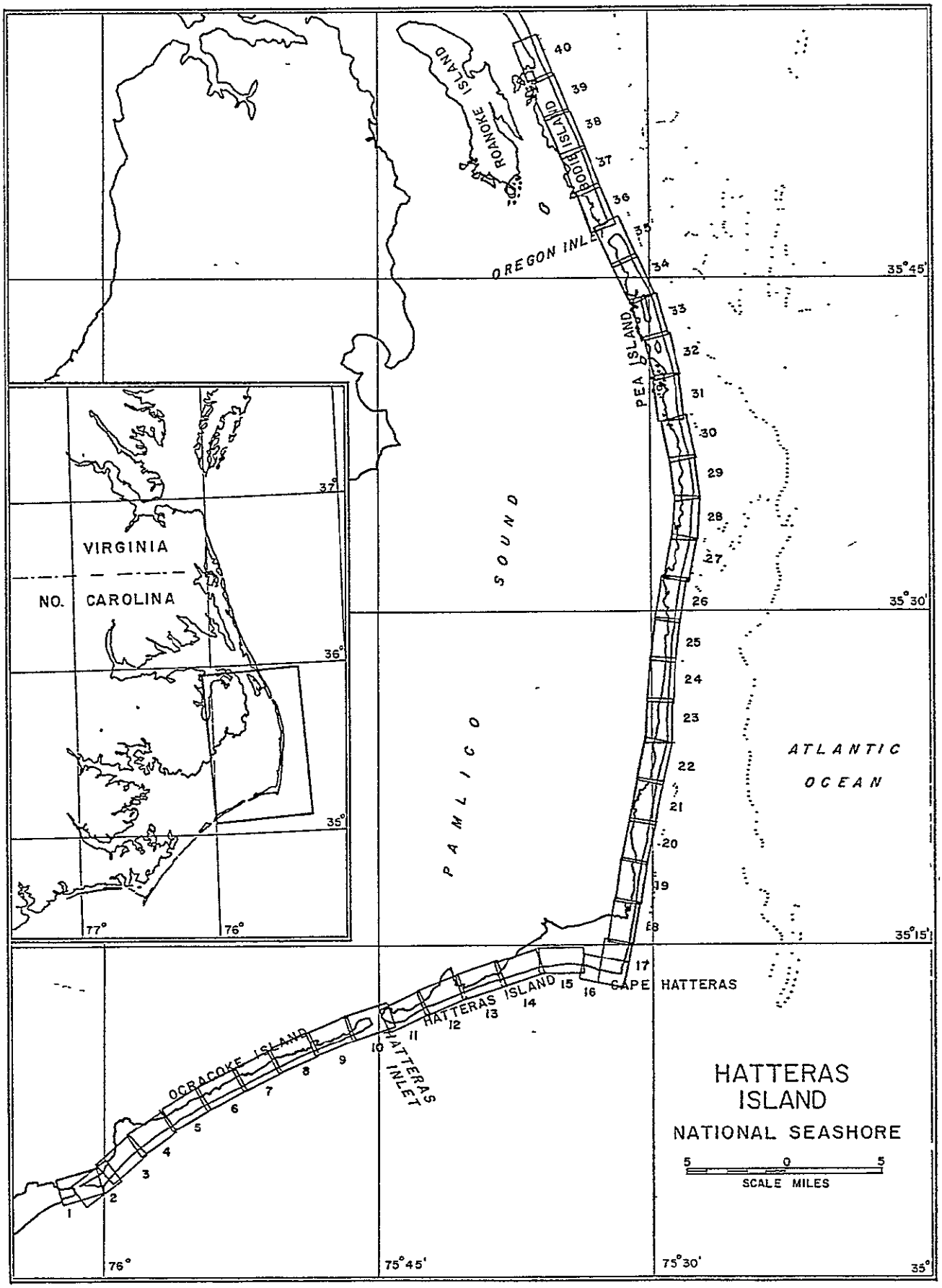

FIGURE 5: Base Maps For Cape Hatteras National Seashore.

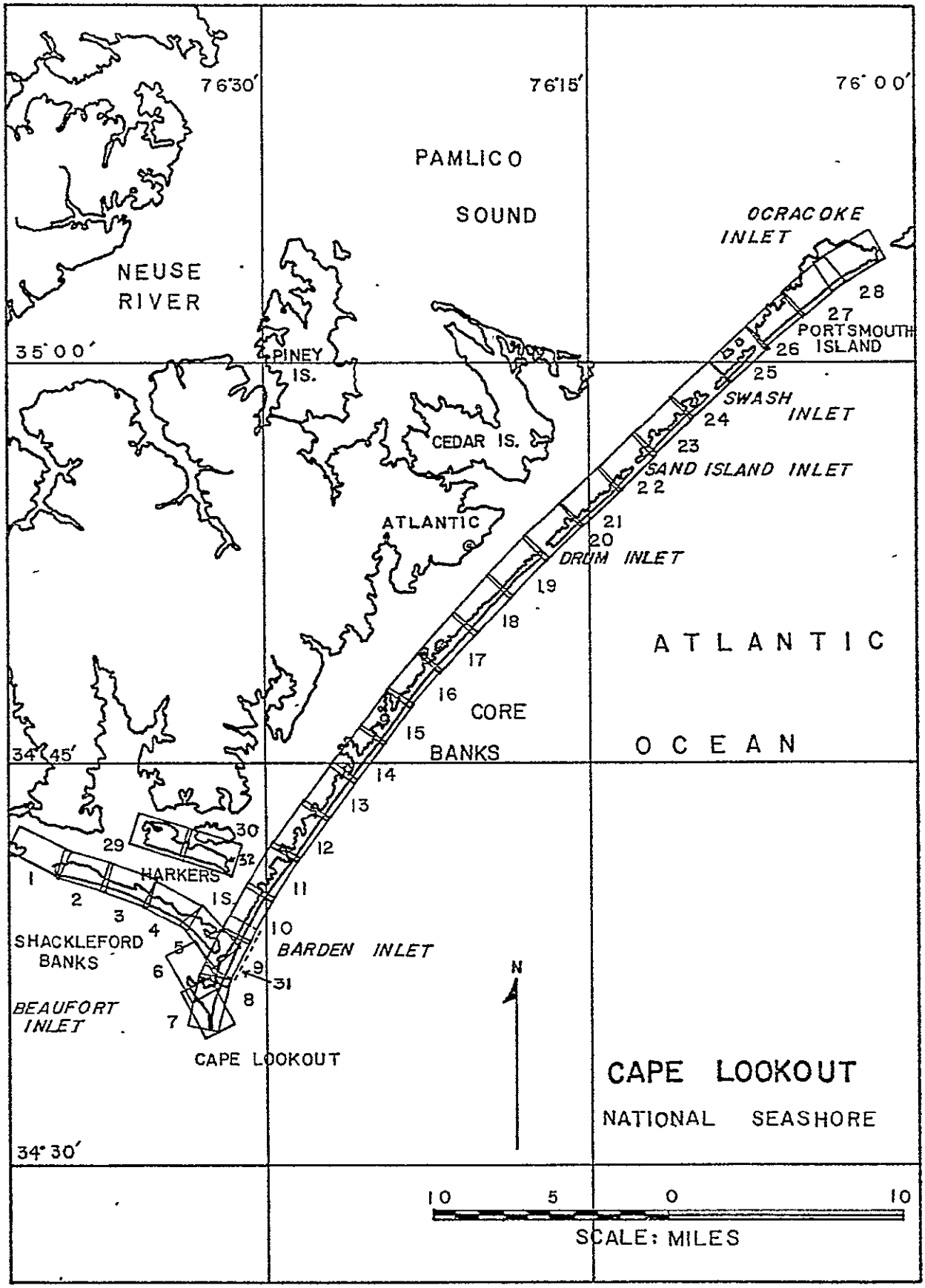

FIGURE 6: Base Maps For Cape Lookout National Seashore.

The base map frames were marked on the most recent available editions of 7-1/2' series U.S.G.S. topographic maps (scale = 1:24,000). The frame of each base map was oriented with the long side parallel to the coastline and positioned over the barrier island so that the shoreline and as much of the island as possible fit within the frame. One long side of each frame, lying entirely over the ocean, was the base line from which all measurements were made, and coincided with the base line of the orthogonal grid. Each base map was precisely located by the grid co-ordinates of at least two uniquely identifiable points on the U.S.G.S. map.

The topographic maps were then enlarged to a scale of 1:5,000 to create the base maps (Figure 7). Each map measured slightly larger than 43 cm. x 73 cm. Initially we manually enlarged the topo maps and created paper base maps on a K&E Kargl Reflecting Projector. Later we decided to photographically enlarge the topo maps and create acetate base maps. The accuracy, expediency, and permanence of the latter method clearly justified the additional cost.

The data source was historical low-altitude aerial photography ranging in scale from 1:5,000 to 1:40,000. The ideal scale to work with was 1:15,000. We used the earliest and latest available sets of photography for each area and photos taken during each decade in between. We included a

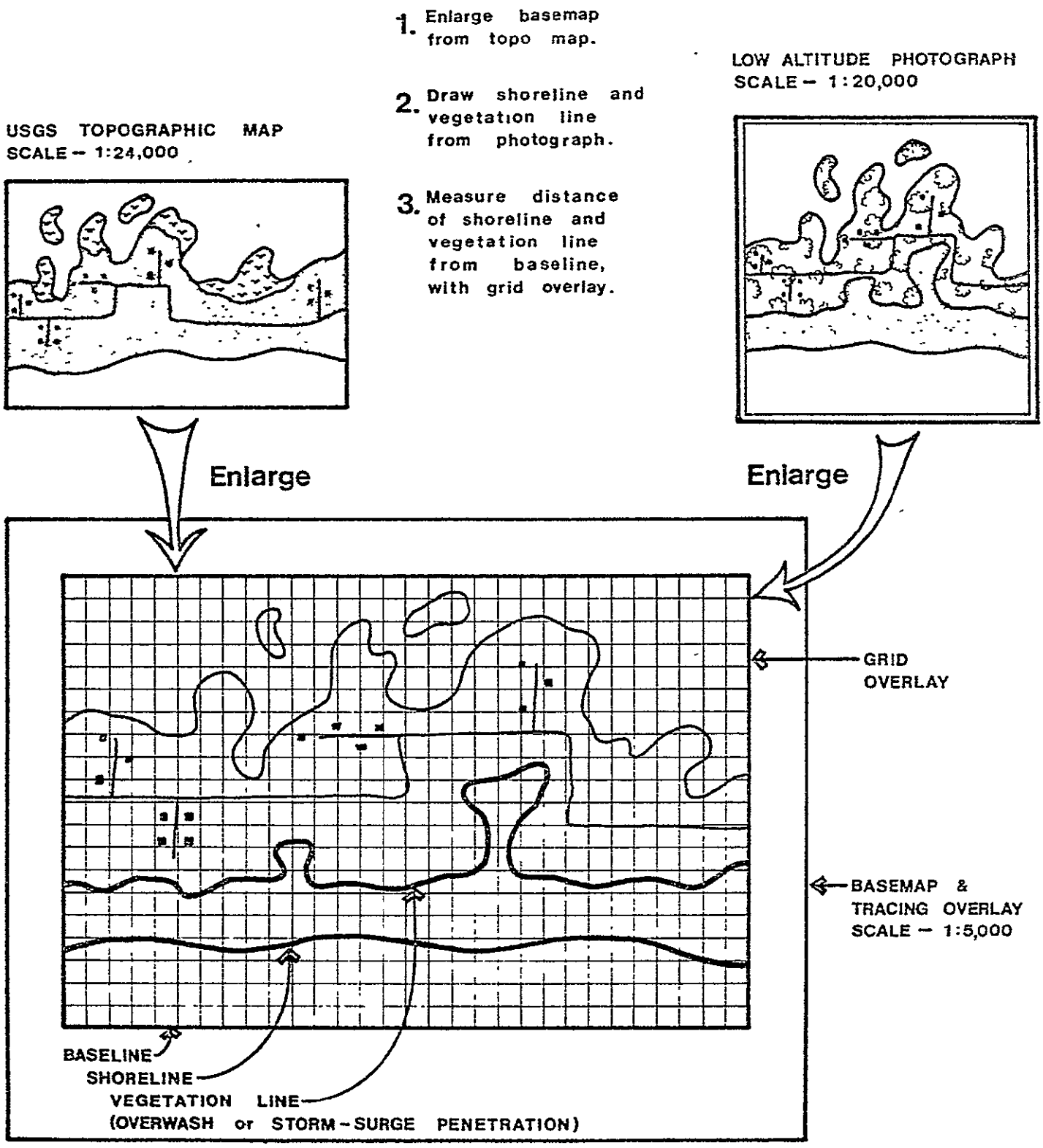

FIGURE 7: Method Of Data Collection Using U.S.G.S. Topographic Maps, Low-altitude Aerial Photography, And An Orthogonal Grid-Address System.

set immediately following the Ash Wednesday storm of March, 1962, which was the largest storm to affect the Atlantic coast in recent history. Thus, most of our study area is covered by at least five sets of photography from the 1930's to the 1970's.

For each base map, the photos were enlarged to 1:5,000 on the Kargl projector until the best possible fit of natural and cultural features between photo and base map was obtained. The shoreline and storm-surge or overwash penetration line was then drawn on an overlay map whose frame coincided with that of the base map. This process was repeated for each historical photograph of the same area.

The shoreline was defined as the high-water mark on the beach. Of the few consistently recognizable linear features of the shoreface on aerial photography, the high-water line is the most constant over a tidal cycle. In 1947 McCurdy identified the high water line (HWL) as a major recognizable feature of the subaerial beach face. Later, McCurdy (1950) and McBeth (1956) indicated that there was only an insignificant difference between the water line of the previous high tide and the HWL line recognized on photographs. The stable nature of the HWL over a tidal cycle was later confirmed by Stafford (1968).

The overwash penetration line (vegetation line) was defined by a smoothed line that separated the beach and dune sand or lightly vegetated sand flats from the relatively contiguous

stands of dense grass and shrub vegetation (Figure 8). The area between the shoreline and overwash penetration line represents the active sand zone which is the most hazardous during times of storm surge.

A transparent orthogonal grid overlay with transects spaced at 100-meter intervals along the coast was used to record to the nearest 5 meters the points at which the shoreline and the vegetation line intersected each across-the-shore transect. All measurements were made with respect to the base line of the grid. There were 36 transects per base map, representing a distance of 3.5 kilometers. The recorded data were then transferred to computer cards. For any given transect, the accuracy of location of the shoreline and vegetation line is within a range of $\pm$ ten meters.

A computer program has been written which lists the following information for every base map (statistics include mean, variance, standard deviation, number of transects over which mean is calculated, maximum value, and minimum value).

1. Location of vegetation line (VL), shoreline (SL), and overwash-penetration distance (OP= VL - SL) for each of the 36 transects along the coast.

2. Line-printer graphs of VL, SL, and OP.

3. Changes and rates of change in VL, SL and OP between selected dates (erosion and accretion statistics).

4. Line-printer graphs of rates of change in VL, SL, and OP.

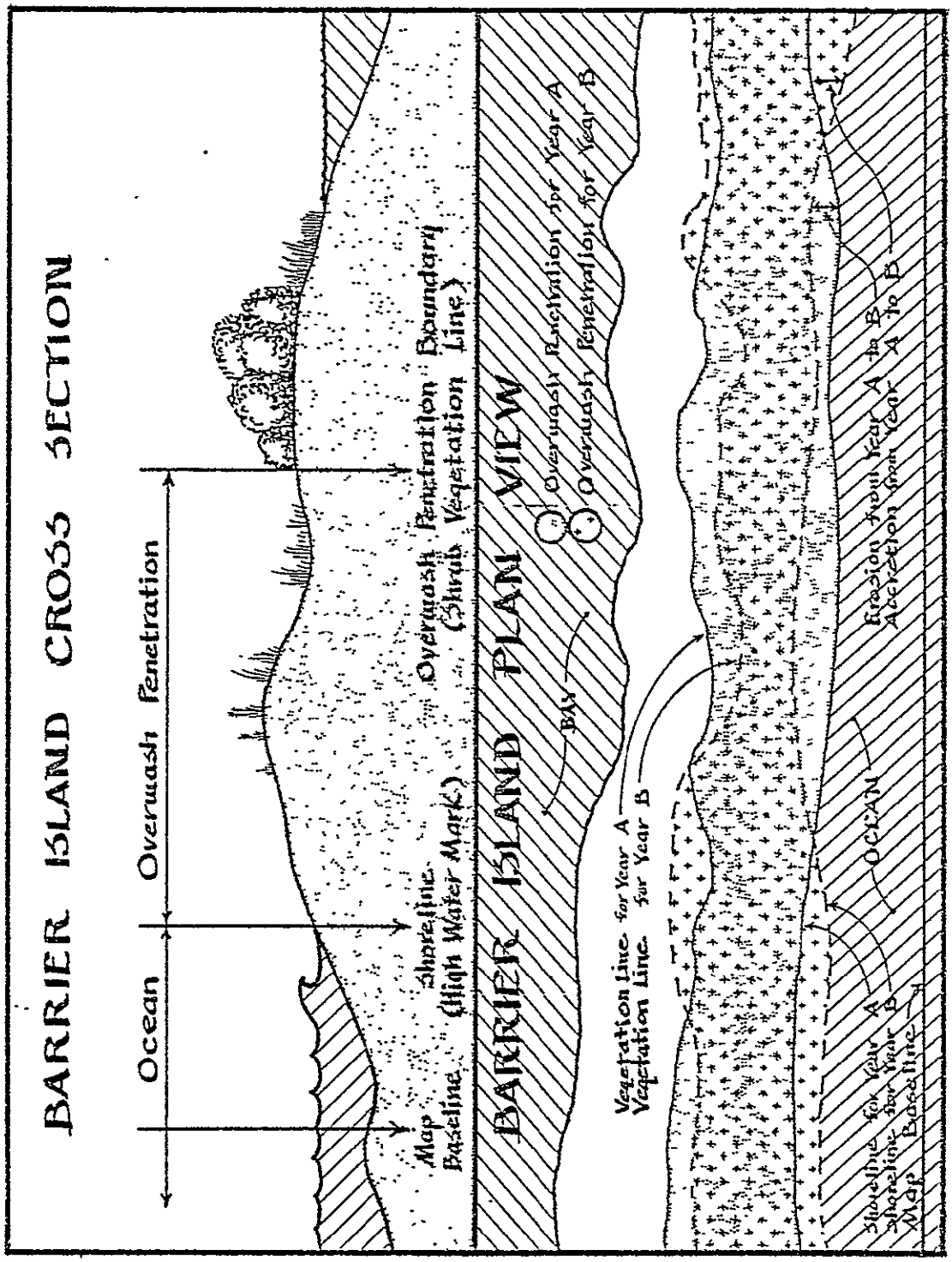

FIGURE 8: Illustration Of Shoreline And Overwash Penetration Line.

5. Line-printer graphs of the mean $\pm$ one standard deviation of rate of change in $\overline{VL}$, SL, and OP (Figure 9).

In addition, the following information is provided for sections of the coast of any desired length.

6. Statistics on OP for each year and statistics on changes and rates of change in VL, SL, and OP between any two years.

7. Frequency distributions of OP for each year and rates of change of VL, SL, and OP between any two years.

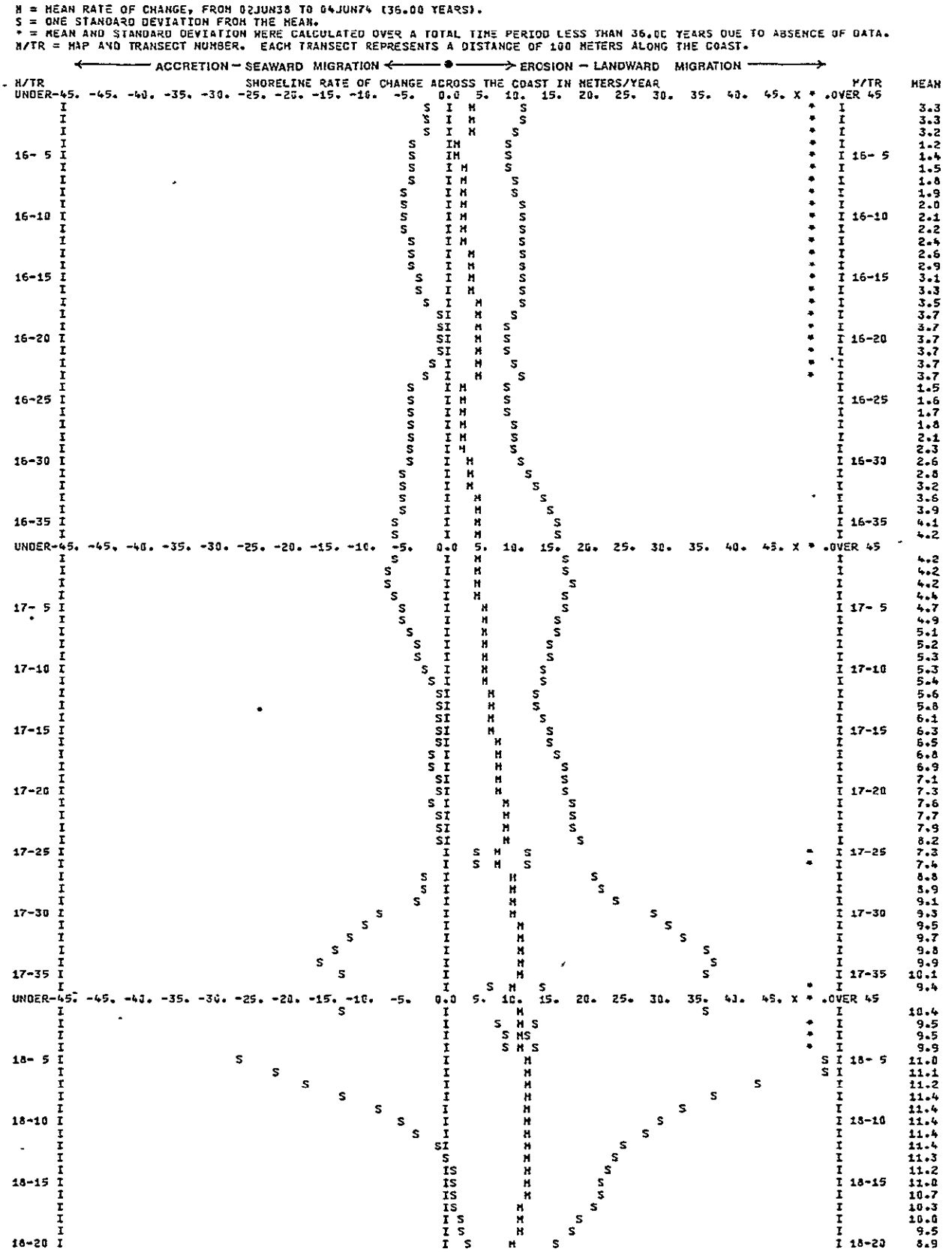

FIGURE 9: Line Printer Graph Of The Mean (M) ± One Standard Deviation (S) Of Shoreline Rate Of Change For The Northern 9 Kilometers Of Assateague Island.

COMPARISON BETWEEN OGAS AND CONVENTIONAL DATA COLLECTION METHOD

The OGAS method of gathering data from aerial photography has numerous advantages over conventional manual methods. Traditionally the method used to measure shoreline change was to: 1) select a recognizable feature on the photograph at or near the area to be measured - the feature must appear on the photos from all dates under study; 2) measure the photo distance from the feature to the shoreline; 3) convert to ground distance using the scale of the photograph.

The OGAS method allows us to make measurements in areas that could not be studied by the traditional method due to lack of "pin-pointed" features to serve as base references. The OGAS method allows us to collect much more data faster and more accurately than the traditional method. Furthermore, the OGAS method provides a uniform set of data that is ideally suited for use with a computer for spatial and temporal analysis. The system is sufficiently flexible to allow studies to be performed at any desired scale; for example, high resolution of one data point per 10 meters or less, or regional scale of one data point per kilometer or more.

MEASURING COASTAL ORIENTATION WITH LANDSAT IMAGERY

Our methods of interpretation of aerial photography and Landsat imagery are simple, and manual rather than automated. Our equipment includes the Kargl Reflecting Projector, mirror and pocket stereoscopes, a "20x" magnification scope, 35 mm and 70 mm cameras, and a darkroom for photographic enlargements. Due to the low resolution of Landsat, the data could not be used to measure shoreline erosion or storm-surge penetration to the degree of accuracy we required. Since Landsat was first placed into orbit in 1972, the data was obviously of no use for historical studies.

We did find, however, that Landsat images were useful in studying coastal orientation. The relationship between coastal orientation and other physical parameters of the coast such as overwash, shoreline change, sand grain size and slope of the swash zone is of both academic and practical interest. Through the application of statistical analyses, we are better able to understand the natural process/response interrelationships in the coastal zone. We are in a better position to classify the natural attributes of the coastal zone, assess the vulnerability of the coast, and make projections of factors such as storm hazard zones.

We used Landsat imagery to determine the azimuthal orientation of straight segments of the coastline - that is, the rotational deviation of straight coastal segments from the

north/south line, measured counter-clockwise in terms of degrees north-of-south (Figure 10). We first selected a suitable cloud free 70 mm transparency of band 7 which included in its entirety a stretch of coast we wished to measure. The single longest stretch of coast we have measured is approximately 80 kilometers of the Outer Banks from Cape Hatteras Point to Nags Head, North Carolina.

We then photographically enlarged the transparency to produce a black and white print at a scale of 1:80,000. In the case of north Hatteras, this continuous print showed a shoreline of more than one meter in length. We had experimented with various scales of enlargement and found that 1:80,000 was a good compromise between an image that was so large that an excess of visible "noise" was introduced, and a smaller image that would eliminate too much detail in coastline configuration. Furthermore, this scale allowed us to match the image with the landforms shown on the 1:80,000 U.S. Coast and Geodetic Survey (C&GS) charts. We were then able to transfer the standard Mercator grid from the C&GS charts onto the Landsat image.

We then placed tracing paper over the image, and using a straight edge, we divided the coast into straight-line segments. The intersection of adjacent segments was defined as a node (Figure 10), and was located to the nearest 100-meter transect previously established on the base maps of our

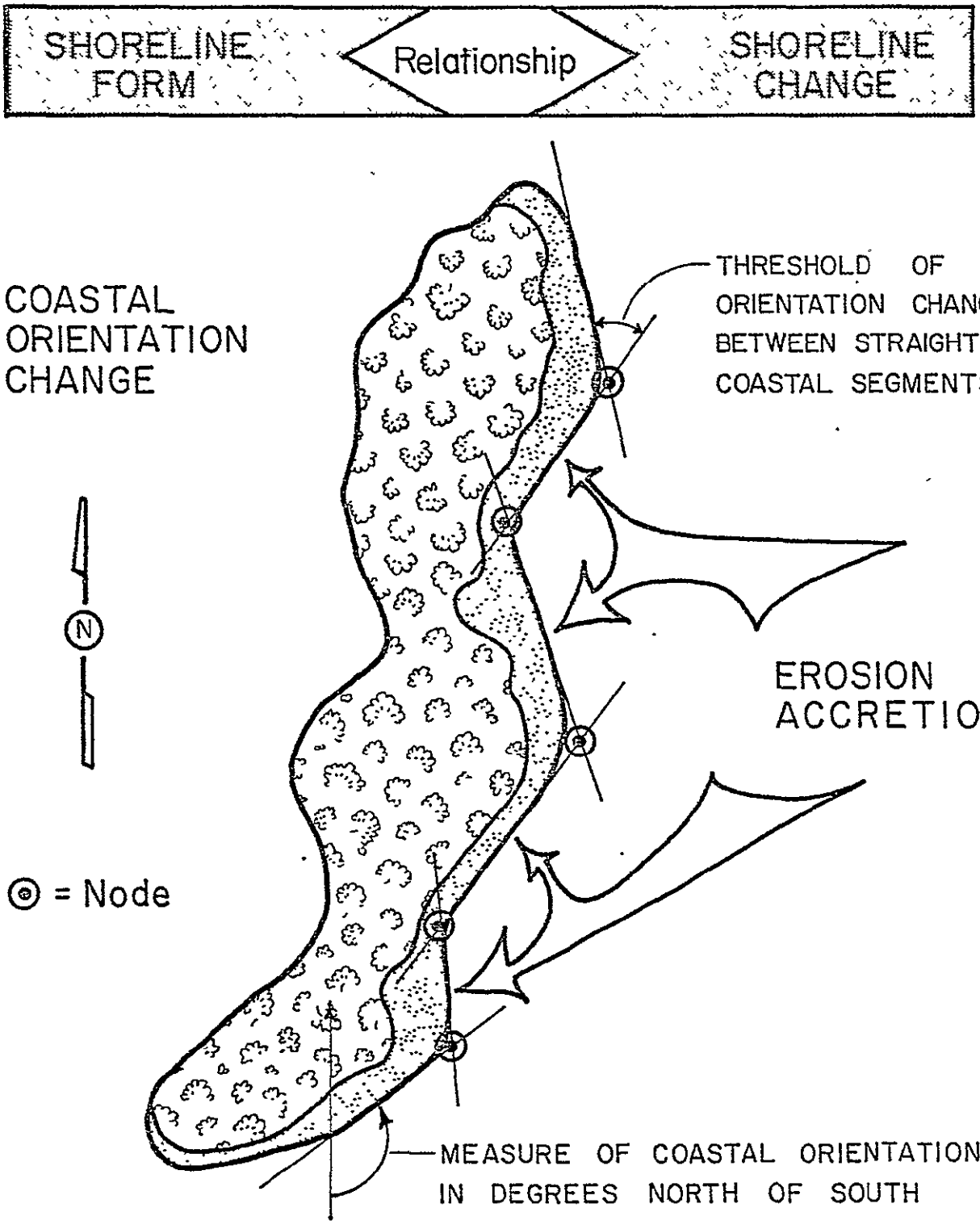

FIGURE 10: Orientation Of Straight Coastal Segments.

orthogonal grid-address system. The orientation of each segment was then measured with respect to the north/south line, and the location of each segment was determined by the nodes. This mapping process was repeated a number of times to allow for interpretive error. All of the data were then submitted to the computer, and a mean orientation of the coastline was determined at each 100-meter transect.

The computer program was written to automatically divide the coast into straight segments whose orientations varied from the orientations of adjacent segments by more than a given threshold value (Figure 10). On successive computer runs, this threshold was increased until the coastline was reduced to three straight-line segments, the minimum number allowed in order to run a regression analysis with N-2 degrees of freedom. For each iteration, correlation studies were performed between coastal orientation and other physical parameters.

It should be noted that due to the way in which the computer algorithm was written, the differences in orientations of adjacent segments of an entire coastline in the printout for a given threshold will not all necessarily be greater or equal to the threshold value. This will become evident in later illustrations which show orientations of barrier island segments. The threshold concept is primarily a tool which the computer uses for internal calculations.

ADVANTAGES OF LANDSAT IMAGERY OVER HIGH-ALTITUDE PHOTOGRAPHY

We found Landsat to be more advantageous than other forms of imagery for the following reasons. The coastal orientation data we required is regional in nature and therefore depends upon a high-altitude platform for a data source. High-altitude photography of 1:130,000 scale would have to be pieced together with a mosaic to include an entire coastline of interest. One Landsat image contains a coastline of more than 160 kilometers in length. It is a simple and inexpensive procedure to enlarge the desired section of coast appearing on a 70 mm Landsat transparency to any scale up to 1:80,000 or larger and produce photographic prints to satisfy our particular requirements. Since measurements were to be made along the coast in the mesoscale range of kilometers rather than meters, the higher resolution of photography was not a critical consideration. More critical was the greater orthogonal accuracy and reduced single-image scale distortion of Landsat compared to high-altitude photos.

RELATIONSHIPS BETWEEN SHORELINE CHANGE AND COASTAL ORIENTATION FOR ASSATEAGUE ISLAND, CAPE HATTERAS, AND CAPE LOOKOUT NATIONAL SEASHORES

Data Base

The historical shoreline change data were obtained from low-altitude aerial photography ranging in scale from 1:5,000 to 1:40,000. The historical photographs were panchromatic and were obtained from various sources including primarily the National Oceanic and Atmospheric Administration and the military. The most recent sets of photos for all three areas were color infra-red supplied by Chesapeake Bay Ecological Program Office at NASA-Wallops.

Assateague Island was divided into 18 base maps as shown in Figure 4. The dates of photography used for each base map are shown in Table 1. Photography for Cape Hatteras base maps (Figure 5) is shown in Table 2. Photography for Cape Lookout base maps (Figure 6) is shown in Table 3.

The current coastal orientation for the three areas was obtained from four different Landsat images - Assateague Island: frame no. 2129-15021-7, acquired on 5/31/75; Cape Hatteras: frame no. 5014-14490-7 and 5014-14493-7, acquired on 5/3/75; and Cape Lookout: frame no. 2147-15033-7, acquired on 6/18/75. Figure 11 shows vector representations of mean orientation and length of coastline of the six barrier island sections for which we ran correlations.

Table 1. Aerial Photography for Assateague Island

Base Map No.	Dates of Photography						
	6/2/38	5/3/49	3/14/55	10/5/59	4/21/61	12/3/62	6/4/74
1-2		x		x		x	x
3-5		x	x	x		x	x
6-7		x	x		x	x	x
8-13			x		x	x	x
14-15	x		x		x	x	x
16-18	x	x	x		x	x	x

Table 2. Aerial Photography for Cape Hatteras

Base Map No.	Dates of Photography					
	7/1/45	10/10/58	3/13/62	12/13/62	10/3/68	6/4/74
1-10		x	x		x	x
11-38	x	x	x	x	x	x
39-40	x		x	x	x	x

Table 3. Aerial Photography for Cape Lookout

Base Map No.	Dates of Photography								
	10/21/40	3/30/43	11/30/54	3/29/55	10/10/58	5/3/62	4/14/69	6/20/75	7/20/76
1-5		x	x		x	x	x		x
6-7	x			x	x	x	x	x	x
8-28	x			x	x	x	x	x	

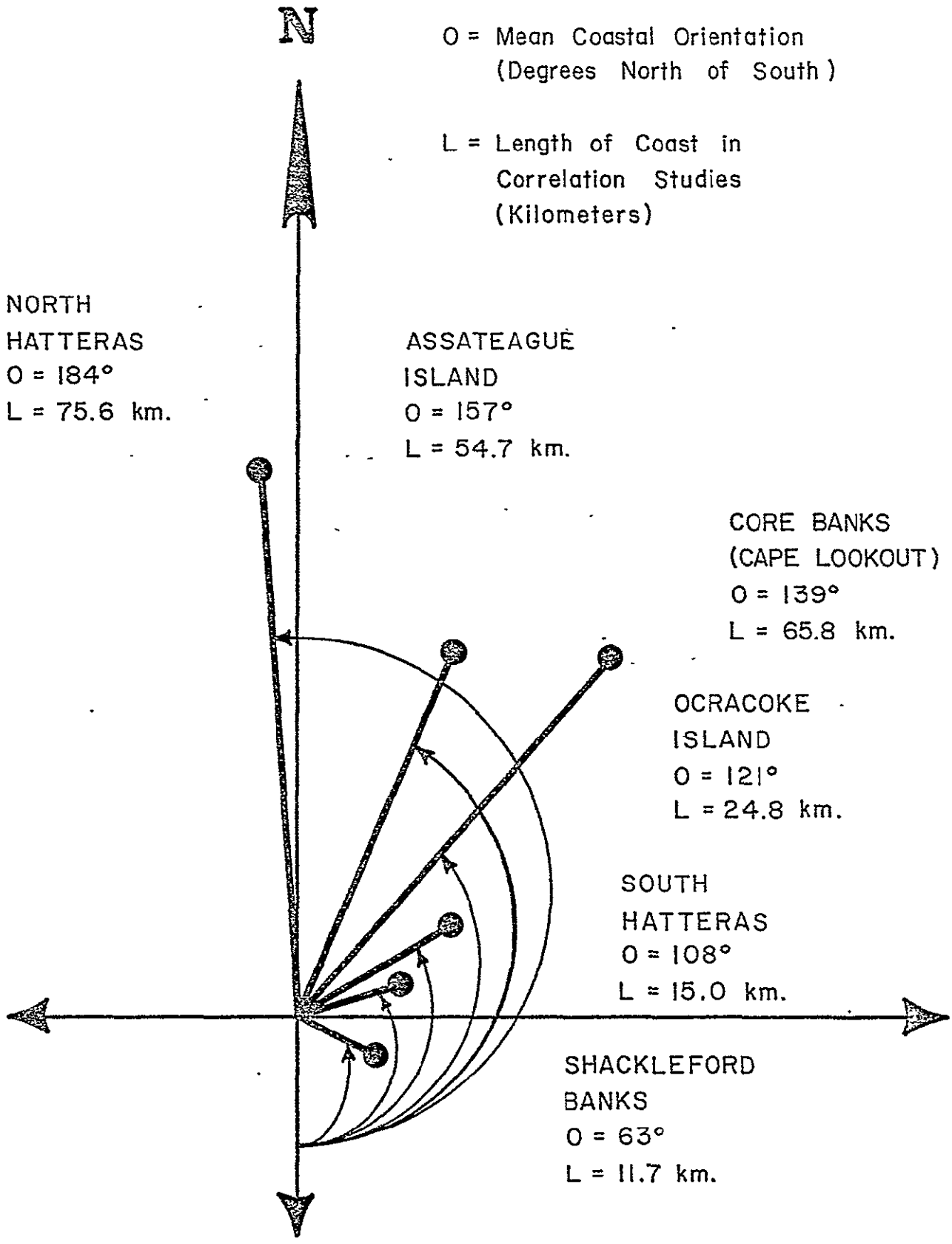

FIGURE 11: Mean Orientation Of Barrier Islands.

Correlation Statistics

If large-scale crescentic coastal landforms are associated in time and space with inshore processes of similar scale, then it is reasonable to assume that there is a measurable relationship between the spatial distribution of shoreline forms and the manifestations of shoreline dynamics (Figure 10). We determined the correlation between current coastal orientation and historical shoreline change (erosion or landward migration, and accretion or seaward migration), in order to quantify these relationships.

As previously described, orientations of "straight-line" segments of the coast were measured in terms of counter-clockwise rotational variation from the north/south line in degrees north of south (Figure 10). The mean rate of shoreline change, and the standard deviation of rate of shoreline change, over time and space were calculated for each coastal segment. Positive change indicated erosion, and negative change indicated accretion. Thus, a positive correlation indicated that as straight-line segments approached a more north/south orientation (as degrees north of south increased), the measured rate of erosion for those segments also increased.

Correlations were calculated between orientation and three measures of shoreline change: mean rate of change; standard deviation of rate of change; and mean plus standard deviation of rate of change. Correlations were performed for each computer iteration of island division into coastal segments.

The statistics are presented in the following tables, graphs, and figures:

Barrier Island	Table	Graph	Figure
Assateague Island (Md/Va)	4	1	12
North Hatteras Island (NC)	5	2	13
South Hatteras Island (NC)	6	3	14
Ocracoke Island (NC)	7	4	15
Core Banks (NC)	8	5	16
Shackleford Banks (NC)	9	6	17

For each table, the following information is provided:

Column A = Orientation Change Threshold for each Computer Iteration

Column B = Number of Coastal Segments

Column C = Mean Length of Coastal Segments

Column D = Correlation Coefficient Between Orientation and Mean Rate of Change in Shoreline (r(m))

Column E = Significance of r (m)

Column F = Correlation Coefficient Between Orientation and Standard Deviation of Rate of Change in Shoreline (r(σ))

Column G = Significance of r (σ)

Column H = Correlation Coefficient Between Orientation and Mean + Standard Deviation of Rate of Change in Shoreline (r (m + σ)).

Column I = Significance of r (m + σ).

Table 4. Correlation Statistics for Coastal Orientation vs. Shoreline Change for Assateague Island.

(Length of Coastline = 54.7 km; Mean Orientation = 157° North of South)

A	B	C	D	E	F	G	H	I
Degree	Segments	Kilometers	r(m)	Sig. [r(m)]	r(σ)	Sig. [r(σ)]	r(m+σ)	Sig. [r(m+σ)]
.5	55	1.0	-.07	.31118	.80	.00001	.58	.00001
1.0	33	1.7	-.30	.04207	.80	.00001	.47	.00318
1.5	25	2.2	-.15	.23828	.83	.00001	.57	.00159
2.0	17	3.2	-.19	.22719	.86	.00001	.54	.01308
2.5	14	3.9	-.36	.10199	.84	.00009	.43	.06334
*3.5	10	5.5	-.41	.11620	.90	.00022	.56	.04880
4.5	8	6.8	.04	.45874	.93	.00036	.68	.03251
5.0	6	9.1	-.09	.43700	.93	.00364	.60	.10220
5.5	5	10.9	-.36	.27455	.92	.01330	.59	.14417
7.0	3	18.2	.22	.42867	.97	.08314	1.00	.02961

*This iteration is illustrated in Figure 12 and Graphs 7 through 10.

Table 5. Correlation Statistics for Coastal Orientation vs. Shoreline Change for Cape Hatteras North from Hatteras Point to Nags Head.

(Length of Coastline - 75.6 km; Mean Orientation = 184° North of South)

A	B	C	D	E	F	G	H	I
Degree	Segments	Kilometers	r(m)	Sig. [r(m)]	r(σ)	Sig. [r(σ)]	r(m+σ)	Sig. [r(m+σ)]
.5	59	1.3	.58	.00001	-.15	.13214	.18	.08270
1.0	45	1.7	.60	.00001	-.13	.18896	.22	.07248
1.5	39	1.9	.55	.00017	-.18	.13187	.13	.22262
2.0	26	2.9	.61	.00042	-.22	.13773	.16	.21332
2.5	18	4.2	.53	.01304	-.23	.17876	.11	.34015
3.0	21	3.6	.56	.00425	-.26	.13146	.11	.31988
3.5	17	4.4	.48	.02691	.03	.45390	.33	.09504
4.0	13	5.8	.74	.00206	-.30	.16552	.32	.14534
4.5	11	6.9	.65	.01447	-.23	.23535	.26	.21567
5.0	10	7.6	.83	.00155	-.18	.29906	.50	.07060
5.5	9	8.4	.86	.00165	-.25	.24915	.56	.06212
*7.0	8	9.5	.83	.00487	-.33	.20702	.66	.03655
9.5	5	15.1	.92	.01193	-.35	.27102	.64	.12758

*This iteration is illustrated in Figure 13 and Graphs 7 through 10.

Table 6. Correlation Statistics for Coastal Orientation vs. Shoreline Change for Cape Hatteras South From Hatteras Inlet to Hatteras Point.

(Length of Coastline = 15.0 km; Mean Orientation = 108° North of South)

A	B	C	D	E	F	G	H	-
Degree	Segments	Kilometers	r(m)	Sig. [r(m)]	r(σ)	Sig. [r(σ)]	r(m+σ)	Sig. [r(m+σ)]
.5	24	.6	.35	.04542	.50	.00727	.50	.00630
1.0	19	.8	.30	.10534	.42	.03382	.42	.03655
1.5	12	1.3	.28	.18757	.41	.09278	.40	.09602
2.0	10	1.5	.42	.11364	.36	.15468	.43	.10566
2.5	9	1.7	.53	.06616	.36	.16881	.49	.09326
3.0	8	1.9	.46	.11721	.42	.15121	.48	.11282
3.5	7	2.1	.38	.20339	.43	.17098	.46	.15204
*4.5	4	3.8	.80	.10113	.22	.38860	.91	.04425
7.0	3	5.0	.83	.18806	.30	.40140	1.00	.02661

*This iteration is illustrated in Figure 14 and Graphs 7 through 10.

Table 7. Correlation Statistics for Coastal Orientation vs. Shoreline Change for Ocracoke Island.

(Lengh of Coastline - 24.8 km; Mean Orientation = 121° North of South)

A	B	C	D	E	F	G	H	I
Degree	Segments	Kilometers	r(m)	Sig. [r(m)]	r(σ)	Sig. [r(σ)]	r(m+σ)	Sig. [r(m+σ)]
.5	24	1.0	-.33	.05798	.86	.00001	.62	.00061
1.0	17	1.5	-.23	.18405	.86	.00001	.66	.00180
1.5	13	1.9	-.27	.17977	.89	.00003	.67	.00621
2.0	11	2.3	-.57	.03303	.87	.00026	.57	.03297
2.5	10	2.5	-.52	.06000	.87	.00047	.62	.02907
3.0	8	3.1	-.67	.03478	.87	.00260	.57	.07259
3.5	7	3.5	-.64	.05940	.86	.00637	.57	.09050
4.5	6	4.1	-.63	.09089	.91	.00600	.69	.06595
*6.0	5	5.0	-.66	.11246	.94	.00963	.73	.08156
7.0	4	6.2	-.52	.23867	.96	.02128	.82	.08948
9.5	3	8.3	-.65	.27719	.96	.09217	.74	.23279

*This iteration is illustrated in Figure 15 and Graphs 7 through 10.

Table 8. Correlation Statistics for Coastal Orientation vs. Shoreline Change for Core Banks from Cape Lookout Point to Ocracoke Inlet.

(Length of Coastline = 65.8 km; Mean Orientation = 139° North of South)

A	B	C	D	E	F	G	H	I
Degree	Segments	Kilometers	r(m)	Sig. [r(m)]	r(σ)	Sig. [r(σ)]	r(m+σ)	Sig. [r(m+σ)]
1.0	82	.8	-.49	.00001	-.70	.00001	-.72	.00001
1.5	62	1.1	-.34	.00316	-.70	.00001	-.69	.00001
2.0	47	1.4	-.54	.00005	-.73	.00001	-.75	.00001
2.5	38	1.7	-.52	.00036	-.74	.00001	-.75	.00001
3.0	32	2.1	-.39	.01331	-.74	.00001	-.74	.00001
3.5	30	2.2	-.28	.06197	-.63	.00010	-.64	.00007
4.0	25	2.6	-.30	.06595	-.67	.00013	-.67	.00011
4.5	19	3.5	-.27	.12756	-.68	.00070	-.67	.00082
5.0	15	4.4	-.36	.09645	-.73	.00109	-.73	.00104
6.0	14	4.7	-.31	.13662	-.70	.00287	-.69	.00306
7.0	12	5.5	-.20	.25975	-.65	.01163	-.63	.01351
8.5	6	11.0	-.52	.13886	-.87	.01268	-.84	.01744
10.5	7	9.4	-.29	.26199	-.85	.00719	-.85	.00821
*14.0	5	13.2	-.51	.19424	-.94	.00964	-.90	.01994
16.5	4	16.5	.07	.47122	-.84	.08142	-.67	.16771

*This iteration is illustrated in Figure 16 and Graphs 7 through 10.

Table 9. Correlation Statistics for Coastal Orientation vs. Shoreline Change for Shackleford Banks.

(Length of Coastline = 11.7 km; Mean Orientation = 63° North of South)

A	B	C	D	E	F	G	H	I
Degree	Segments	Kilometers	r(m)	Sig. [r(m)]	r(σ)	Sig. [r(σ)]	r(m+σ)	Sig. [r(m+σ)]
.5	41	.3	.28	.04085	.67	.00001	.54	.00014
1.0	28	.4	.24	.11124	.71	.00001	.51	.00289
1.5	21	.6	.14	.27654	.76	.00003	.50	.01113
2.0	17	.7	.27	.14491	.78	.00012	.62	.00383
2.5	16	.7	.40	.06487	.72	.00083	.65	.00307
3.0	12	1.0	.24	.22782	.79	.00116	.62	.01587
3.5	11	1.1	.37	.13082	.78	.00251	.69	.00909
4.0	10	1.2	.35	.16398	.81	.00224	.71	.01032
4.5	9	1.3	.40	.14446	.82	.00347	.74	.01171
5.0	8	1.5	.44	.13586	.82	.00602	.74	.01783
6.5	7	1.7	.54	.10715	.82	.01118	.78	.01919
8.0	6	2.0	.60	.10399	.80	.02922	.83	.02049
*10.5	5	2.3	.65	.11750	.85	.03370	.82	.04285
11.0	4	2.9	.64	.17994	.93	.03726	.81	.09494
14.0	3	3.9	.57	.30681	.97	.07624	.81	.19855

*This iteration is illustrated in Figure 17 and Graphs 7 through 10.

ASSATEAGUE ISLAND

MEAN COASTAL ORIENTATION = 157° NORTH OF SOUTH.

●——● = r For Orientation Vs. Mean Shoreline Rate Of Change.

■——■ = r For Orientation Vs Standard Deviation Of Shoreline Rate Of Change.

▲——▲ = r For Orientation Vs Mean Plus Standard Deviation Of Shoreline Rate Of Change.

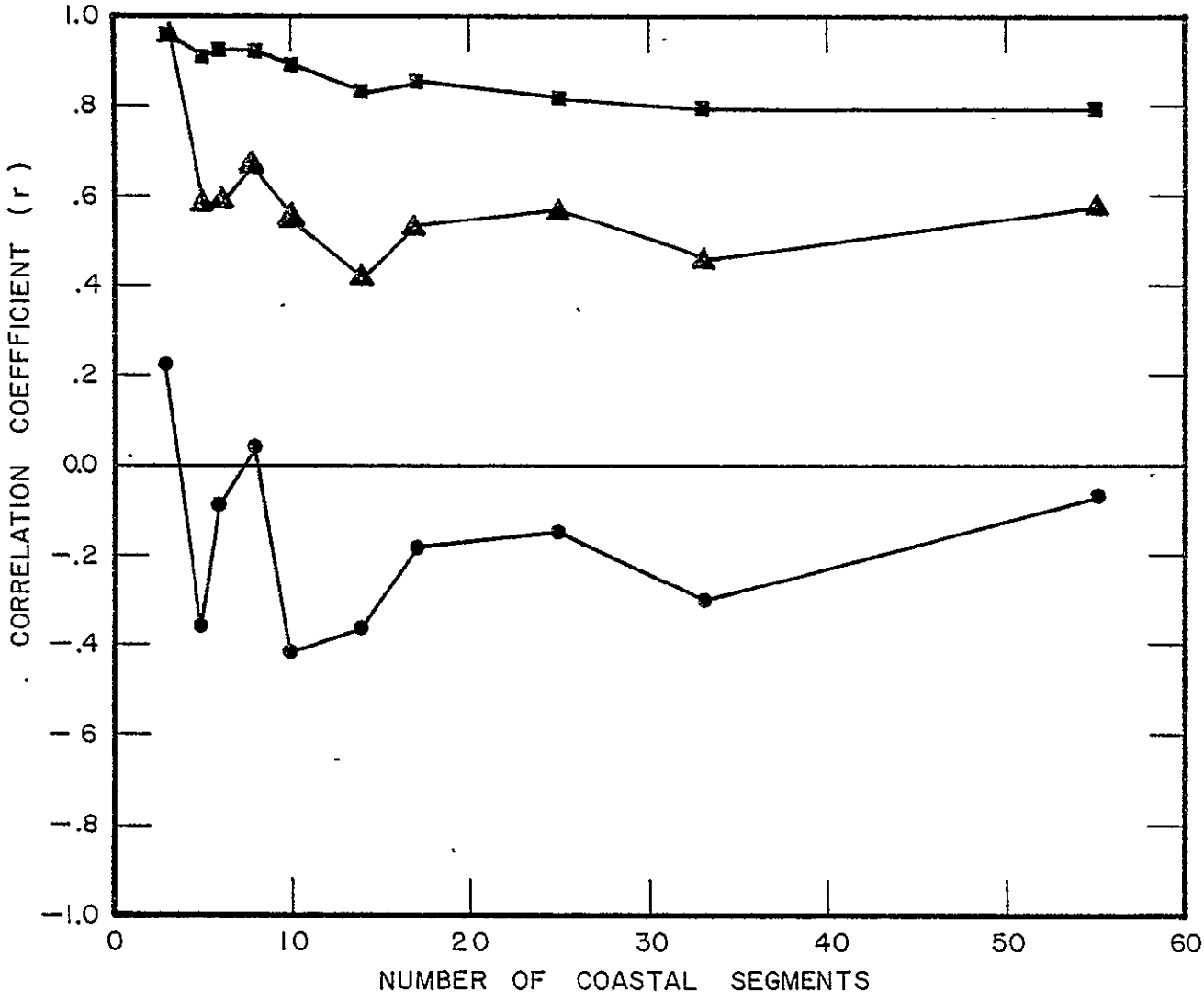

GRAPH 1: Assateague Island: Correlation Of Coastal Orientation And Shoreline Rates Of Change Vs. Number Of Coastal Segments.

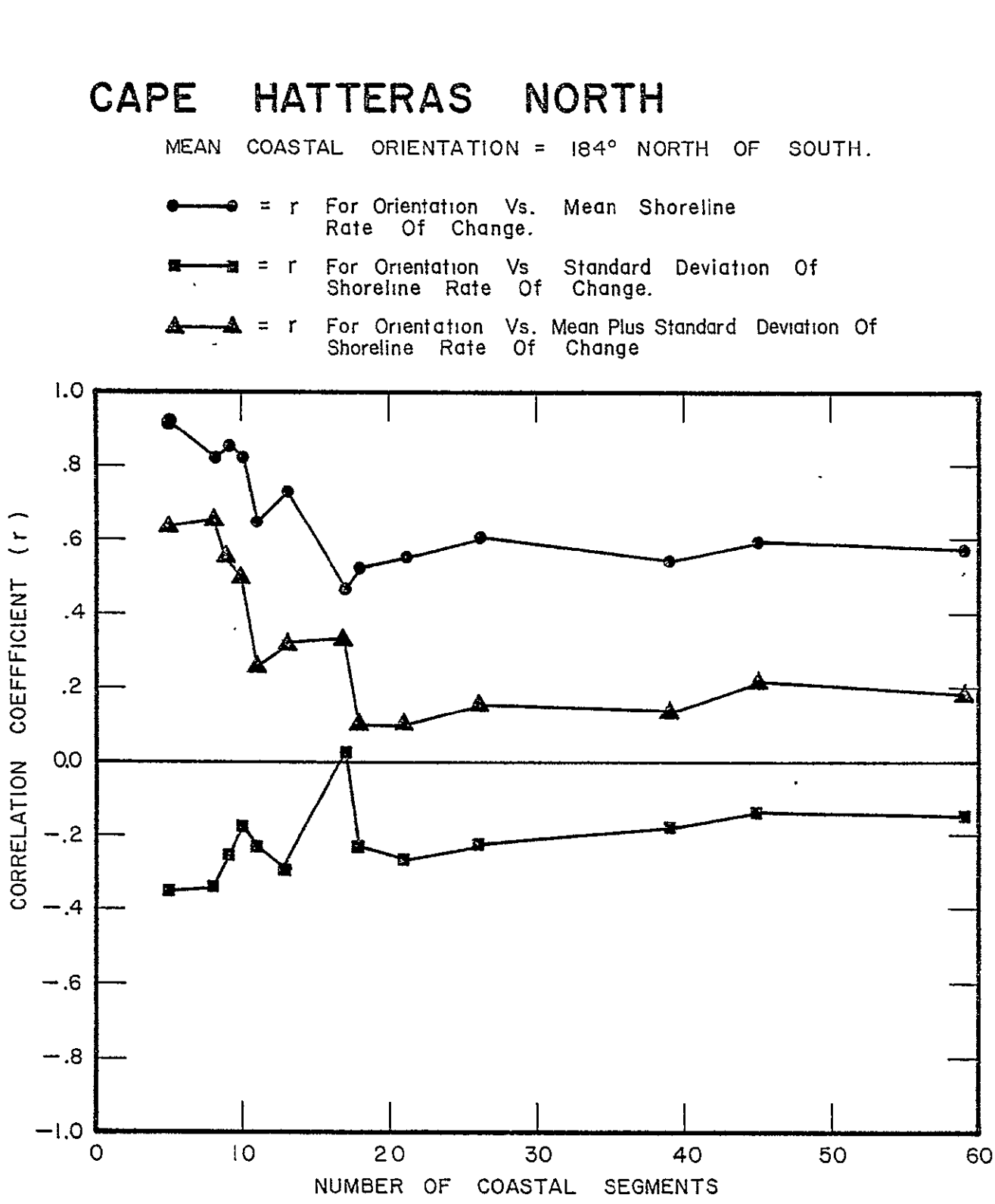

GRAPH 2: Cape Hatteras North: Correlation of Coastal Orientation And Shoreline Rates Of Change Vs. Number Of Coastal Segments.

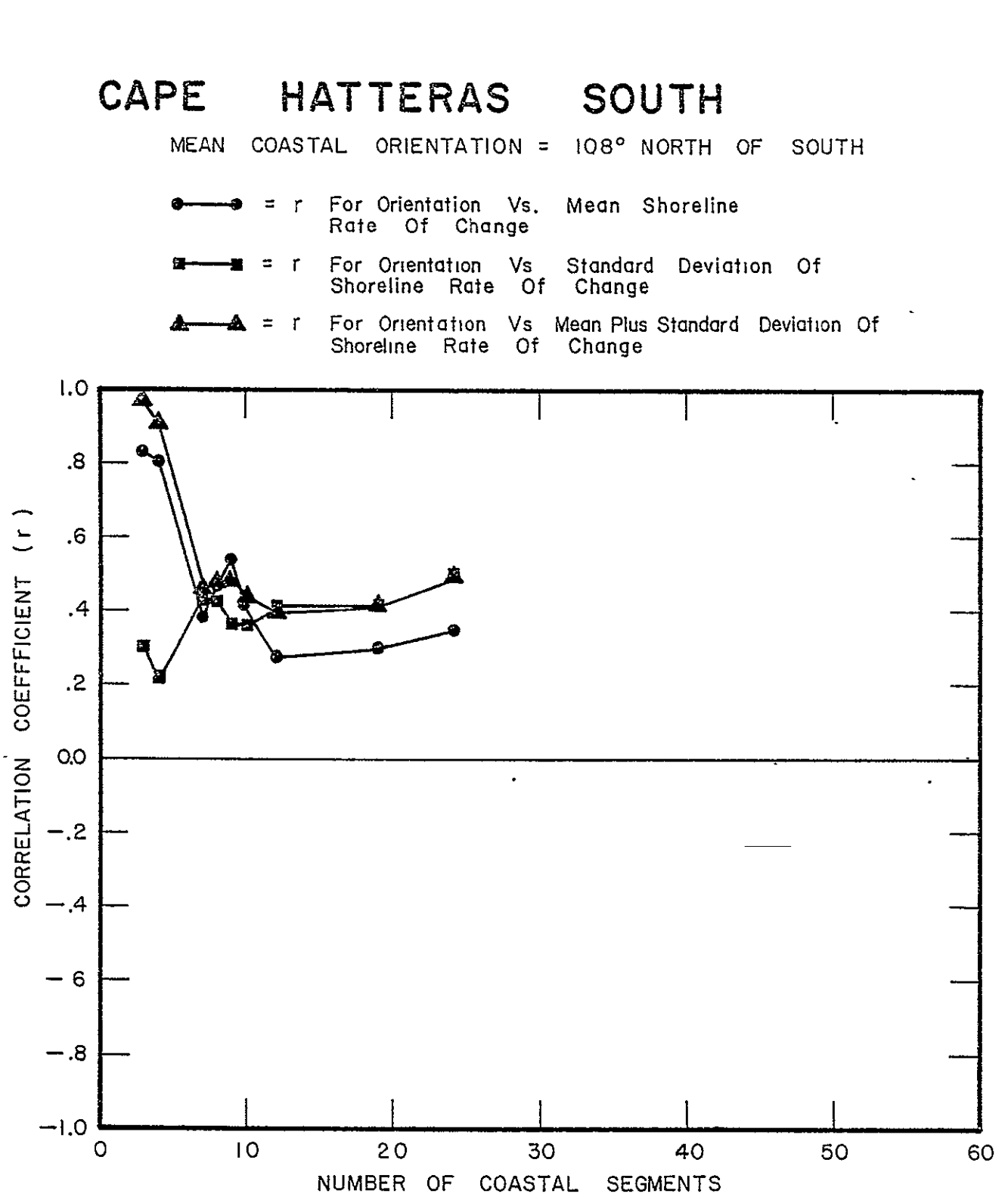

GRAPH 3: Cape Hatteras South: Correlation Of Coastal Orientation And Shoreline Rates Of Change Vs. Number of Coastal Segments.

OCRACOKE ISLAND

MEAN COASTAL ORIENTATION = 121° NORTH OF SOUTH

= r For Orientation Vs. Mean Shoreline Rate Of Change

= r For Orientation Vs Standard Deviation Of Shoreline Rate Of Change.

= r For Orientation Vs. Mean Plus Standard Deviation Of Shoreline Rate Of Change

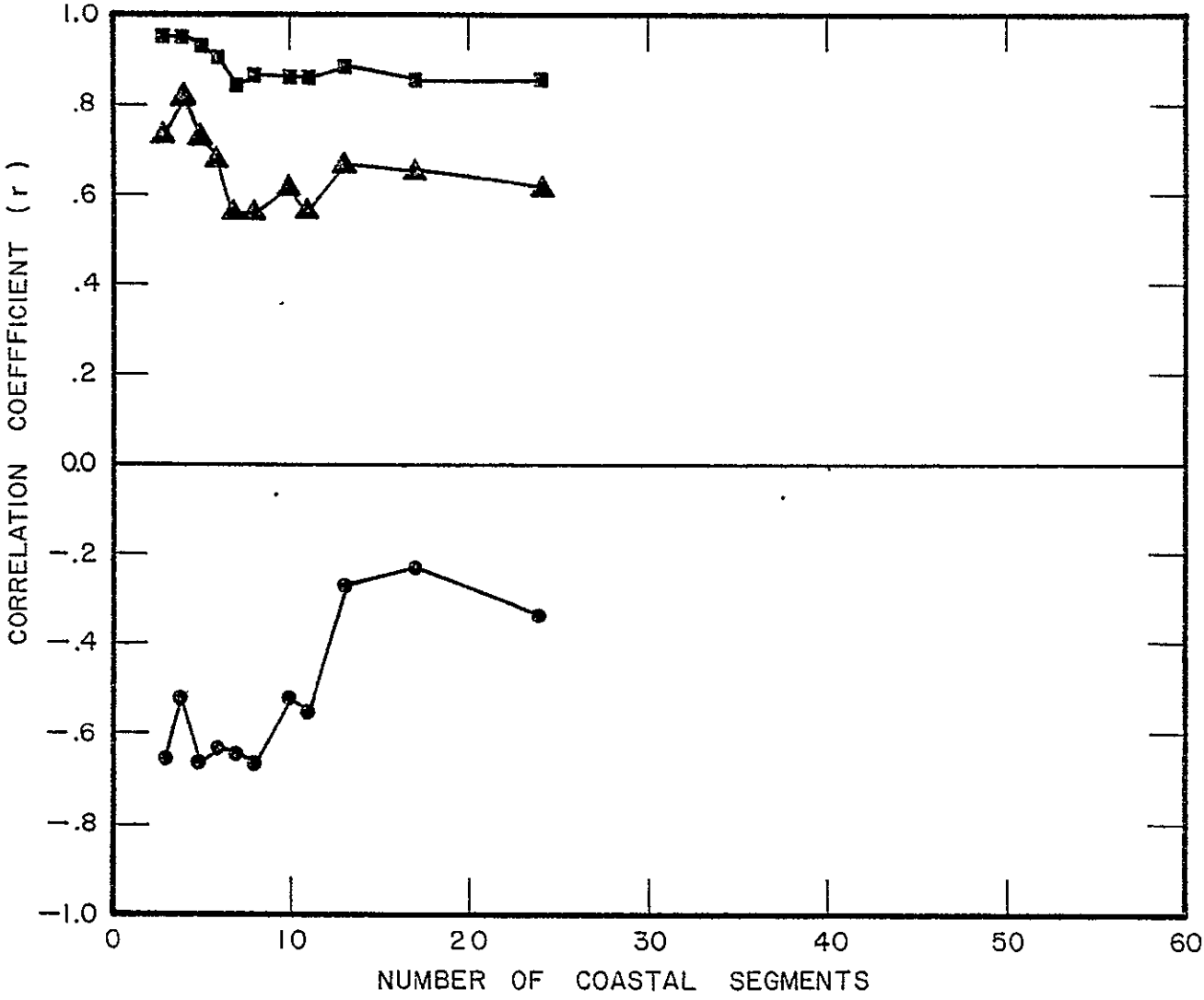

GRAPH 4: Ocracoke Island: Correlation Of Coastal Orientation And Shoreline Rates Of Change Vs. Number Of Coastal Segments.

CORE BANKS

MEAN COASTAL ORIENTATION = 139° NORTH OF SOUTH.

●——● = r For Orientation Vs. Mean Shoreline Rate Of Change.

■——■ = r For Orientation Vs. Standard Deviation Of Shoreline Rate Of Change

▲——▲ = r For Orientation Vs Mean Plus Standard Deviation Of Shoreline Rate Of Change.

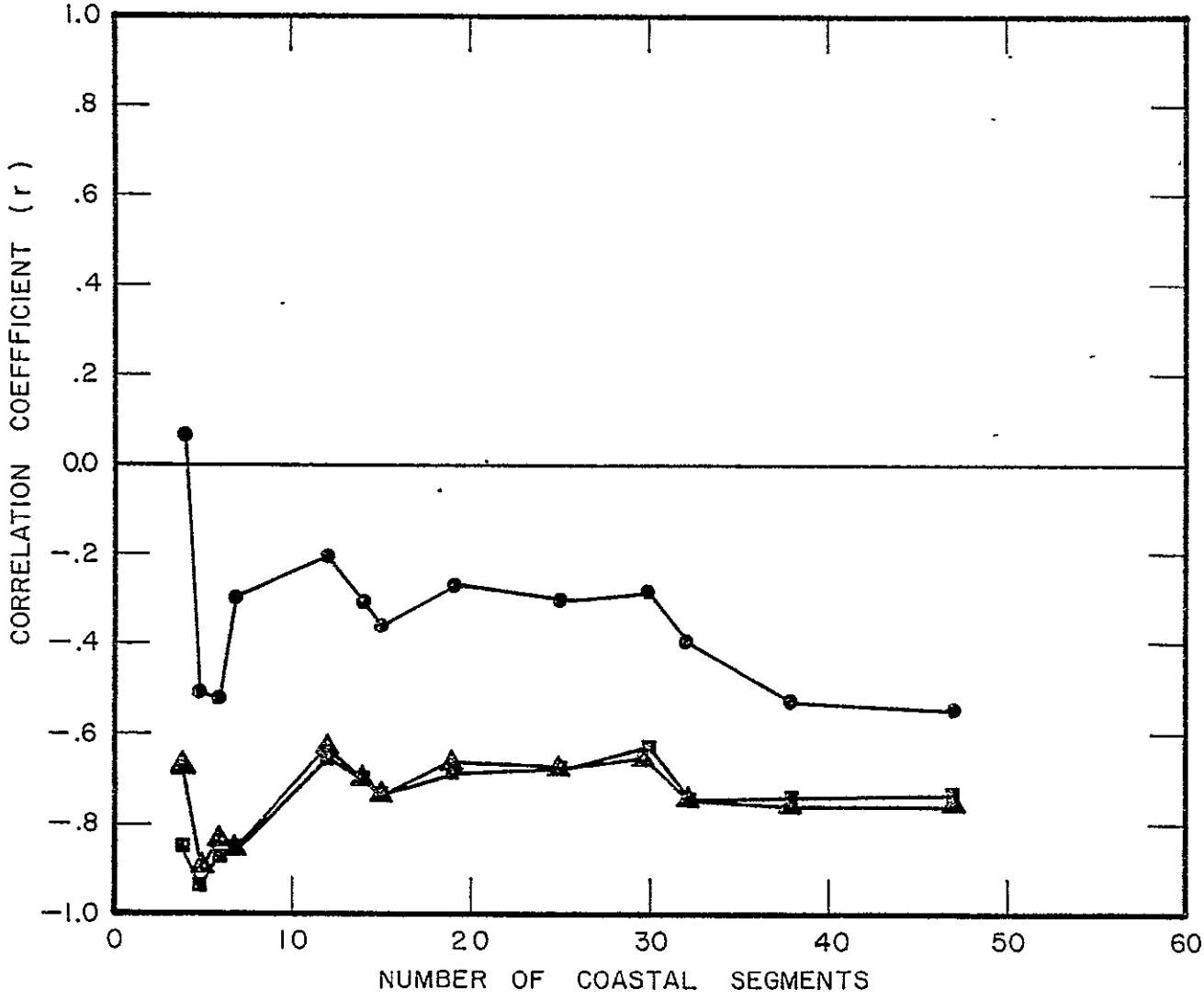

GRAPH 5: Core Banks: Correlation Of Coastal Orientation And Shoreline Rates Of Change Vs. Number Of Coastal Segments.

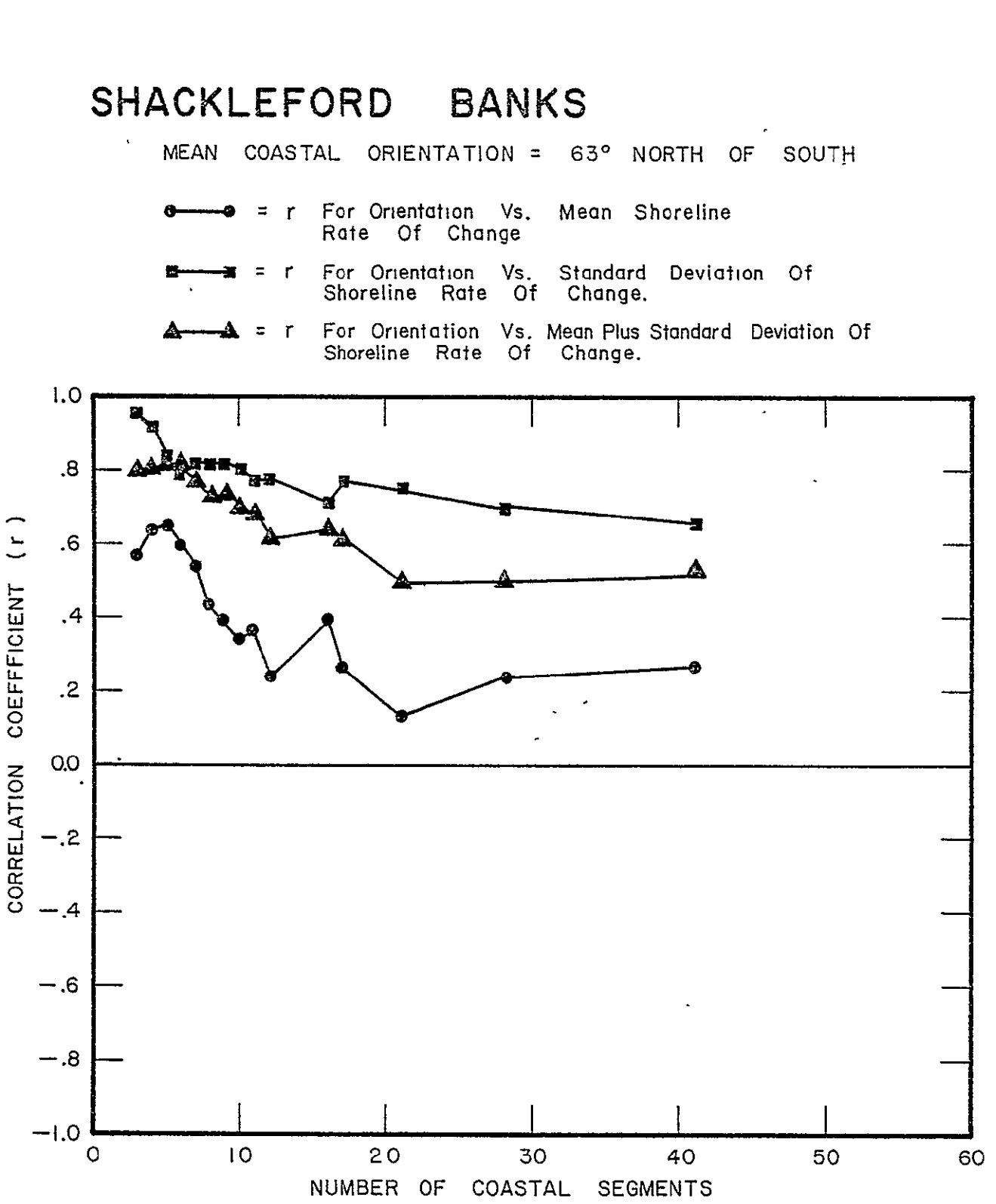

GRAPH 6: Shackleford Banks: Correlation Of Coastal Orientation And Shoreline Rates Of Change Vs. Number Of Coastal Segments.

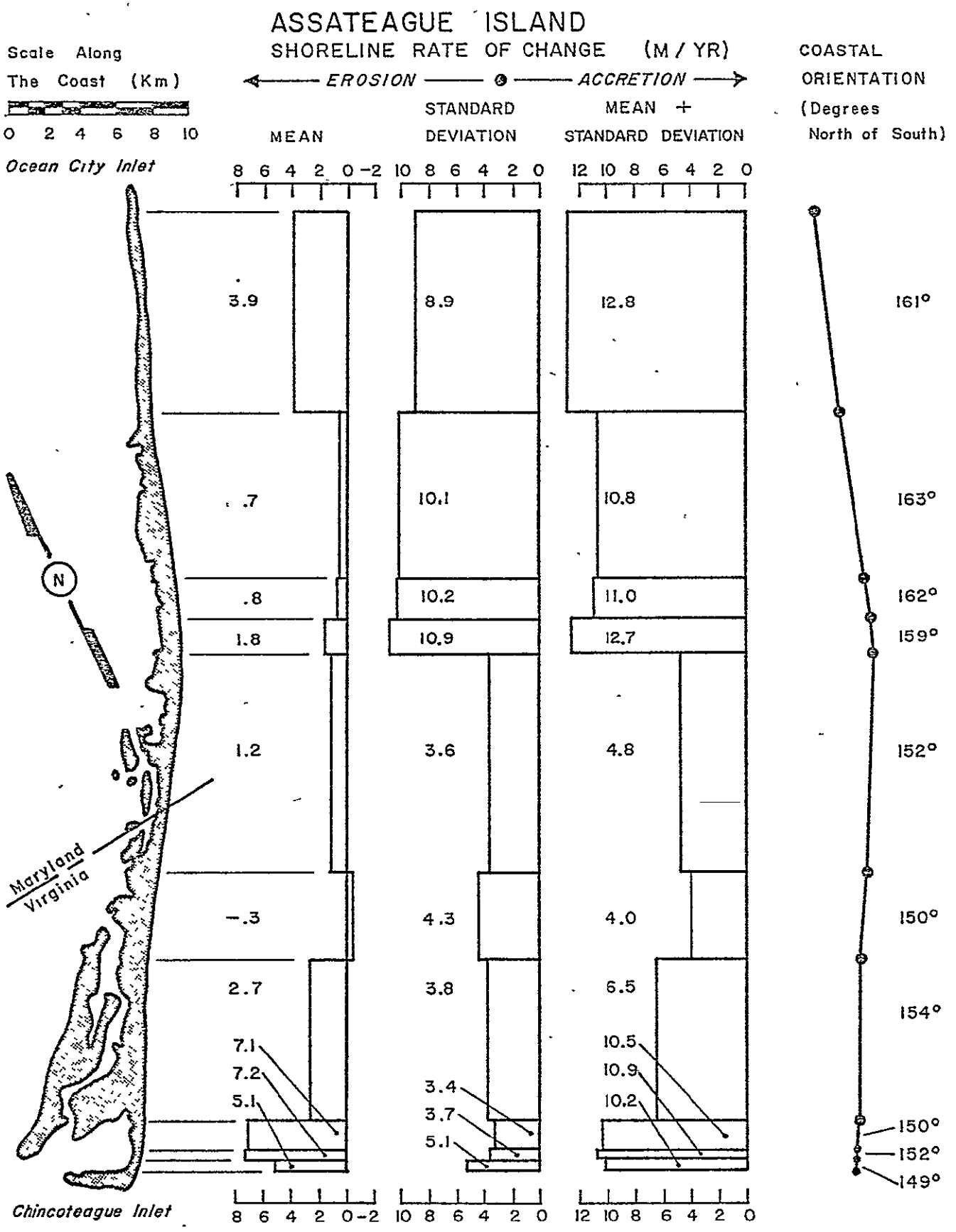

FIGURE 12: Assateague Island: Rate Of Shoreline Change And Coastal Orientation For 3.5° Threshold And 10 Coastal Segments.

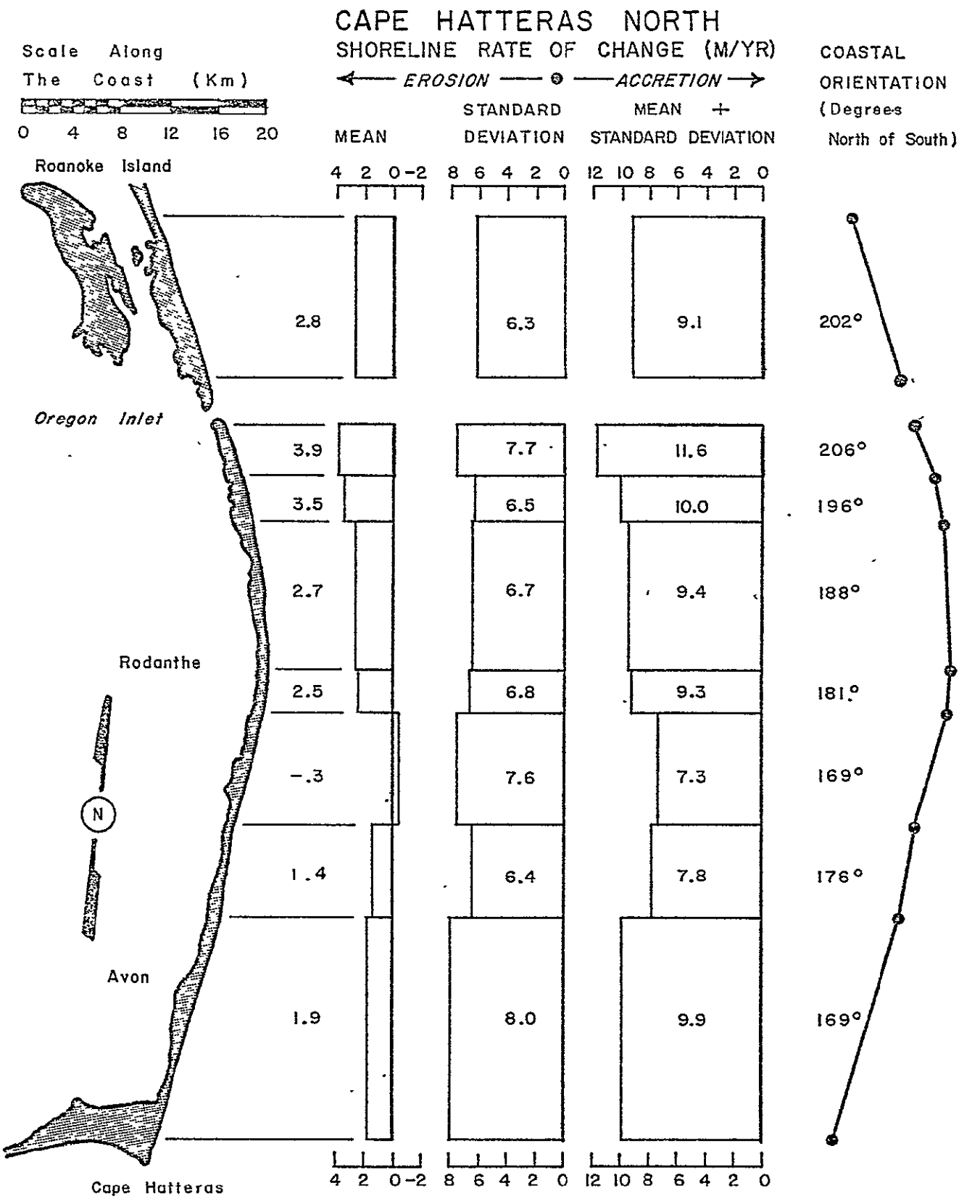

FIGURE 13: Cape Hatteras North: Rate Of Shoreline Change And Coastal Orientation For 7.0° Threshold And 8 Coastal Segments.

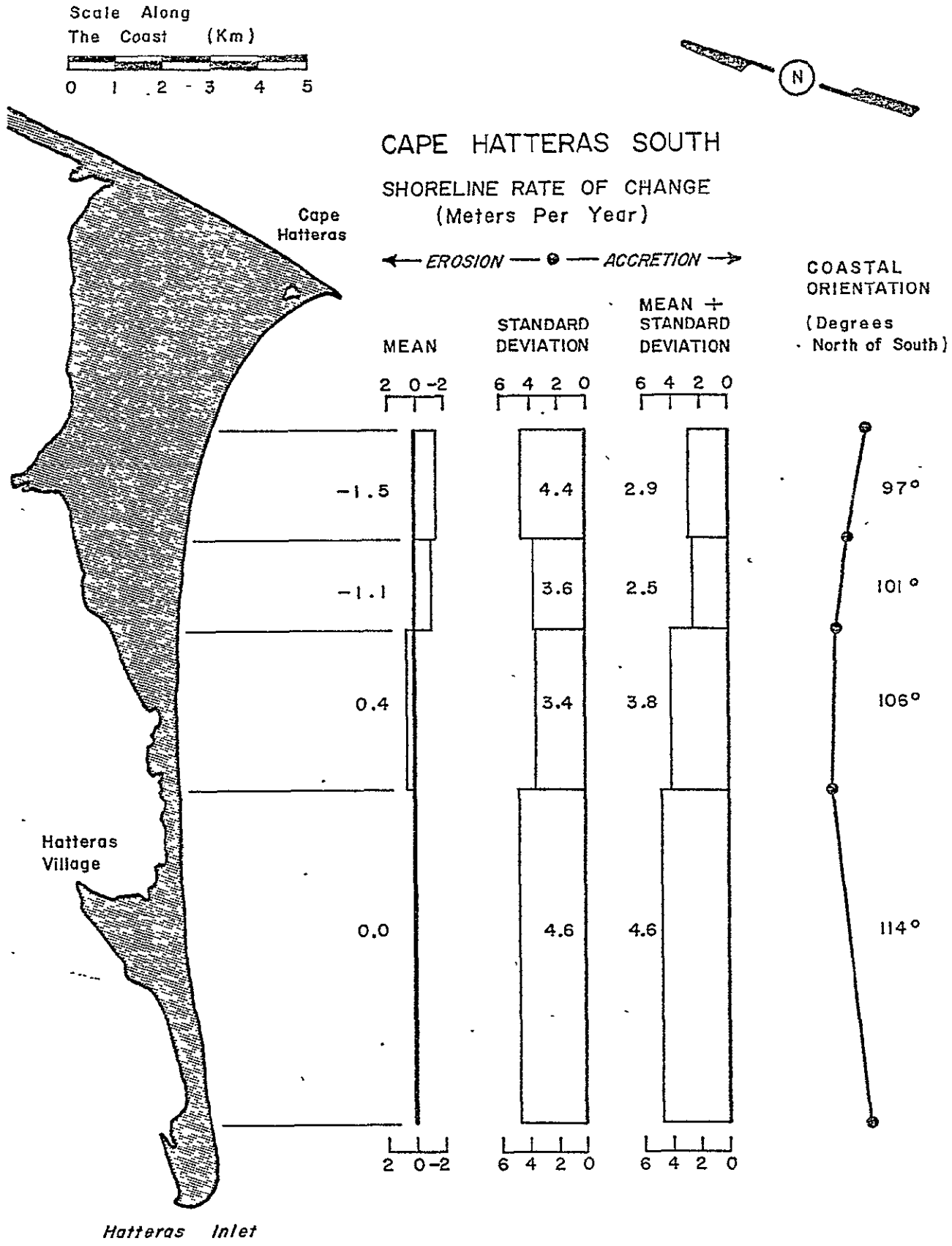

FIGURE 14: Cape Hatteras South: Rate Of Shoreline Change And Coastal Orientation For 4.5° Threshold And 4 Coastal Segments.

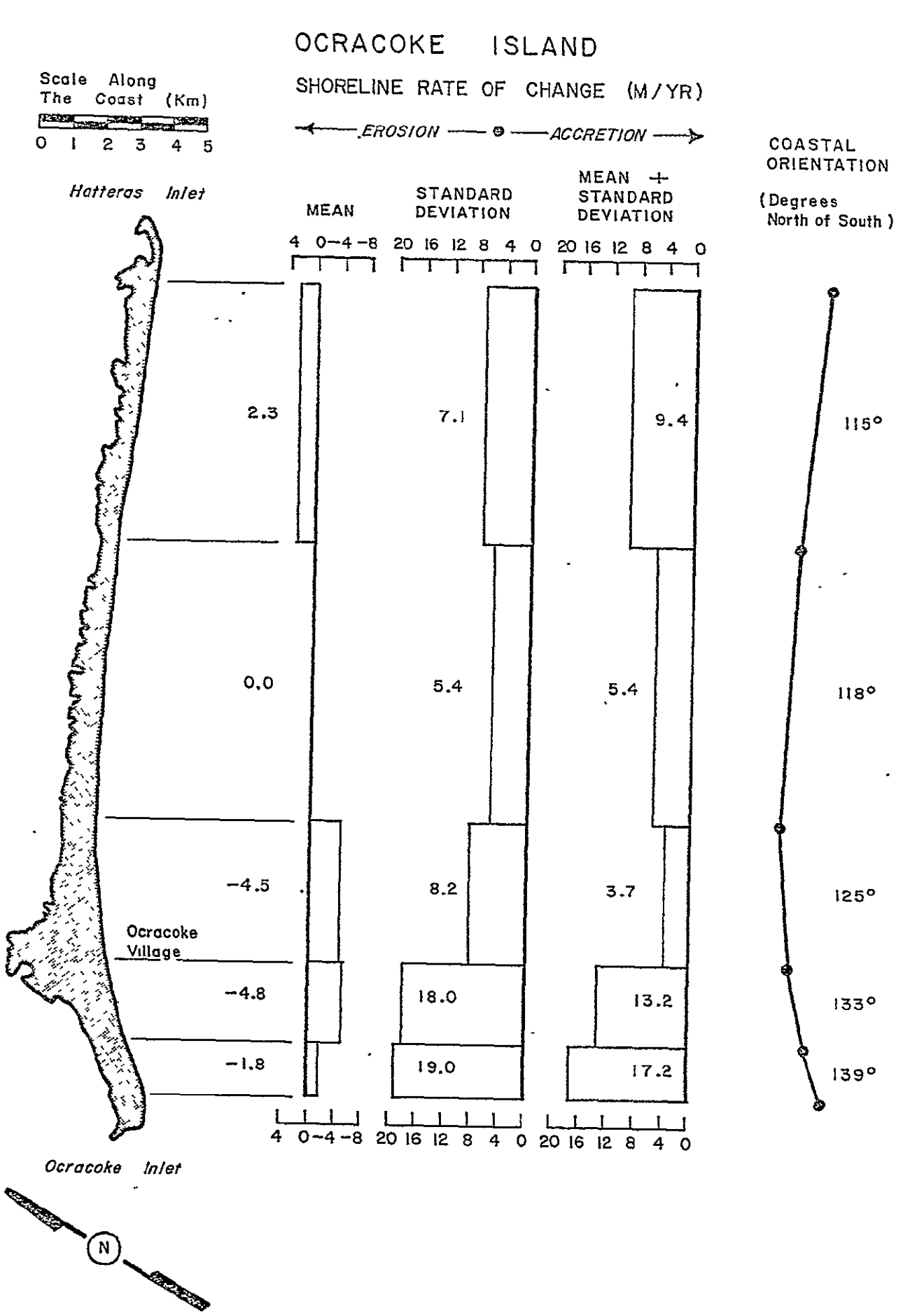

FIGURE 15: Ocracoke Island: Rate Of Shoreline Change And Coastal Orientation For 6.0° Threshold And 5 Coastal Segments.

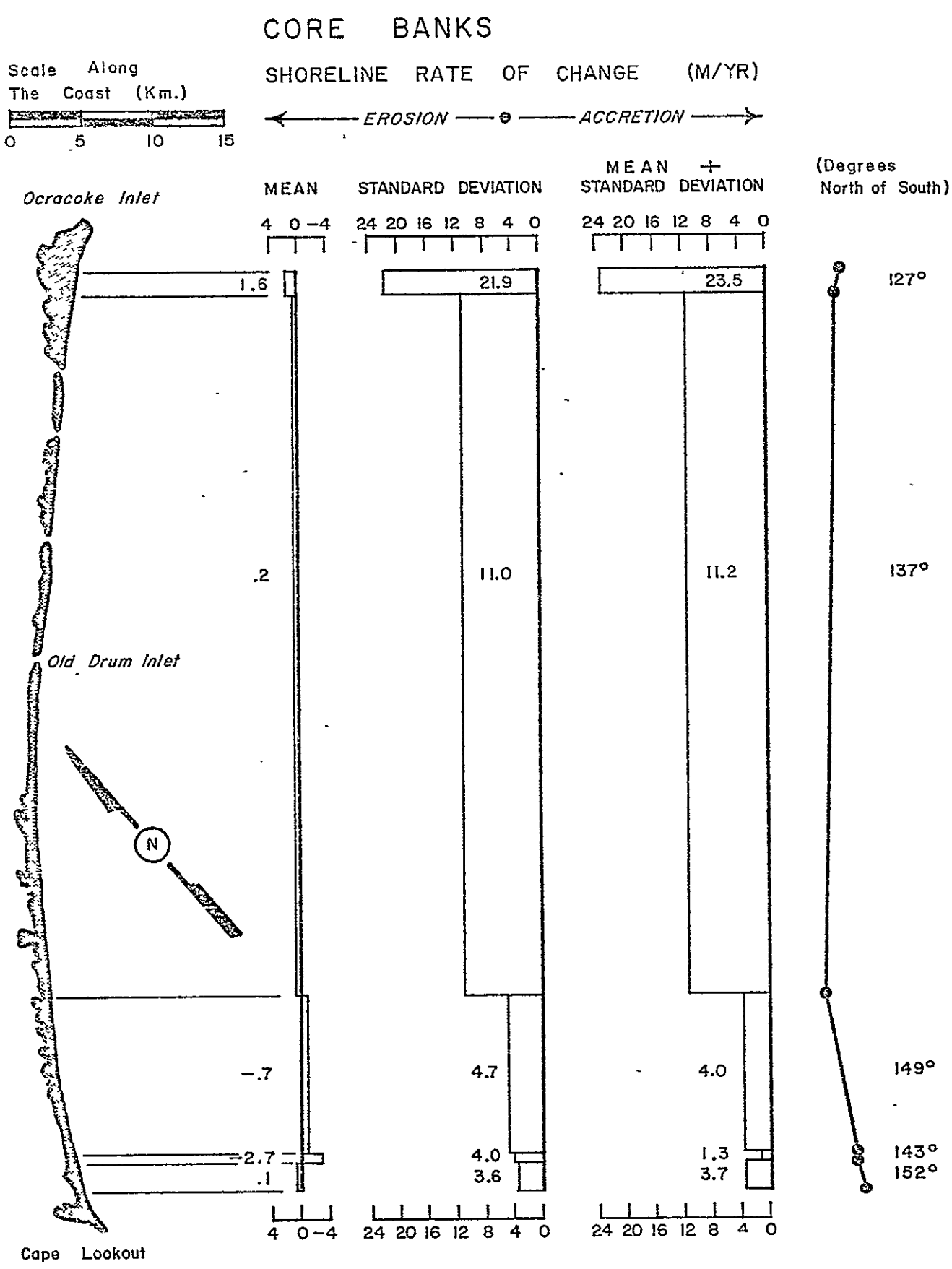

FIGURE 16: Core Banks: Rate Of Shoreline Change And Coastal Orientation For 14.0° Threshold And 5 Coastal Segments.

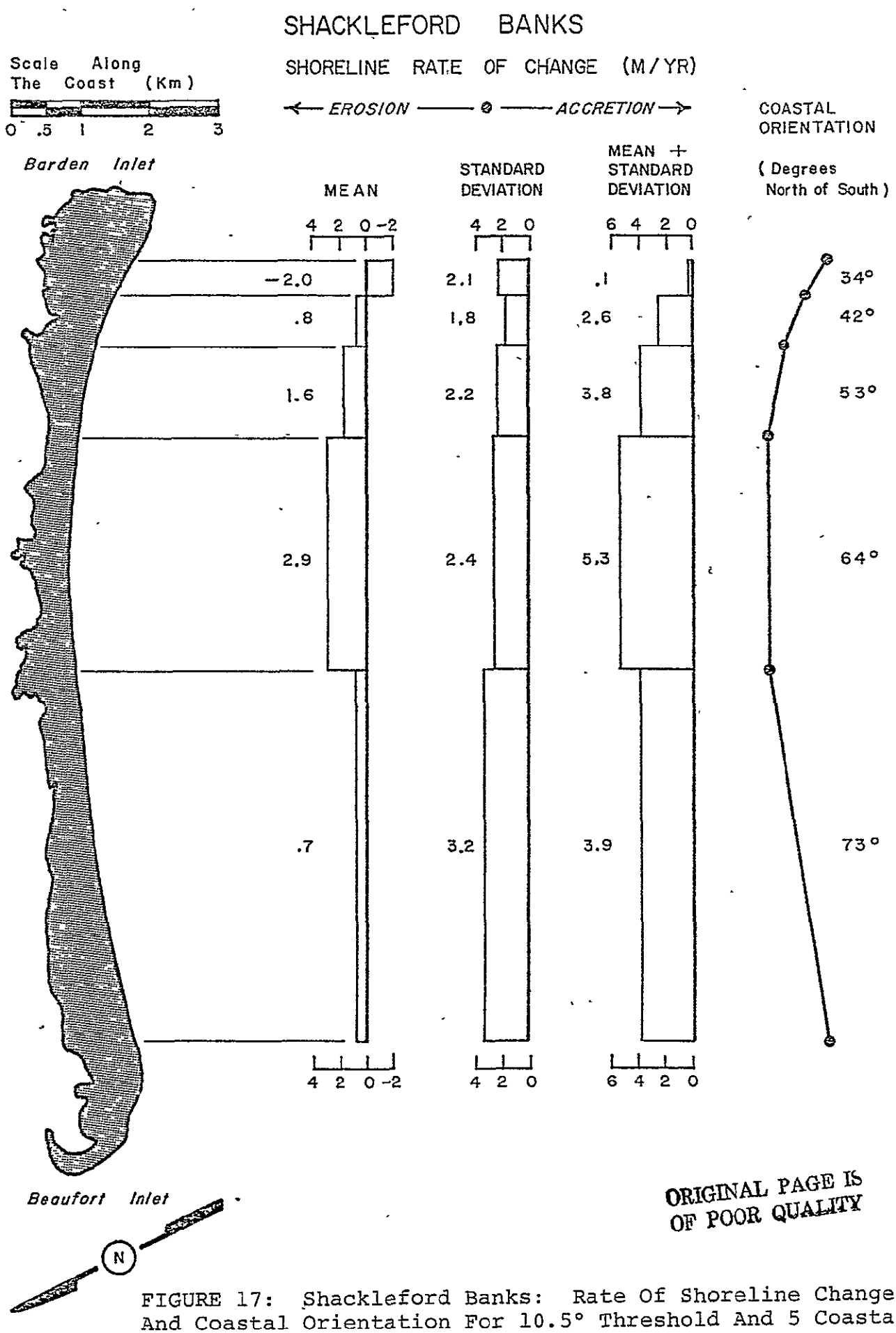

FIGURE 17: Shackleford Banks: Rate Of Shoreline Change And Coastal Orientation For 10.5° Threshold And 5 Coastal Segments.

Significant Results

In our quarterly report dated 18 June 1976, we presented correlations between orientation and the standard deviation of rate of shoreline change for Assateague Island, Cape Hatteras, and Ocracoke Island. The data suggested that for those barrier islands whose mean coastal orientations were in the vicinity of a northeast/southwest direction, there should be a high positive correlation between orientation and standard deviation of rate of shoreline change for individual straight-line segments of the coast. The mean orientation for the 65.8 km. stretch of Core Banks that we studied was 139° north of south (Figure 11). Since this was nearly ideally northeast/southwest, we expected a very high positive correlation. Our results, however, were opposite of what we had expected. The correlations were high, but negative rather than positive, and significant at the 1% level.

In the following discussion, we will treat the data on an island-by-island basis and then make some general observations. Graphs 1-6 are useful visual aids for interpreting the data in Tables 4-9.

It is important to look at correlations for all three measures of rate of shoreline change, because each has a different relation to the physical environment. The mean rate of change represents the long-term trend of shoreline migration. This is most important in terms of long-range planning. The

standard deviation over time allows us to assess the variability of shoreline movement from point to point or segment to segment along the coast. It in turn is the best indicator of vulnerability to individual storms. The mean + standard deviation of rate of change combines the long-term trend state with the episodic eddy state of shoreline movement. It is the best indicator of the shoreline's overall response to daily and seasonal coastal processes. Figures 12-17 show the orientations and erosion rates for selected computer iterations for all the islands.

On Assateague Island, the standard deviation is the best measure of shoreline rate of change to relate to coastal orientation (Table 4, Graph 1, Figure 12). For two iterations, the correlation was .93 at the 1% level of confidence. This indicates that if we were to compare the variability of shoreline change between two relatively straight segments of the coast, we could say with a high degree of certainty that the segment that was closer to the north/south orientation (measured counterclockwise) would show greater variation in shoreline migration (erosion and accretion) over time. However, that same segment would show a lower long-term rate of erosion, since the correlations involving the mean are primarily negative. We cannot make the second conclusion with very much confidence, because the correlations are low and the levels of significance are low.

The reverse is true in the case of Hatteras Island from Cape Hatteras Point to Nags Head (Table 5, Graph 2, Figure 13). We find that the mean rates of erosion of coastsl segments

increase as the orientations of those segments increase their rotation north of south. We can be more confident of this relationship when the average segment length exceeds 7 kilometers. The correlation is then greater than .8 at the 1% level of significance. We can also say, with less confidence, since the correlations are low and not very significant, that the variability in shoreline change decreases as the orientation north of south increases, because the correlations are negative.

The strongest relationship for southern Hatteras Island from Hatteras Inlet to Cape Hatteras Point (Table 6, Graph 3, Figure 14), is between orientation and the mean plus standard deviation. The only high correlations with relatively acceptable confidence levels (better than 5%), are for the last two iterations, with the longest coastal segments. Other than the fact that all correlations were positive, little can be said about this section of Hatteras Island with any degree of certainty. This is not surprising since we are working with a relatively short stretch of coast, and we expect the highest correlations to occur when we examine the longer coastlines.

The relationship between orientation and shoreline change for Ocracoke Island (Table 7, Graph 4, Figure 15) is very similar to that for Assateague Island. The standard deviation of rate of change is a very strong indicator, having positive correlations with orientations at high levels of significance, whereas the mean rate of change is a weaker indicator, with

lower negative correlations of lower significance. It is interesting to note that these similarities exist between Assateague and Ocracoke even though the overall shoreline form for Assateague is convex, whereas it is concave for Ocracoke.

The correlations for the 65.8 km. stretch of Core Banks from Cape Lookout Point to Ocracoke Inlet (Table 8, Graph 5, Figure 16) were totally unexpected. The standard deviation of rate of shoreline change was associated with very high, but negative correlations with orientation, at the 1% level of significance. Correlations involving the mean rate of erosion were lower, less significant, but also negative. Also of interest is the fact that on the Core Banks, the mean plus standard deviation is a more significant indicator of the relationship between orientation and erosion than for any other coastline we studied, with high negative correlations at the 1% level of significance. More simply stated, we can be confident that on the Core Banks, the least changing segments of the shoreline are those whose orientation have the greatest counterclockwise deviation from the north/south line - the opposite condition from Ocracoke or Assateague Islands.

All correlations for Shackleford Banks (Table 9, Graph 6, Figure 17) were positive. The only other section of the coast where this occurred was South Hatteras, the mean orientation of which (108° north of south) was closest to that of Shackleford Banks (63° north of south). For Shackleford, the

standard deviation was the best indicator, but not as significant as for some of the other islands.

In comparing all islands together, it is difficult to spot strong trends in correlations vs. mean orientation for each island (Graph 7). The graph suggests that islands whose mean orientations are approximately 140° north of south will have different relationships between orientation and erosion from the islands whose mean orientations are greater or less than 140°.

Graphs 8-10 show linear regression lines from scatterplots of the data for all six islands and for the three sets of correlations between orientation and rate of erosion for selected computer iterations. For each island, the iteration that was chosen was the one that gave the all-around highest and most significant correlations for the three tests. The degree threshold and correlation coefficients are listed on the graphs and may be compared to the figures in Tables 4-9.

We see that in all three graphs, the six island segments appear to segregate into two groups of similar process/response relationships as suggested by the slopes of the regression lines. One group contains Assateague Island, Ocracoke Island, and Core Banks. The other group includes North Hatteras, South Hatteras, and Shackleford Banks. Core Banks appears to be in a subgroup of its own. (Note island groupings in Figure 11).

In most cases, the standard deviation shows the strongest relationship between orientation and shoreline change. In

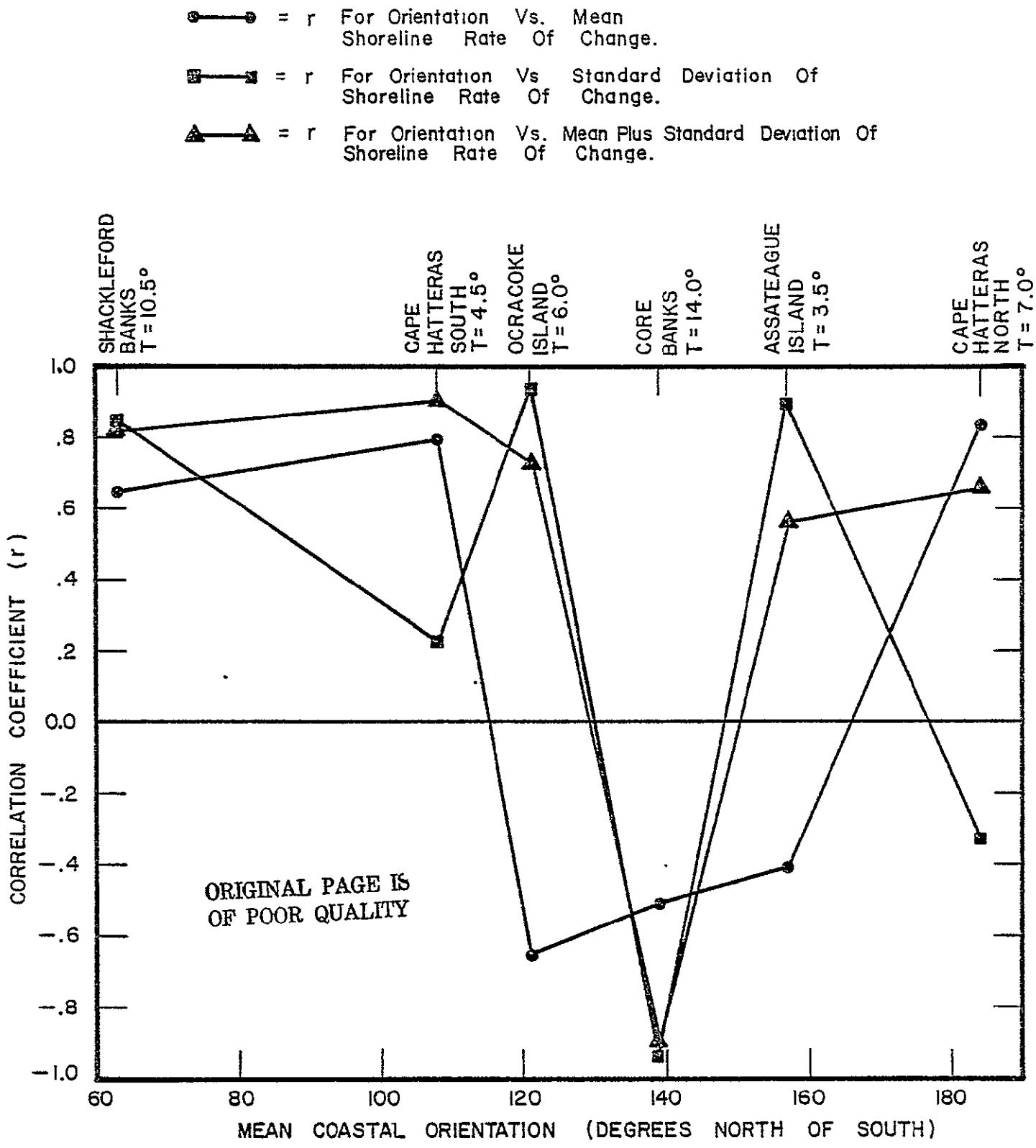

T = Orientation Change Threshold (See Tables 4 - 9).

GRAPH 7: Correlation Of Coastal Orientation And Shoreline Rate Of Change Vs. Mean Orientations of Six Barrier Islands.

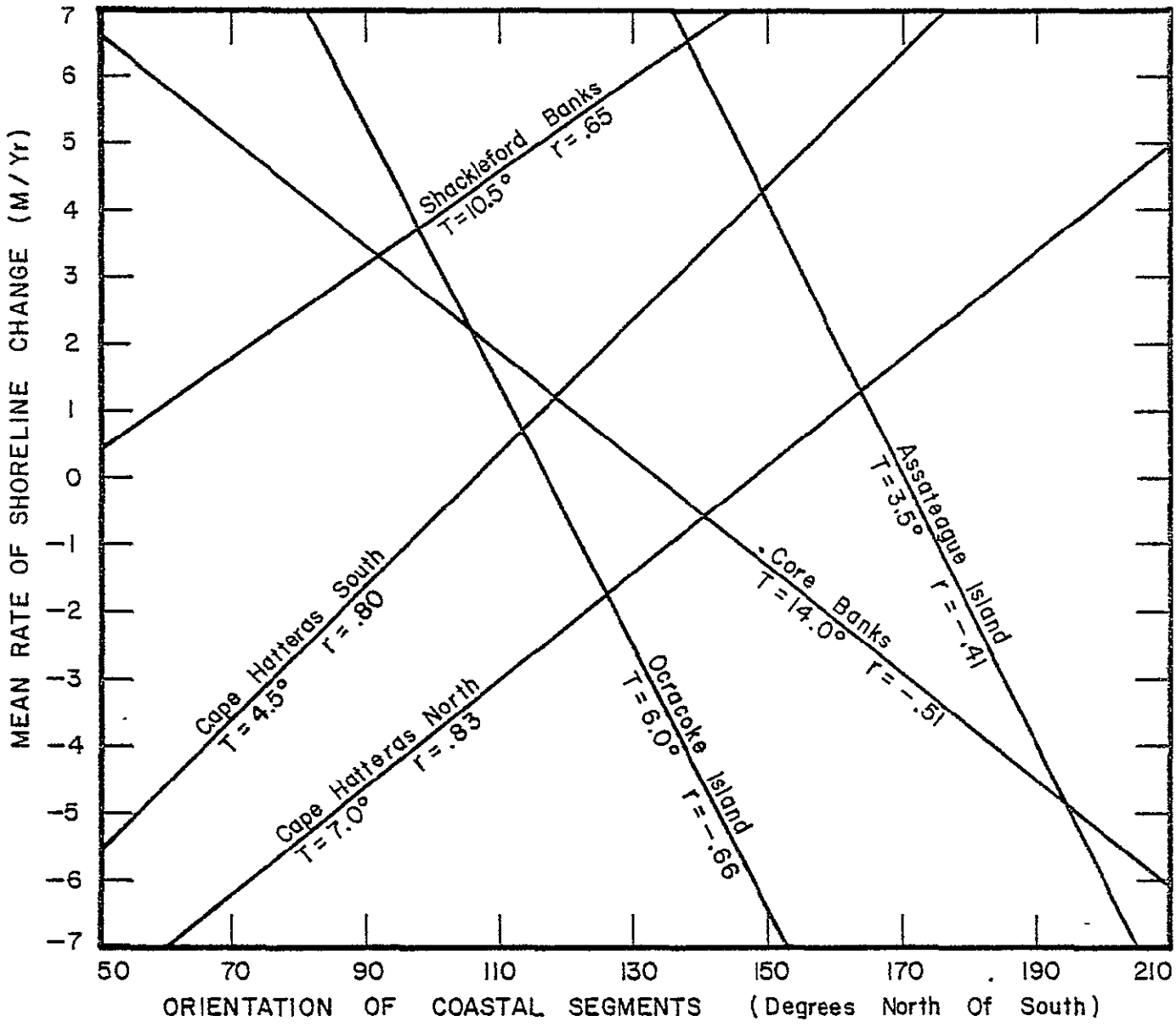

T = Orientation Change Threshold (See Tables 4-9).

r = Correlation Coefficient.

GRAPH 8: Regression Lines For Coastal Orientation Vs. Mean Rate Of Shoreline Change For Six Barrier Islands.

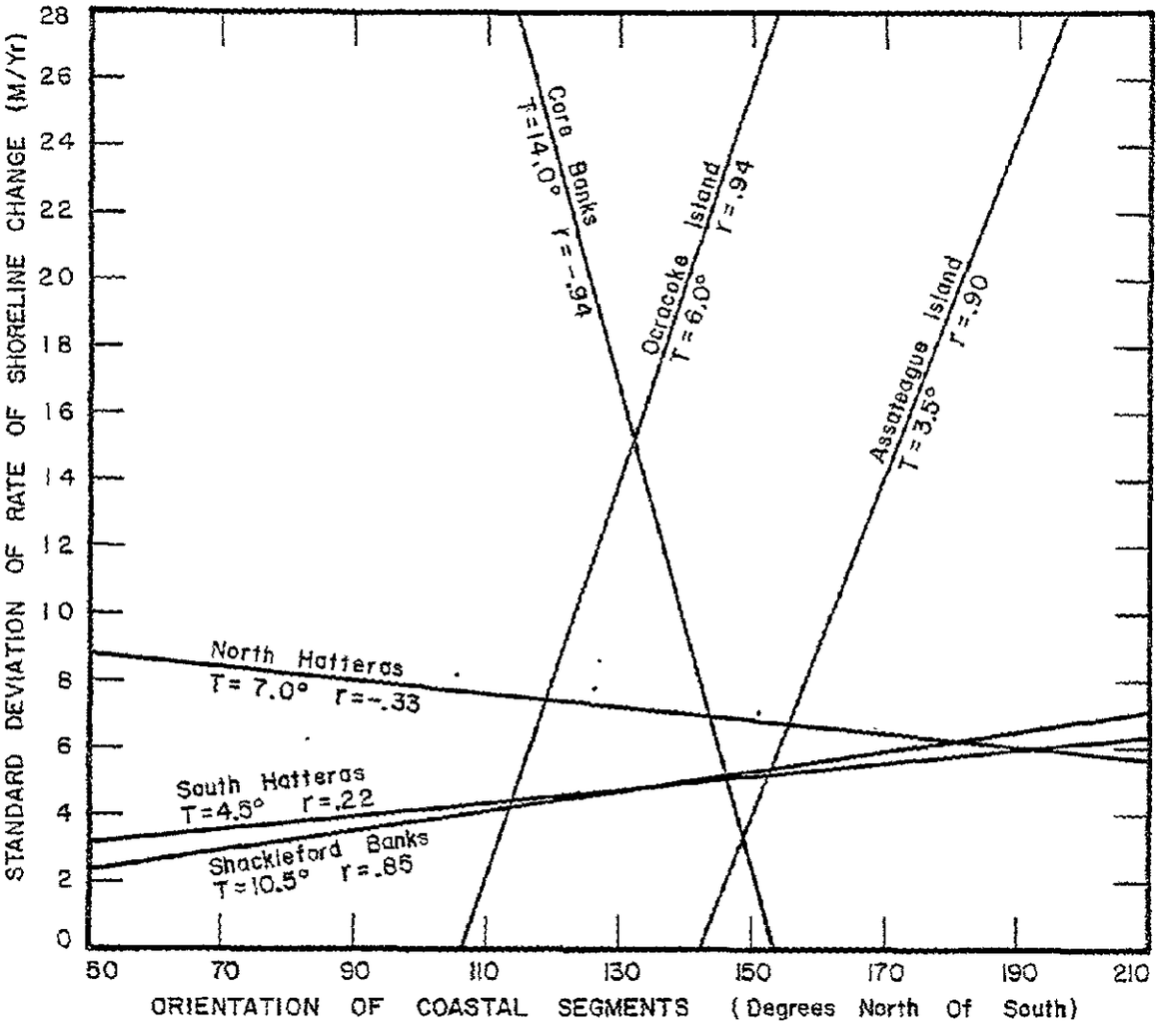

T = Orientation Change Threshold (See Tables 4 – 9).

r = Correlation Coefficient.

GRAPH 9: Regression Lines For Coastal Orientation Vs. Standard Deviation Of Rate Of Shoreline Change For Six Barrier Islands.

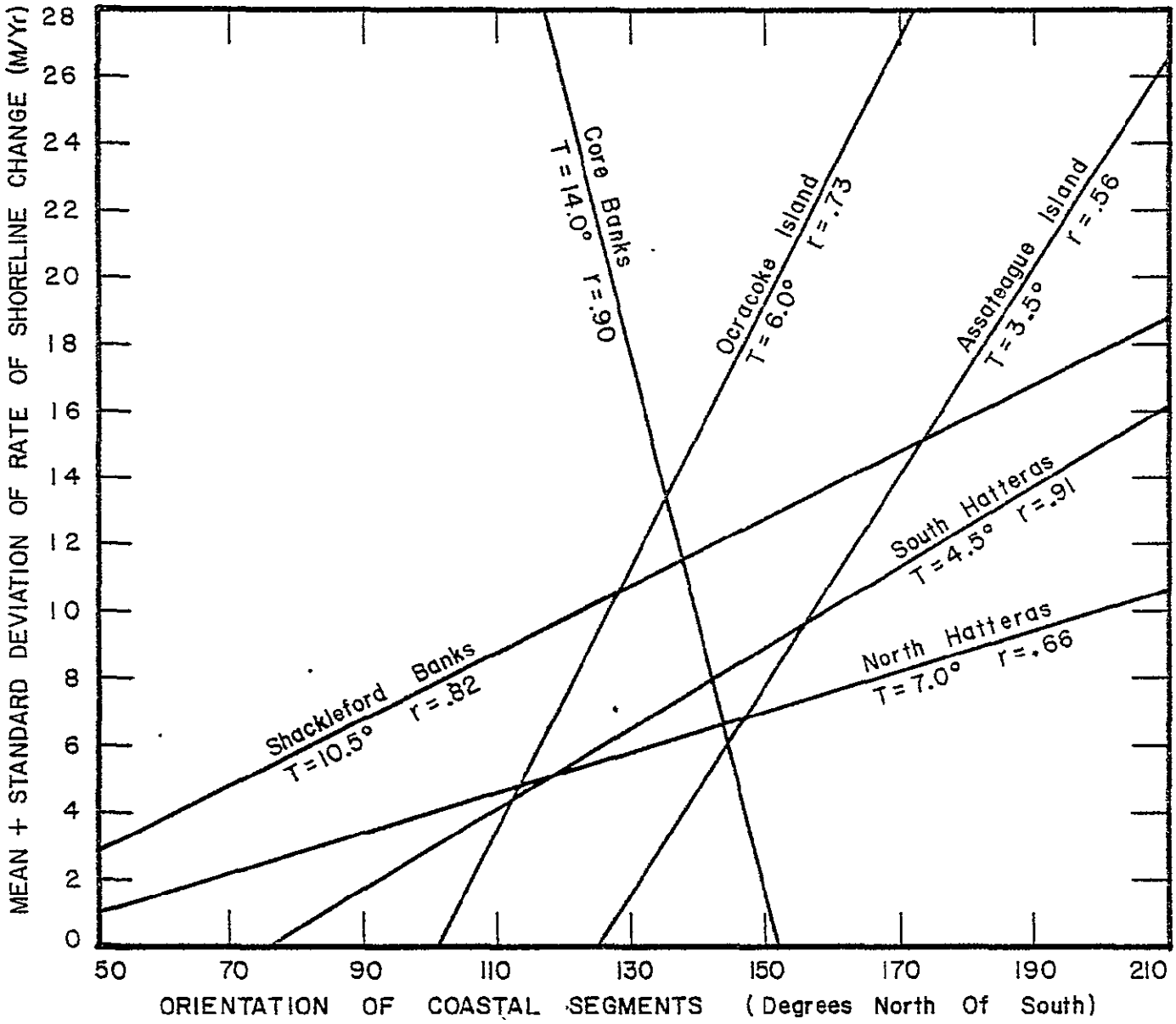

T = Orientation Change Threshold (See Tables 4-9).

r = Correlation Coefficient.

GRAPH 10: Regression Lines For Coastal Orientation Vs. Mean + Standard Deviation Of Rate Of Shoreline Change For Six Barrier Islands.

general, correlations for the mean + standard deviation fall between those for the mean alone and those for the standard deviation alone. Only for Core Banks does the mean + standard deviation show a significantly strong relationship between orientation and shoreline change. For all areas except Hatteras North, the weakest relationship was between orientation and the long-term mean rate of shoreline change.

Finally, as previously stated, it is the larger coastal landforms that are the most significant in determining where the rapid environmental changes occur along the shoreline. The data tend to support this theory, because in most cases, correlation coefficients increased as the mean segment lengths increased.

Given that it is the longest reaches of the islands which show strong process/response relationships, it seems clear that a regional model is needed to explain these relationships. The results presented here will serve as raw material for subsequent analysis and modelling. We have already begun work on creating a model for barrier island migration. We are also preparing a paper which will examine barrier island classification based primarily on the shoreline change and coastal orientation data.

Problems

Our major problems were all concerned with imagery interpretation. The most difficult job was being consistent in defining the overwash line via the correct vegetation line. In some areas, especially following major storms when beaches were broad and flat, the high water line was difficult to establish due to small-scale features, such as ridges and runnels. Whenever there was sufficient doubt in the mapper's mind, a second and often a third opinion were called upon. Because of the inherent subjectivity and constant decision-making involved in drawing these lines, the task is tedious and time-consuming. This is the phase of a coastal zone monitoring system wherein automation would be most beneficial. This idea is discussed more fully in the Appendix.

Another problem with interpretation occurred in defining straight segments of the coast with Landsat imagery. This task was also based on subjective decision-making by the mapper. In order to maximize accuracy, multiple measurements of each coastline were taken and averaged to determine a mean orientation of coastal segments.

A problem which caused delays and occasional gaps in our historical data sets was the availability of low-altitude aerial photography. Although we compiled the most extensive index of aerial photography known to exist for Assateague Island, Cape Hatteras, and Cape Lookout (Handbook for Remote Sensing,

Dolan et al., 1977), we believe that there may be many other sets of photos of those areas that we were unable to locate. This is one reason why we are recommending the establishment of a single Federal agency responsible for providing routine annual coverage of sedimentary coasts and for the storage and dissemination of this imagery and data.

Finally, a problem that was somewhat bothersome, but not critical, was slow-turn-around time for high-altitude aerial photography and Landsat transparencies. This problem was most acute in the beginning of the project when we had few or no Landsat images with which to work.

Conclusions

We have concluded that for long individual sections of the coast which contain smaller straight coastal segments with similar orientations (within approximately 40°), measurable relationships exist between coastal orientation and rate of shoreline change. These relationships differ, however, from island to island.

We have found that we cannot determine historical shoreline erosion trends based solely on coastal orientation. Therefore, we cannot predict areas of coastal vulnerability based solely on orientation of coastal segments. It is necessary to develop a more comprehensive model of a more regional nature.

We feel that the most reliable method of assessing coastal vulnerability is through direct measurement of shoreline migration through the use of low-altitude historical aerial photography.

When historical erosion data and coastal orientation data for a given section of coast are obtained, and correlations are determined, orientation alone can be useful in assessing vulnerability of that coastline.

Correlations between coastal orientation and shoreline change can be used as a method of classifying coastlines with respect to process/response relationships.

Finally, the high, significant correlations we obtained for some of the barrier island coastlines we studied cannot

be ignored. We have explored only a small segment of the data we have collected, and we have expanded our knowledge of the barrier island environment with new discoveries. There is much more analysis of the already existing data that must be done, and we are continuing our research which will lead to more general models. We feel we have still just scratched the surface, for the type of research and analysis with which we are involved has a snowballing effect. We expect numerous professional papers to evolve in the near future from our efforts in this field.

RELATIONSHIPS AMONG SHORELINE CHANGE, COASTAL ORIENTATION, AND BEACH FEATURES

In our quarterly report dated 28 September 1976, we described field work that was conducted in May and June, 1976, on Ocracoke, Hatteras, and Assateague Islands. At 270 sites distributed over nearly 200 kilometers of coastline, measurements of beach features were made, and sand samples were gathered. The objective of this work is to study relationships among physical beach features, coastal orientation, and shoreline change using simple correlations, multi-variate statistics, and eigenvector analysis.

We presented initial results of our data analysis for Assateague Island in the quarterly report dated 16 March 1977. Fourteen variables were studied:

1. Orientation of coastal segments
2. Mean rate of shoreline change
3. Standard deviation of rate of shoreline change
4. Mean plus standard deviation of rate of shoreline change
5. Sub-aerial beach width (dune to berm)
6. Sub-aerial beach slope (dune to berm)
7. Swash width
8. Swash slope
9. Foredune height
10. Foredune slope
11. Median sand-grain size at base of foredune, measured by rapid sediment analyzer (RSA)
12. Sand-grain size sorting at base of foredune, measured by RSA
13. Median sand-grain size at berm, measured by RSA
14. Sand-grain size sorting at berm, measured by RSA.

In addition to relationships between orientation and shoreline change previously discussed, our initial analysis of the

Assateague data showed highest correlations to exist between orientation and swash slope (positive), foredune slope and beach width (negative), foredune height and mean plus standard deviation of rate of shoreline change (negative), and swash width and standard deviation of rate of shoreline change (negative). Since our analysis of the data has not progressed past the stage of simple correlations, our results are inconclusive.

Before we publish our results we will incorporate similar data for Cape Hatteras and Cape Lookout into our findings. The data for Cape Hatteras has been processed by the computer and awaits analysis. In June, 1977, we gathered field data on the above beach features at 36 sites on Cape Lookout National Seashore, including Shackleford Banks, Core Banks, and Portsmouth Island. This data has yet to be processed by the computer.

ANALYSIS OF COASTAL EROSION AND STORM-SURGE HAZARDS

As previously mentioned, the data that we record from historical low-altitude aerial photography is the location at a given point in time of the shoreline and a vegetation line. This in turn defines the active sand zone, or the zone of storm-surge penetration. This is the most hazardous area of the coast in which to place roads, structures, or utilities. The changes in width of this zone over time, coupled with the migration of the shoreline, are useful in projecting hazard zones into the future. This information can aid in the establishment of set back lines for zoning and establishing high risk areas.

With additional funding through the Federal Flood Insurance Program of the Department of Housing and Urban Development, we conducted a demonstration project using our OGAS methods along the southern New Jersey coast. Changes in the position of the shoreline and storm surge penetration line were mapped from Cape May to Little Egg Inlet, a distance of 90 km (Figure 2), with five sets of aerial photography spanning the period from 1930 to 1971. We developed formulas based on probability levels that can be used to determine projected hazard zones of varying risks. Our methods can be applied to any sedimentary coastline in the world. We have written two papers dealing with the subject that are soon to be published in the Coastal Engineering journal: "A New Photogrammetric

Method for Determining Shoreline Erosion," and "Analysis of Coastal and Storm Surge Hazards."

BARRIER ISLAND MIGRATION MODEL

One of the major benefits from the data gathered during the NASA project will be the development of a model for barrier island migration. We are now working on a paper dealing with this subject which will be presented at the Symposium on Threshold Geomorphology in the Fall of 1978. The paper will be published along with the other papers to be presented, in a hard-bound book (title as yet unknown) prior to the convening of the symposium.

The paper will present a brief geological history of barrier islands. It will discuss the various dynamic states into which a barrier island can be classified, such as steady, trend, eddy, or extant state. It then presents a mathematical model of barrier island migration based on momentum transport of barrier island mass, and the velocity of change in the shoreline and the storm-surge penetration line. The model incorporates spatial and temporal variability in rate of change as well as the mean rate of change. Our data for Core Banks and Assateague Island is then applied to the model, and a discussion of the differences in dynamics of the two islands is presented.

SPATIAL RESPONSES TO COASTAL PROCESSES ON BARRIER ISLANDS

Part of the funding from our NASA Contract contributed to a master's thesis effort by Laura Stottlemyer entitled "Variations in Spatial Responses Along the Virginia Barrier Islands." Ms. Stottlemyer studied a chain of eleven islands on the Delmarva Peninsula from Wallops south to Smith Island (Figure 18) for similarities in individual island configuration with respect to the organization of spatial responses of fourteen variables to coastal processes. The variables included three vegetation zones, six soil zones, transect orientation, erosion rate, two measures of island lengths, and one measure of island width. Eigenvector, or principal components analysis was used to determine the principal modes of variation in the response variables of the individual islands and of the island chain.

The results suggest that the variation of spatial responses along the Virginia barrier islands is organized in a systematic manner. For purposes of classification, the islands can be considered as three groups, each exhibiting a distinctive pattern of behavior. The northern group (I), including Wallops, Assawoman and Metomkin Islands, and the southern group (III), including Cobb, Wreck, Ship Shoal, Myrtle and Smith Islands, are characterized by shorter, narrower islands and generally narrower vegetation and soil substrate zones. The orientation of these islands is more easterly, and the erosion rate is less.

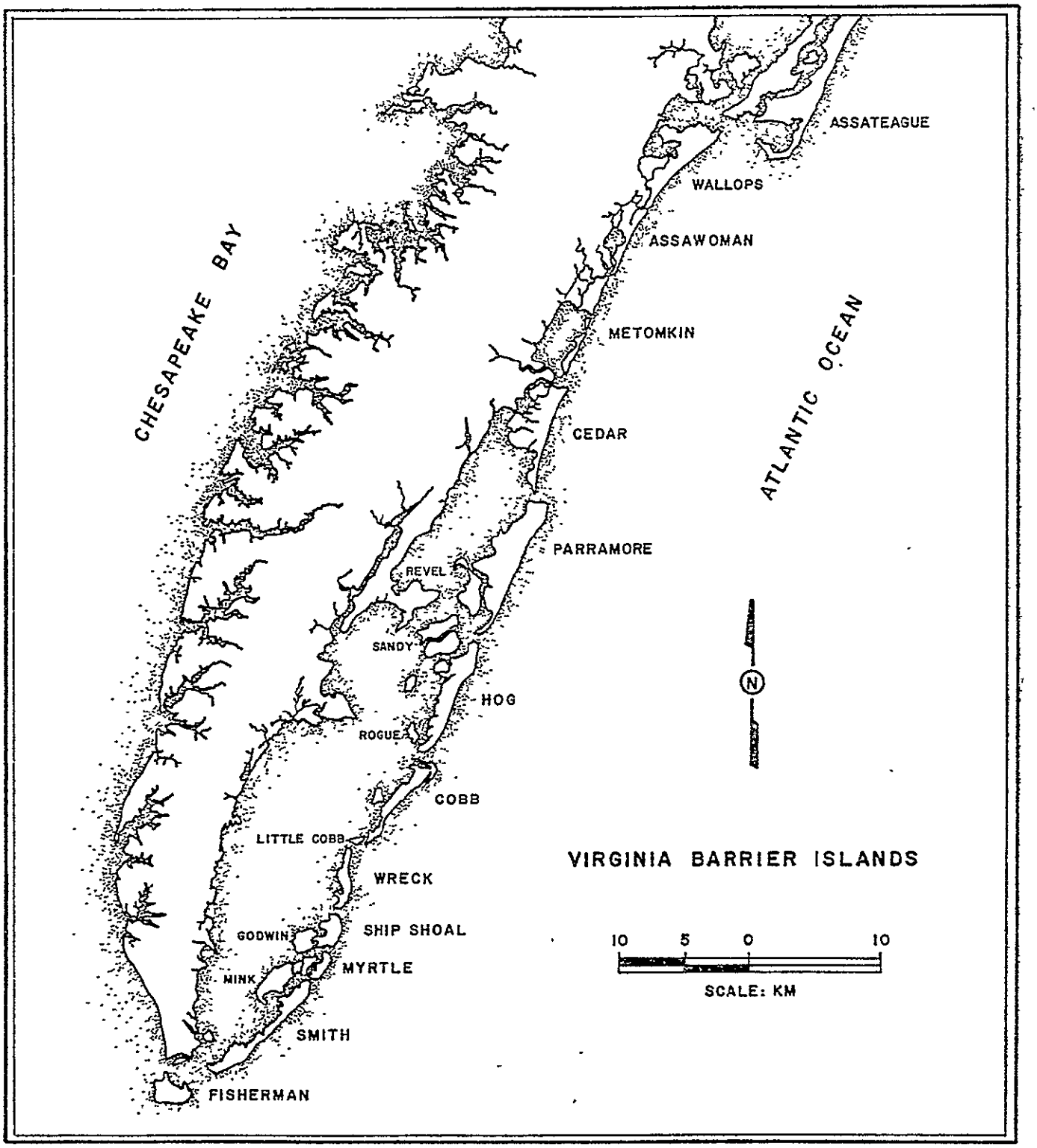

FIGURE 18: Spatial Responses Of Fourteen Landscape Variables To Coastal Processes Have Been Studied For The Virginia Barrier Islands.

The central group (II), including Cedar, Parramore, and Hog Islands, is characterized by much larger islands with wider vegetation and soil substrate zones and a more northerly orientation accompanied by a greater rate of erosion.

Ms. Stottlemyer concludes that the behavior of each island in the chain is dependent upon the behavior of the islands to the north and south. The implication is that any physical alteration to a particular island which alters the process of that island will have a direct impact on the behavior of adjacent islands.

The site for this study, although in the mesoscale range, is relatively small when compared to the mid-Atlantic coast from New Jersey to Cape Lookout. Based on the success of this study, we hope to apply similar methods of examining process/response relationships to the entire mid-Atlantic coast. The historical shoreline erosion data base for this study was not as extensive as that for other areas we have examined and did not allow for the incorporation of variability in change over time.

In order to study temporal as well as spatial variability in coastal responses at a large regional scale, we must first obtain for the Virginia and North Carolina coasts from Chincoteague Inlet to Nags Head, the same degree of historical data on shoreline change and storm-surge penetration as we have obtained elsewhere. We will then have nearly 650 kilometers of continuous coastline on which to test our models and hypotheses.

COMPARISON OF LANDSAT IMAGERY WITH HIGH-ALTITUDE AND LOW-ALTITUDE AERIAL PHOTOGRAPHY FOR MEASURING CHANGES IN COASTAL CONFIGURATION

In our quarterly report dated 28 September 1976, we described our efforts to assess the usefulness of Landsat imagery compared to high-altitude aerial photography (1:130,000) and low-altitude aerial photography (1:24,000), in quantifying the change in land area at the southern end of Assateague Island over a nine-month period from spring, 1975 to winter, 1976. This land mass adjacent to Chincoteague Inlet and known as Fishing Point (Figure 4) has been one of the most rapidly changing areas in our study site. We photographically enlarged 70 mm negative transparencies of band 7 to a scale of 1:80,000 before taking our area measurements. These were compared to measurements made on contact prints of aerial photography at 1:130,000 and 1:24,000 scales.

Our results were somewhat inconclusive because we could not obtain sets of all three types of imagery flown simultaneously, and because of tidal differences between obtention times. However, we were able to measure a change in land area as small as 2.5% from 2.560 km^2 to 2.624 km^2 with Landsat. We feel that the resolution of Landsat must increase before changes in area smaller than this can be measured reliably.

In all our work, we have found Landsat to be most useful in situations where detailed accuracy is not essential, where large land masses (many kilometers in length) are to be studied,

where orthogonal accuracy and lack of image distortion is important, and where measurements are made on a regional rather than site-specific basis. Our only use of Landsat to obtain quantified data was in measuring coastal orientation. We found Landsat to be extremely useful in discussions and study sessions concerning coastal configuration, simply by projecting 70 mm transparencies onto a screen. As previously stated, we are primarily interested in the larger cusp-like features of the coastline such as large sand waves and inlet-to-inlet and cape-to-cape shoreline forms. These are ideally represented on Landsat enlargements of band 7. In many cases, it has been the qualitative studies of Landsat imagery that has led to our quantification of coastal processes.

We have also used high-altitude photography in strip mosaics as a visual aid in our discussions about shoreline form. However, it is more cumbersome to handle and much more costly than Landsat imagery.

We have found there was no substitute for low-altitude aerial photography for making accurate measurements of barrier island response to coastal processes at the site-specific level. The ideal scale range for our purposes was 1:15,000 to 1:20,000.

PUBLICATIONS

In an effort to make public our methods for gathering data from Landsat imagery and aerial photogrpahy, and to present results of our research, we have produced a number of publications.

One of the most effective reports used to present our work is the Atlas of Environmental Dynamics for Assateague Island National Seashore. It is a 44-page document including fold-out maps which makes extensive use of graphics to describe the geology of barrier islands, process/response relationships in the coastal zone, methods of monitoring island dynamics, and how this information might be useful in barrier island management. Data on storm/wave climate and shoreline erosion for Assateague is also presented. The Atlas was funded by NASA/Goddard and the National Park Service and is now being distributed.

Another in-house document entitled, Handbook for Remote Sensing - Mid-Atlantic Coast National Seashores: Assateague Island, Cape Hatteras, and Cape Lookout, reviews the advantages and disadvantages of different types of remote sensing for use in interpreting coastal zone features. We present a case study on how we have used remote sensing, including Landsat, in the coastal zone, and we give specifications on various types of remote sensing equipment. Finally, we include an inventory of most of the aerial photography of the three national seashores

available up to August, 1976. The Handbook was sponsored by NASA/Wallops and the National Park Service and was distributed early in 1977.

Our first published article dealing with the relationship between coastal orientation and shoreline change appeared in "Science" magazine in 1977 and was entitled Shoreline Forms and Shoreline Dynamics. This was an outgrowth of a paper we presented in 1976 at a Symposium on Research Techniques in Coastal Environments. That paper is yet to be published in the R.J. Russell Memorial volume of "Geosciences and Man" series, Louisiana State University, under the title of Shoreline Configuration and Shoreline Dynamics: A Mesoscale Analysis.

Two related articles describing our OGAS method of data collection and the use of our data in a case study of shoreline erosion of the southern New Jersey coast will appear in the "Coastal Engineering" journal in 1978. A New Photogrammetric Method for Determining Shoreline Erosion and Analysis of Coastal Erosion and Storm Surge Hazards also deal with the establishment of set back lines and different risk areas in the coastal zone, based on projections of historical shoreline erosion and overwash penetration.

In 1976, a paper entitled Vegetation Changes Associated with Barrier-Dune Construction on the Outer Banks of North Carolina was published in the Journal of "Environmental Management." Michael Schroeder, a graduate student member of our research

team, used our OGAS method and aerial photography to study vegetation response to sand-dune construction on Ocracoke Island. He has used the same methods to study vegetation changes on Assateague Island following the Ash Wednesday storm of March, 1962. His results were published in a master's thesis in 1977.

Laura Stottlemyer's thesis entitled Variations in Spatial Responses Along the Virginia Barrier Islands is now available. As mentioned earlier in this report, her thesis deals with the analysis of the spatial variation of 14 variables on a chain of eleven barrier islands in Virginia.

Two other graduate students in our program, Robert Clerman and Deborah Elmer, will publish their master's theses in 1978 on the subject of vegetation response to coastal processes on Assateague Island. Both are using aerial photography and field work in their studies.

Finally, other professional papers, such as the one previously mentioned dealing with barrier island migration, will be published in 1978. Additional papers based on the methods developed and data collected during the NASA project will be forthcoming in the following years.

PRESENTATIONS

On numerous occasions, we made presentations to various gatherings to describe how we were using remote sensing to answer questions and help solve problems in the coastal zone, to educate people about the advantages of using remote sensing as a tool, and in some cases to request additional funding for our research. Visual aid material for our talks included slides, large picture boards, aerial photo mosaics, Landsat enlargements, and computer printout.

The first presentation of our work relating coastal orientation to shoreline erosion was given to a group of scientists at the Symposium on Research Techniques in Coastal Environments, held in March, 1976, at Louisiana State University. In the spring of 1976 and 1977 we presented our work to coastal researchers at Assateague Shore and Shelf meetings held in Ocean City, Maryland, and Lewes, Delaware.

In the spring of 1977 we gave a presentation to a group of high school science teachers from Richmond, Virginia, during a field trip to Cape Hatteras. This presentation was very well received. We were impressed with how little the otherwise well-educated general public knows about the uses and availability of aerial photography and Landsat imagery.

A presentation to officials at NASA-Langley in 1977 led to a small grant from the Flight Electronics Division. This resulted in a report entitled Definition of an Aircraft Experiment for Shoreline Sensitivity Mapping, written in October,

1977. Presentations to the Department of Housing and Urban Development in Washington led to additional funding to study the coast of southern New Jersey in an attempt to establish more meaningful criteria on which to base a program of coastal zone property insurance. As a result of these efforts, the National Oceanic and Atmospheric Administration has expressed an interest in applying our methods of measuring shoreline change to the entire coastline of the United States. Other presentations of our use of remote sensing have been given to National Park Service officials in Washington, Denver, and other locations in the United States.

Locally, we have contributed to a Virginia state effort in organizing a remote sensing program through the State Air Pollution Control Board in applying Landsat imagery and aerial photography to the solution of appropriate state-wide problems in land use, agriculture, and coastal zone management. We also participated in the Virginia Coastal Zone Management Workshop.

In October, 1978, we will present a paper on Barrier Island Migration to scientists at a Symposium on Threshold Geomorphology to be held in Binghamton, New York. This paper, based on our work with aerial photography, is discussed in another section of this report.

Each semester, we make at least one presentation to University of Virginia students covering all aspects of our research with remote sensing. These lectures are oriented towards applied

research and hopefully kindle an interest in the students to take future advantage of the many uses of remote sensing.

AERIAL PHOTOGRAPHY AND LANDSAT USER BENEFITTS

The benefits of using aerial photography in coastal zone studies are enormous. Aerial photos are the least expensive and fastest method for gathering large volumes of surface processes data over large areas. These data are extremely important for planning, environmental, and economic purposes. The information that can be obtained from aerial photos is directly related to numerous state and federal programs. This is covered in more detail in the Appendix, which contains excerpts from a report written for NASA-Langley in October, 1977.

A number of public agencies are making use of our data for planning purposes. The Denver Service Center of the National Park Service is studying our shoreline erosion and overwash penetration data for Assateague Island, Cape Hatteras, and Cape Lookout. Using our OGAS methods, we have supplied erosional data for Barden Inlet to the managers of Cape Lookout National Seashore. Accelerated erosion is endangering the lighthouse near the inlet.

The Delaware Department of Natural Resources and Environmental Control is using our data in coastal zone planning efforts on Fenwick Island (Figure 3). They feel the data will be useful in establishing building setback lines.

We found Landsat to be of limited quantitative use in our studies. As previously stated in this report, we were

able to best use Landsat enlargements to measure orientation of relatively straight coastal segments. Landsat was also valuable in providing a good view of large, regional areas in our study site. Band 7, which best shows the land/sea interface, was especially useful for studying shoreline forms in the mesoscale range. However, unless the resolution of Landsat is greatly improved, approaching 10 meters, we feel that aerial photography is a better source of shoreline change and overwash penetration data.

The concept of using a dedicated, high resolution, optical-mechanical scanner to obtain regional synoptic data in a coastal zone monitoring system is a good one. Our ideas on this subject are also included in the Appendix.

RECOMMENDATIONS

Our major recommendation is that the Federal Government should establish a coastal zone monitoring program which would include at least one low-altitude pass over all the sedimentary coastlines of the United States each year.

1. Imagery should include, as a minimum, color infra-red film for interpretation of land cover and land/water interface. Panchromatic or true color film would be valuable for studies of offshore sedimentation patterns and shallow submarine features. Scanning data and imagery would be useful for many purposes (see Appendix).

2. The most useful scale of the photography would be 1:15,000 to 1:24,000. At this scale, accurate analyses can be made with contact prints, and resolution is excellent. High-altitude photography does not have sufficient resolution at contact-print size for most requirements, and most users would not have sufficient in-house capability to enlarge the photo to an acceptable scale and retain high resolution.

3. The best time for the annual flight is late summer, prior to the onset of fall storm activity. At this time the vegetation is in full bloom and can best be seen on color infra-red. The period of the least storm activity throughout the year (for Atlantic and Gulf coasts) has just passed and the beaches are in their most "dormant" or "typical" configuration. The beach slope is steeper than at other times of

the year, and the horizontal displacement of the shoreline (high water mark) over a tidal cycle is at a minimum. This allows for the most accurate mapping of shoreline location. This is also a reason to schedule annual flights for the same month and time of tidal cycle each year, weather permitting. The ideal time of flight is a high tide during a spring tide (highest tide of the month).

4. Due to the relatively low topographic variation in the coastal zone, 60% within-line overlap of frames is not as critical as it would be with other types of landscapes. However, it is still more desirable to have 60% rather than 30% overlap in order to increase mapping accuracy and allow for stereo viewing in those cases where there is enough topography or development to show relief.

5. One federal agency should be assigned the responsibility of obtaining and storing the photography on an annual basis. Such an agency might be the EROS Data Center or National Oceanic and Atmospheric Administration (NOAA). There are many potential users of this photography including private landowners, educational and research institutions, commercial and industrial developers, state planning agencies, and federal agencies such as the National Park Service, NOAA, Department of Housing and Urban Development, and the U.S. Army Corps of Engineers. In the past, gaps in coverage of an area from decade to decade have hindered research efforts. The difficulty

in locating historical photography for a given area is significant due to the multitude of sources, some of which are obscure. The State of New Jersey is one of the few coastal states that systematically flew its coastline on an annual basis.

6. Additional flights over selected areas would be accomplished on an as-needed basis throughout the year, such as following major storms for damage assessment. Such flights should be made routinely rather than waiting for specific requests from authorized users. The need may not be critical at the time of storm impact, but future studies and research may well depend on the data. In this respect, we have found the Chesapeake Bay Ecological Program Office at NASA-Wallops to be very responsive to our needs regarding aerial coverage of our study sites throughout this project.

Regarding the improvement of Landsat imagery, we feel the resolution must be increased before it could be of quantitative use in measuring detailed changes in coastal features. Furthermore, it would be useful to be able to order a continuous 100-mile square image of any segment of an orbit, rather than being constrained to order pre-determined sections. For example, it is very difficult to obtain a complete image of Assateague Island on one frame. It is frustrating to learn that the sharpest, most cloud-free image of a study site is cut in half by the pre-determined sectioning for that particular orbit.

We recommend that efforts to educate the public regarding the availability and use of Landsat and aerial photography be continued and increased. It is especially important to target those individuals, agencies, and institutions who can best use remote sensing in work in which they are already involved, not to mention new work that would evolve as a result of familiarity with the subject. We have found such potential users who have been simply ignorant of the numerous advantages of remote sensing. Where necessary, funding and technical assistance should be made available to educational institutions to include remote sensing courses in their curricula.

Finally, we recommend that research into the process/response relationships on barrier islands be continued toward the end of developing predictive models in ecological responses, island migration, and coastal vulnerability to storm damage. Such information will have significant economic impact on the public and private sector in terms of shoreline and inlet stabilization efforts, dredging activity, zoning, site planning, and coastal zone management and development in general.

DATA USE

All of our Landsat data was in image format rather than digital data. We received over 200 frames of the Atlantic coast from Long Island, New York, to Cape Fear, North Carolina, over the 2-year period from May, 1975, to April, 1977. Most of the frames were 70 mm transparencies of bands 4, 5, 6, and 7. For a short time we also received 9" prints. We photographically enlarged most of the band 7 transparencies to make 11" x 11" prints (~1:700,000). We selected four frames with which to measure coastal orientation at an enlarged scale of 1:80,000:

1) Frame no. 2129-15021-7, 31 May 1975, Assateague Island;

2) Frame no. 5014-14490-7, 3 May 1975, northern Hatteras Island;

3) Frame no. 5014-14493-7, 3 May 1975, southern Hatteras Island, and Ocracoke Island;

4) Frame no. 2147-15033-7, 18 June 1975, Core Banks from Cape Lookout to Portsmouth Island, and Shackleford Banks.

AIRCRAFT DATA

We received high-altitude (1:130,000) color infra-red aerial photography from five different flights over various sections of our study site:

1) Flight No. 75-056B, 8 May 1975, Cape Henlopen, Delaware, to the Virginia/North Carolina border;

2) Flight No. 75-061B, 11 May 1975, Cape Henry, Virginia, to Cape Fear, North Carolina;

3) Flight No. 76-023, 25 February 1976, Chincoteague, Virginia, to Santee River, South Carolina;

4) Flight No. 76-073, 22 May 1976, Cape Henlopen, Delaware, to Fisherman's Island, Virginia;

5) Flight No. 76-142, 30 August 1976, Long Island, New York, to Cape Lookout, North Carolina.

We bought and borrowed historical low-altitude aerial photography from numerous sources, including the Corps of Engineers, Defense Intelligence Agency, National Archives, New Jersey Office of Shore Protection, NOAA, USGS, and military and commercial agencies. Recent low-altitude color infra-red coverage of our study site was provided by the Chesapeake Bay Ecological Program Office at NASA-Wallops.

APPENDIX

Excerpts from Definition of an Aircraft Experiment for Shoreline Sensitivity Mapping written for the Flight Electronics Division of NASA-Langley Research Center in October, 1977 (pp. 1-5, 24-37 with minor deletions).

I. INTRODUCTION

A) Background of Coastal Dynamics

Some of the most dynamic landforms in the United States are the mid-Atlantic and Gulf coast barrier islands. Their geological substrate is composed primarily of sand, and their shorelines are under constant attack by ocean currents, wind and waves, and occasional storm surge. Barrier island configuration is therefore undergoing continuous change. The most apparent manifestation of this change is in shoreline erosion (landward migration), or shoreline accretion (seaward migration).

In some areas, the net change may be imperceptible over a time span of many years. In other areas, the change may be dramatic, such as at the northern end of Assateague Island where the shoreline has been eroding at a rate in excess of 11 meters/year for more than four decades. Some sections of the coast experience severe erosion (tens of meters) overnight due to storm activity, while other sections are only slightly affected by the same storm. Some sections of the coast exhibit a consistent long-term trend of erosion or accretion; whereas, other sections are more temporally erratic, showing rapid erosion during one time period and minimal erosion, or accretion during another period.

Normally, this is of little concern in a natural system. But in a region which man has developed or is planning to

develop, the natural coastal processes present many uncertainties and potential hazards. In the past, coastal losses have run into the millions of dollars each year. There is no reason to believe future losses will not escalate unless building and siting practices and government policies regarding coastal zone development are changed. Therefore, from an economical and human welfare point of view, we should develop a system of coastal zone monitoring that will allow us to measure long-term trends of change, short-term aberrations from these trends, and episodic or instantaneous changes brought about by major storms. The ensuing data would provide the most reliable framework on which to determine coastal zone hazard areas, and would become a necessary input to coastal zone management plans.

B) Relationship to State and Federal Programs

The information derived from the coastal zone monitoring system described in this report would benefit numerous programs created by federal legislation. Foremost of these is the Coastal Zone Management Act of 1972 (CZMA), with Amendments of 1976.* The Act provides participating states with funds to develop comprehensive programs to protect and manage their coastal areas. An important facet of each management

*An excellent review of the provisions of the Coastal Zone Management Act is contained in the Natural Resources Defense Council publication entitled "Who's Minding the Shore" (August, 1976).

E-2

program is to collect and update information about the state's coast. This information should include data on shoreline change and on the most dynamic and vulnerable area of the coast - the zone of storm-surge, or overwash penetration. More specifically, under Section 305(b) (3), the states are instructed to include "an inventory and designation of areas of particular concern within the coastal zone" in their management program. Examples include areas where development would disrupt important natural processes, and areas of significant hazard if developed, due to storms, floods, erosion, overwash, etc. The CZMA Amendments of 26 July 1976 added a new planning element to the states' 305 program for shoreline erosion. States now have additional time for planning, up to September 30, 1979. The new Section 310 allows for financial grants to states to carry out research, studies, and training required to support their programs.

Other acts creating programs that would benefit from a coastal zone monitoring system include:

1. The National Environmental Policy Act of 1969 (NEPA), which requires that an environmental impact statement be prepared in connection with any proposal for major federal action having a significant impact on the environment. Dredging and construction of groins, jetties, and foredunes are activities that have altered and will continue

to impact the coastal environment in ways which can be discovered and measured through the monitoring system we propose.

2. The Flood Disaster Protection Act of 1973, which requires communities to restrict development in areas which might be flooded once every hundred years - such as flood plains and along the coast - in order for individuals within the community to be eligible for mortgage loans from private banks, as well as for federal construction funds and flood insurance. Data from a coastal zone monitoring system can be used to identify areas subject to overwash and flooding, and can be used to establish zones of varying risks based on probabilities of the future occurrence and extent of overwash events and shoreline erosion. The information would also form a basis for establishing insurance premiums.

3. The Interstate Land Sales Act of 1969, which requires a developer of 50 or more lots to make a full disclosure of the subdivision's significant aspects. The wise land buyer would want to carefully examine the data on coastal erosion and overwash on his prospective property that could be supplied by a coastal monitoring system. The seller could reasonably adjust his prices based on this information. Numerous parcels of undeveloped private landholdings on the northern end of Assateague Island are now completely submerged due to the landward migration of the island. If this erosion could have been foreseen and made public, the sales transactions would probably not have occurred.

4. The National Historic Preservation Act of 1966, which provides for federal consideration of historic values prior to the alteration or demolition of selected buildings or districts, and for preservation grants. The erosion at Cape Hatteras, North Carolina, which is endangering the Cape Hatteras lighthouse, has been common knowledge for many years. As a result, steps have been taken to retard the erosion in an effort to save the lighthouse. More recently, we have become aware of the increasing rate of shoreline erosion on the bay side of Core Banks, North Carolina, at Barden's Inlet. As a result of studies based on historical aerial photography, we have concluded that the Cape Lookout lighthouse will be awash in Barden's Inlet before the year 2000. Another example of the importance of the ability to identify the impending destruction of historical structures through shoreline monitoring is the fate of the Coast Guard station at Drum Inlet, North Carolina. The station was destroyed within the past decade as a result of shoreline erosion.

5. The Water Resources Development Act of 1974, which authorizes the Army Corps of Engineers to assist states in comprehensive planning for the coastal zone. The Corps has tremendous amounts of historical data on the coastal environment that would be useful for planning purposes. Current, synoptic data from a coastal monitoring system would be an ideal supplement.

III. IMPROVEMENTS IN CURRENT WORK

A) The Need for a Dedicated Remote Sensor

The major improvement in our state-of-the-art methods for measuring changes in the shoreline location, overwash penetration, and coastal orientation would be to automate the system. The primary areas of automation would be in data acquisition, data processing and display, and to some extent, data analysis.

A dedicated, aircraft-mounted, optical mechanical scanner would replace the photographic camera as a data source. Such a scanner is being developed at the Flight Electronics Division of NASA-Langley Research Center. The scanner as shown in Figure 19 is displayed on a .9m x 1.5m (3'x5') platform with a Hasselblad camera. The scanner is initially designed to provide 6-meter (20-foot) resolution when flown at an altitude of 3,050 meters (10,000 feet). This resolution is an improvement over our current accuracy with the manual mapping method and is expected to be improved. The total field of view is 60°, or 3.2 kilometers (2 miles) at 3,050 meters (10,000 feet). There are eight spectral channels from the visible to the infrared plus a thermal channel. The scanner can be flown in any of the aircraft now being used as platforms for 23cm x 23cm (9"x9") format cameras. Specifications are summarized in Figure 20.

The expected advantages with using a scanner to monitor coastal change rather than aerial photography are three-fold:

ORIGINAL PAGE IS
OF POOR QUALITY

AIRCRAFT-MOUNTABLE OPTICAL MECHANICAL SCANNER
DEVELOPED BY FLIGHT ELECTRONICS DIVISION
NASA - LANGLEY RESEARCH CENTER
SHOWN WITH HASSELBLAD CAMERA ON 3' x 5' PLATFORM

Figure 19.

1) Faster turn-around-time for data products; 2) Reduction in man-hours of labor in image interpretation, and in data transfer and display; 3) Greater objectivity and accuracy in defining the shoreline and overwash penetration line.

The required time from flight to imagery output, and to digital and graphical data and statistics is not expected to be any longer than the time has been in the past from flight to photographic print. After the software is written, most of the process will be automated. By our manual methods, we estimate that there is nearly one man hour of labor required per kilometer of coast to arrive at the stage where the data for one flight is on punched cards ready for submission to the computer. In any case, rapid turnaround time from flight to product is not a critical issue with the scanners. Two weeks should be adequate speed for foreseeable applications.

Resolution of the scanner should be as high as possible; for example, 1 meter (3 feet) or greater - especially if monitoring is to take place on an annual basis or more frequently. However, the current resolution of 6 meters (20 feet) should be acceptable for assessing the usefulness of the scanner in identifying the shoreline and overwash penetration line.

Perhaps the biggest unknown is the capability of the scanner and data processor to accurately locate the correct

continuous shoreline, and the correct continuous overwash penetration line. Ground truth will probably be required at selected locations along the coast during each flight to establish the proper spectral response signatures for critical landcover, such as wet beach sand, dry beach sand, unvegetated sand flats, lightly vegetated sand flats, thickly vegetated sand flats, and solid shrub vegetation.

The scanner output must be properly registered with respect to some co-ordinate system. The standard Mercator grid may be appropriate. As an alternative, a grid could be established with one axis parallel to the overall trend of the shoreline for the section of coast under study. Registration marks will be required on all images and graphical output, and location stations will be required on all digital output. Whatever design is chosen will establish the need for ground references.

Finally, each flight should take place under uniform tidal, wave height, and storm surge conditions. This will insure that detectable changes in the shoreline represent erosion or accretion rather than changes in ocean surface conditions.

B) Types of Data Products Desired

The data from the scanner would be automatically processed by appropriate computer programs and would be displayed

in both digital and graphical format, as well as grey tone images. The precise format and content of the output will depend primarily on the capabilities of the scanner and available computer hardware. However, as a minimum, the output should contain the information now available through our manual methods. Registration marks, such as Mercator grid coordinates, should appear on all imagery and computer graphs, and location stations along the coast should accompany the digital output. Specifically, the following output should be available on command:

1. Grey tone prints and/or transparencies of scanner images in all channels, and color enhanced images in selected combinations of channels, not unlike Landsat products. If displayed on 23 cm x 23 cm (9"x9") frames, the images would be at the approximate scale of 1:15,000, which is a useful scale for general interpretive work.

2. Digital data and statistics describing the location of the shoreline (SL) and overwash penetration line or vegetation line (VL) with respect to a fixed base line, and the overwash penetration distance (OP=VL-SL) for each flight; the change and rate of change in SL, VL, and OP between any pair of flights; the mean and standard deviation over time of rate of change in SL, VL, and OP, and the mean and standard deviation over time of the OP distance. Units would be in meters and meters per month or meters per

year, depending upon the frequency of flights. The base line could be a single straight line, parallel to the overall trend of the section of coast under study, and lying sufficiently offshore to allow for expected future shoreline accretion. Measurements would be made perpendicular to the base line. The frequency of data points along the coast would depend on computer capacity, logistical ease in storing the data and in handling the output, and user needs. As a minimum, data should be available for every 10 meters along the coast. The user should be able to obtain data/statistical printouts for frequency intervals ranging from 10 meters to 1,000 meters along the coast.

3. Continuous line output for any historical or recent flight showing the location of the SL and VL with respect to registration marks, at scales that could vary from 1:130,000 (for comparison with high-altitude photos) to 1:5,000 (for detailed analysis). These lines could be enhanced on the original images for ease in identification. This line output would also include a graph of the OP distance, drawn on a straight-line axis which "parallels" the shoreline. It would be especially useful to obtain line output for SL, VL, and OP for more than one flight on the same printout for visual comparison purposes. This would require coding of the lines for identification.

4. Continuous line graphs of the change and/or rates of change in SL, VL, and OP for any selected time period.

5. Continuous line graphs of the mean and one standard deviation over time of rate of change in VL, SL, and OP, and the mean and standard deviation over time of the OP distance.

6. Frequency distribution statistics and statistics on change and rate of change in SL, VL, and OP for any desired section of the coast.

7. Continuous line output showing coastal orientation at designated scales ranging from 1:130,000 to 1:5,000, and for successive iterations of coastal segment definition as determined by increasing threshold values. Figure 21 shows the coastal orientation of Assateague Island for an iteration defining 11 segments of the coast. Digital data would be printed next to each segment, indicating the numerical value of that segment's orientation. The capability should exist to show orientations from more than one flight on the same printout for purposes of comparison.

If a coastal monitoring program such as we are describing is developed, future uses for the data which we are not now considering are certain to evolve. Different output formats will be required. Additional statistics will be requested as routine output. The concept may be expanded to measure more lines than the ocean shoreline or overwash penetration line. For example, it may be desirable to monitor changes in the

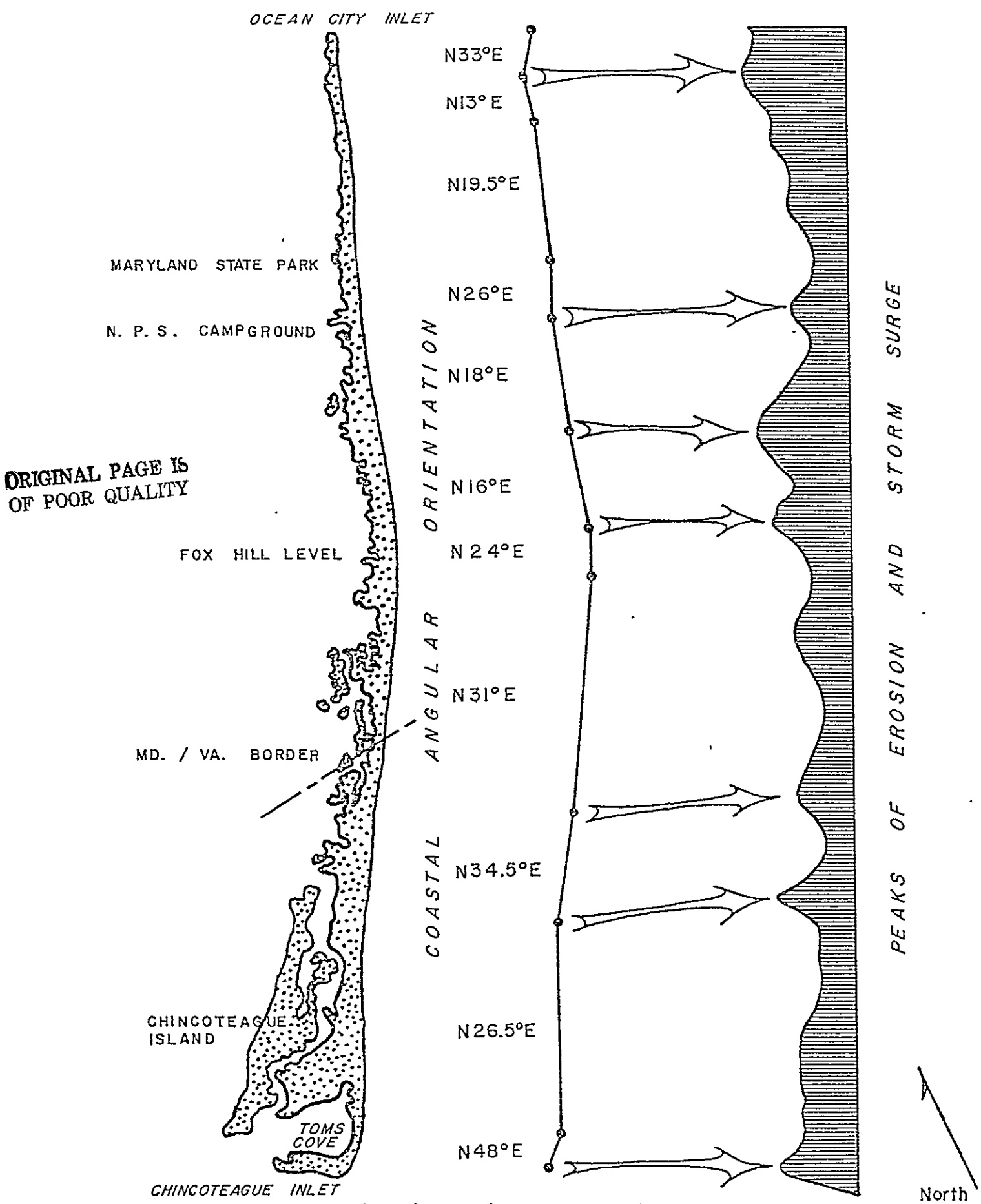

FIGURE 21: Coastal Orientation For Assateague Island With 11 Coastal Segments Defined.

Scale=1:250,000

bay shoreline, or changes in vegetation zones such as high marsh, low marsh, and shrub communities (Figure 22). The computer software should be sufficiently flexible to allow the output to be modified and expanded to become increasingly responsive to the user's needs as analysis becomes more sophisticated.

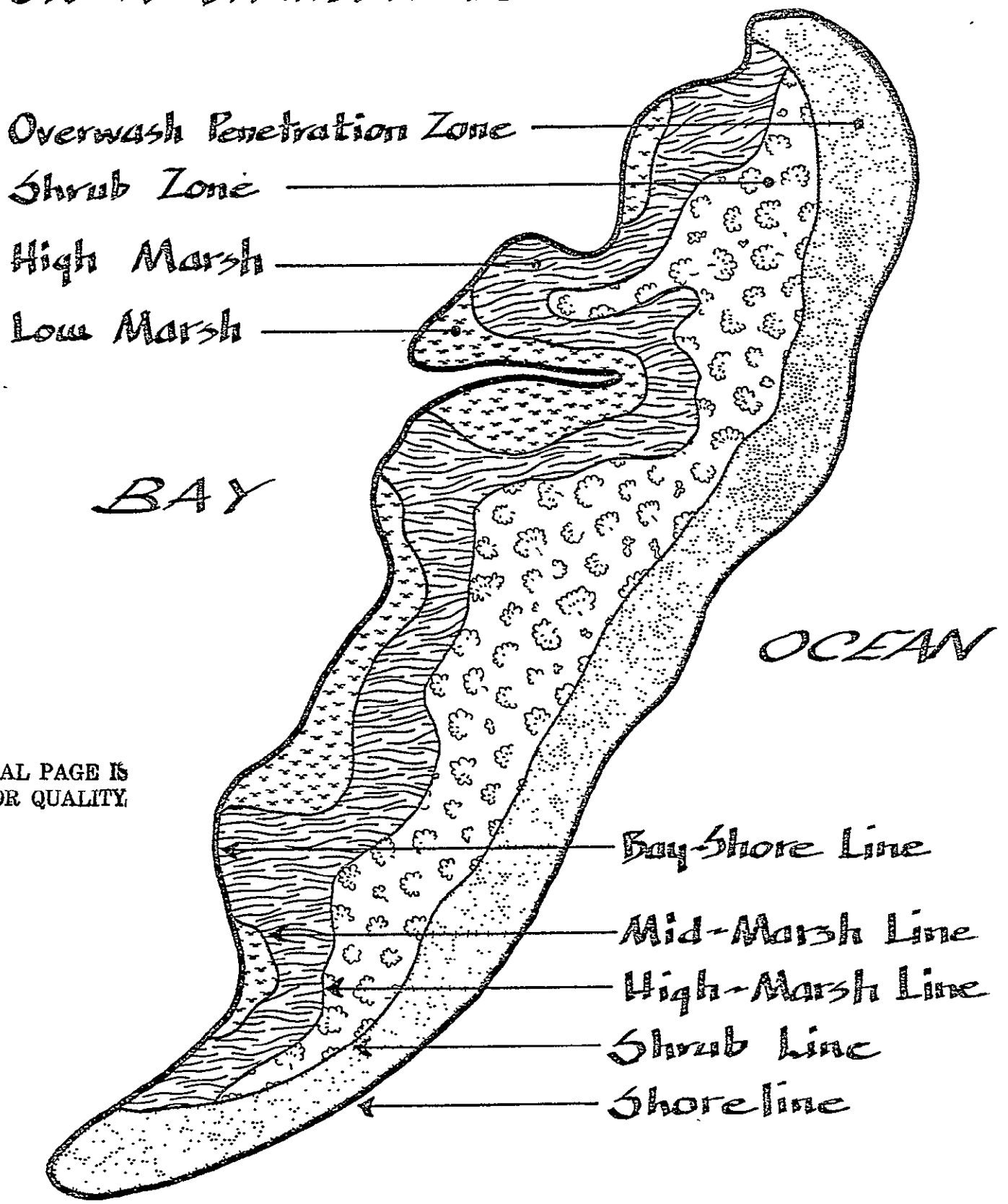

FIGURE 22: The Optical Mechanical Scanner Could Be Used To Detect Changes In Vegetation Zones In A Coastal Monitoring Program.

IV. EXPERIMENT DEFINITION FOR PROOF OF TECHNIQUE

A) Test Site

Coastlines over which test flights will be made should coincide with those which we have already studied (see Summary of Research). If the entire coast from Little Egg Inlet, New Jersey, to Cape Lookout, North Carolina, cannot be covered for reasons such as cost, then sections of the coast which we have found to be most dynamic, and which are closest to the aircraft base should be chosen. Assateague Island best fits these criteria. Cape Hatteras would be the second choice due to the dynamic nature of the shore zone.

B) Flight Considerations

The aircraft to be used will be chosen by NASA-Langley, and will fly along the coastline at an altitude of 3,050 meters (10,000 feet). The position of the aircraft should be centered directly over the active sand zone, or overwash penetration zone from the shoreline to the vegetation line. In addition to the operation of the scanner, the Hasselblad camera should take color infra-red transparencies at a frequency to provide 60% overlap within the flight line. Ocean surface conditions should be as quiet as possible. The tidal cycle should be at high tide, since this would indicate the landward most extent of the swash. Personnel should be stationed at selected points along the coast to take readings

of the spectral response characteristics of the landscape at the time the aircraft passes overhead. Other important considerations are cloud cover and sun angle.

C) Frequency of Flights

The first flight should take place as soon as the scanner and data processing equipment are operational. The second flight should occur during the first quiet period following a major storm. That which constitutes a major storm will be determined by University of Virginia personnel.

The data from both flights will be assessed to determine the usefulness of the scanner. If the scanner proves to be successful, we recommend that a minimum of two flights be scheduled annually: one in August or September, before the end of the growing season and prior to the onset of the winter storm season; and one in March or April, following the winter storm season and prior to the growing season.

D) Data Considerations

Ideally, data from each flight would include output as described under "Improvements in Current Work." However, initially it is more realistic to expect only grey-tone images of the spectral data. These would be useful to compare with the Hasselblad photographs and with aerial photos at the University of Virginia. Assessments could be made of the resolution of the images and the ability to manually identify lines and

zones of interest. Work would proceed on developing the automated process of providing digital and graphical output in the desired formats.

E) Predictions of Shoreline Damage

We already have sufficient data from historical aerial photography and Landsat to make predictions regarding shoreline damage. We cannot predict the extent of damage at any given point other than by stating the probability that an overwash event will penetrate the shorezone a given distance from a storm of a given magnitude. However, we should be able to predict the relative vulnerability along the coast of different sections of the coastline to any major storm. We are now basing our predictions primarily on past overwash occurrences and shoreline change rather than on crescentic forms. We have found strong relationships to exist between shoreline erosion and coastal configuration for some, but not all of the mid-Atlantic coastlines we have studied. Part of our ongoing research at the University is to probe deeper into these relationships.

One of the major reasons for our interest in a coastal monitoring program is to identify changes in established trends of coastal zone dynamics. This will in turn effect predictions of shoreline damage.

BIBLIOGRAPHY

Bowen, A.J. and Inman, D.L., 1971. "Edgewaves and crescentic bars." J. of Geophysical Research, V. 76, 36, p. 8667-71.

Bruun, P., 1954. "Migrating sand waves or sand humps, with special reference to investigations carried out on Danish north seacoast." Proceedings 5th Conference on Coastal Engineering, p. 460-68.

Dolan, R., Hayden, B., and Heywood, J., 1978. "A new photogrammetric method for determining shoreline erosion." Coastal Engineering, accepted for publication.

_____1978. "Analysis of coastal erosion and storm-surge hazards." Coastal Engineering, accepted for publication.

Dolan, R., Hayden, B., Heywood, J., and Alfonsi, P., 1977. Handbook for remote sensing: mid-Atlantic coast national seashores: Assateague Island, Cape Hatteras, Cape Lookout. Natural Resources Report No. 10, National Park Service.

Dolan, R., Hayden, B., Heywood, J., and Vincent, C., 1977. "Shoreline forms and shoreline dynamics." Science, V. 197, 4298, p. 49-51.

Dolan, R., Vincent, C., and Hayden, B., 1974. "Crescentic coastal landforms." Z. für Geomorphologie, V. 18, 1, p. 1-12.

Dolan, R., 1972. "Barrier dune system along the Outer Banks of North Carolina: a reappraisal. Science, V. 176, p. 286-88.

_____, 1971. "Coastal landforms; crescentic and rhythmic." Bull. Geol. Society of America, V. 82, p. 177-80.

Dolan, R. and Ferm, J., 1968. "Crescentic landforms along the Atlantic coast of the United States." Science, V. 159, p. 627-729.

Guza, R.T. and Inman, D.L., 1975. "Edgewaves and beach cusps." J. of Geophysical Research, V. 80, 21, p. 2997-3012.

Hom-ma, M. and Sonu, C., 1962. "Rhythmic pattern of longshore bars related to sediment characteristics." Proceedings 8th Conference on Coastal Engineering, p. 248-78.

Komar, P.D., 1971. "Nearshore cell circulation and the formation of giant cusps." Bull. Geol. Society of America, V. 82, p. 2643-2650.

Langfelder, J., Stafford, D., and Amein, M., 1968. "A reconnaissance of coastal erosion in North Carolina." Project ERD-238. Department of Civil Eng., North Carolina State University at Raleigh, 126 p.

_____, 1970. "Coastal erosion in North Carolina." J. of Waterways, Harbors Coastal Eng. Div., Am. Soc. Civ. Engrs. WW2, p. 531-45.

McBeth, F.H., 1956. "A method of shoreline delineation." Photogram. Engr. 22(2), p. 400-05.

McCurdy, P.G., 1947. Manual of coastal delineation from aerial photographs. U.S. Navy Hydro. Off. Pub. No. 592. U.S. Navy Hydrographic Office, Washington, D.C.

_____, 1950. "Coastal delineation from aerial photographs." Photogram. Engr. 16(4), p. 550-555.

Russell, R.J., 1958. "Long, straight beaches." Ecologae Geologicae Helvetiae, V. 51, p. 592-598.

Schroeder, P.M., 1977. "Vegetation changes on Assateague Island following the Ash Wednesday storm of March, 1962." Master's thesis, University of Virginia, Charlottesville, Virginia.

Schroeder, P.M., Dolan, R., and Hayden, B., 1976. "Vegetation changes associated with barrier-dune construction on the Outer Banks of North Carolina." Environmental Management, V. 1, 2, p. 105-114.

Sonu, C.J., 1972. "Field observation of nearshore circulation and meandering currents." J. of Geophysical Research, V. 77, 18, p. 3232-47.

Stafford, D.B., 1968. "Development and evaluation of a procedure for using aerial photographs to conduct a survey of coastal erosion." Report prepared for the State of North Carolina, Dept. of Civil Engineering, North Carolina State University, Raleigh, North Carolina. (Also unpublished PhD Thesis).

Stafford, D.B. and Langfelder, J., 1971. "Air photo survey of coastal erosion." Photogram. Engr. V. 37, p. 565-75.

Stottlemyer, L.L., 1977. "Variations in spatial responses along the Virginia barrier islands." Master's Thesis, University of Virginia, Charlottesville, Virginia.

Vincent, C.L. 1973. "Quantification of shoreline meandering." Technical Report No. 7, Office of Naval Research, Washington, D.C.

for terrain cells are described more fully in subsequent paragraphs.

Hilbert Transformer

When processing 13.3 and 1.6 GHz scatterometer data, the signals must be sign-sensed and then frequency components corresponding to the desired angle of incidence must be extracted. To perform the sign-sensing operation, a Hilbert transformer can be used. Ideally, a Hilbert transformer is an all-pass filter with a ± 90° phase shift for positive frequencies and a ± 90° phase shift for negative frequencies. Mathematically, this can be written as

$$H(\omega) = \begin{cases} \pm j & \text{for } \omega > \\ \mp j & \text{for } \omega < \end{cases}$$

where

$$j = \sqrt{-1}\,.$$

By passing the quadrature channel through a Hilbert transformer which has a + 90° phase shift for positive frequencies and a - 90° phase shift for negative frequencies, the resulting signal is

$$\text{Quadrature Channel: } \frac{F(\omega) - A(\omega) + F(-\omega) - A(-\omega)}{2}$$

Adding this signal to the cosine channel, the result becomes

$$F(\omega) + F(-\omega)$$

thus, obtaining only fore data. By subtracting the two channels, it is possible to obtain only aft data.

After the data have been sign-sensed, the output is passed through a digital bandpass filter with a center frequency corresponding to some given angle of incidence. Then a digital root-mean-square is taken and the output is displayed or stored. A block diagram of the processor is shown in Figure 7.

The FIR Hilbert transform was designed using a computer program utilizing the Remez Exchange Algorithm [8] A typical impulse response for a Hilbert transformer is shown in Figure 8. Since a digital filter is a causal system, the impulse response must be shifted by N/2 points so as to start at zero. To preserve the ± 90° phase shift caused by the Hilbert transform, the channel not being Hilbert transformed must also be delayed by N/2 points. Designing a Hilbert transformer of length 39, the following specifications can be obtained (all frequencies normalized to the sampling frequency).

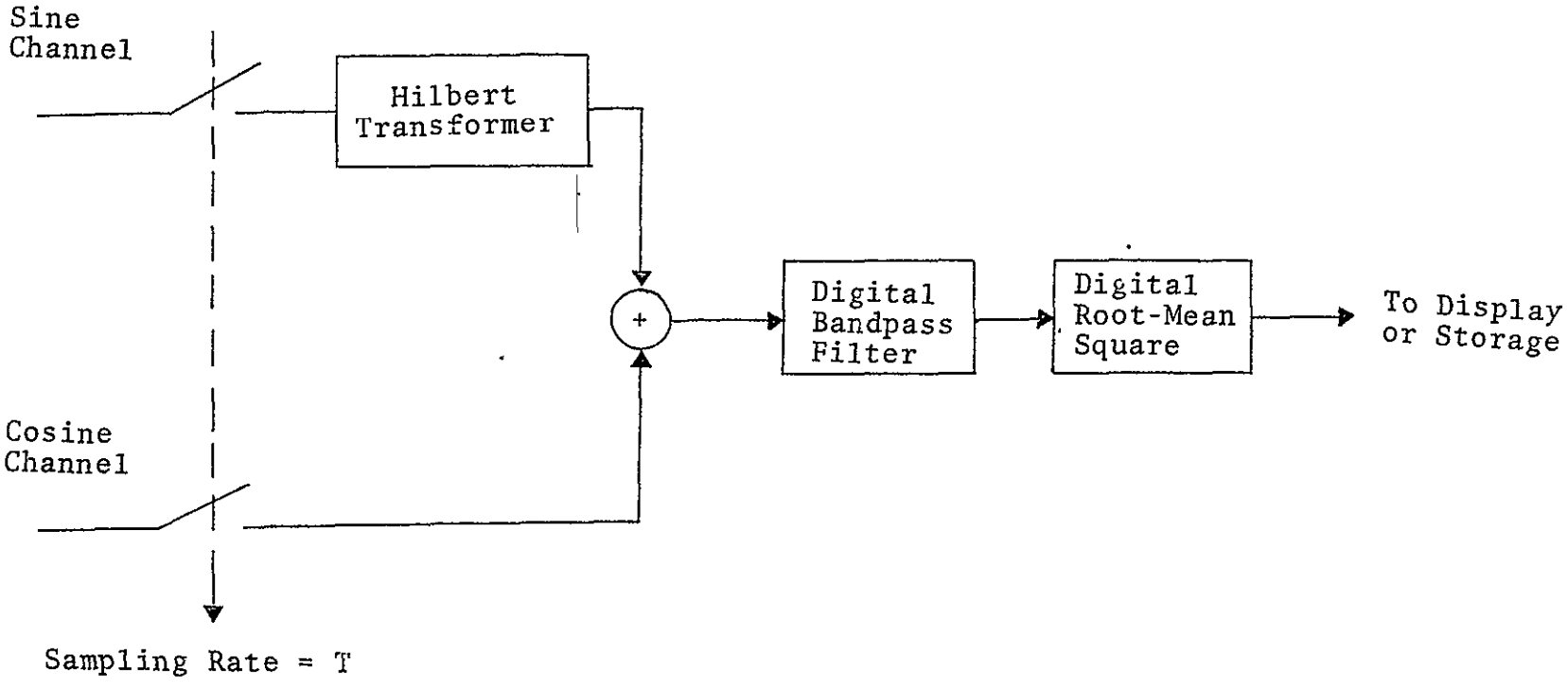

Figure 7. Block Diagram of a Digital Processor.

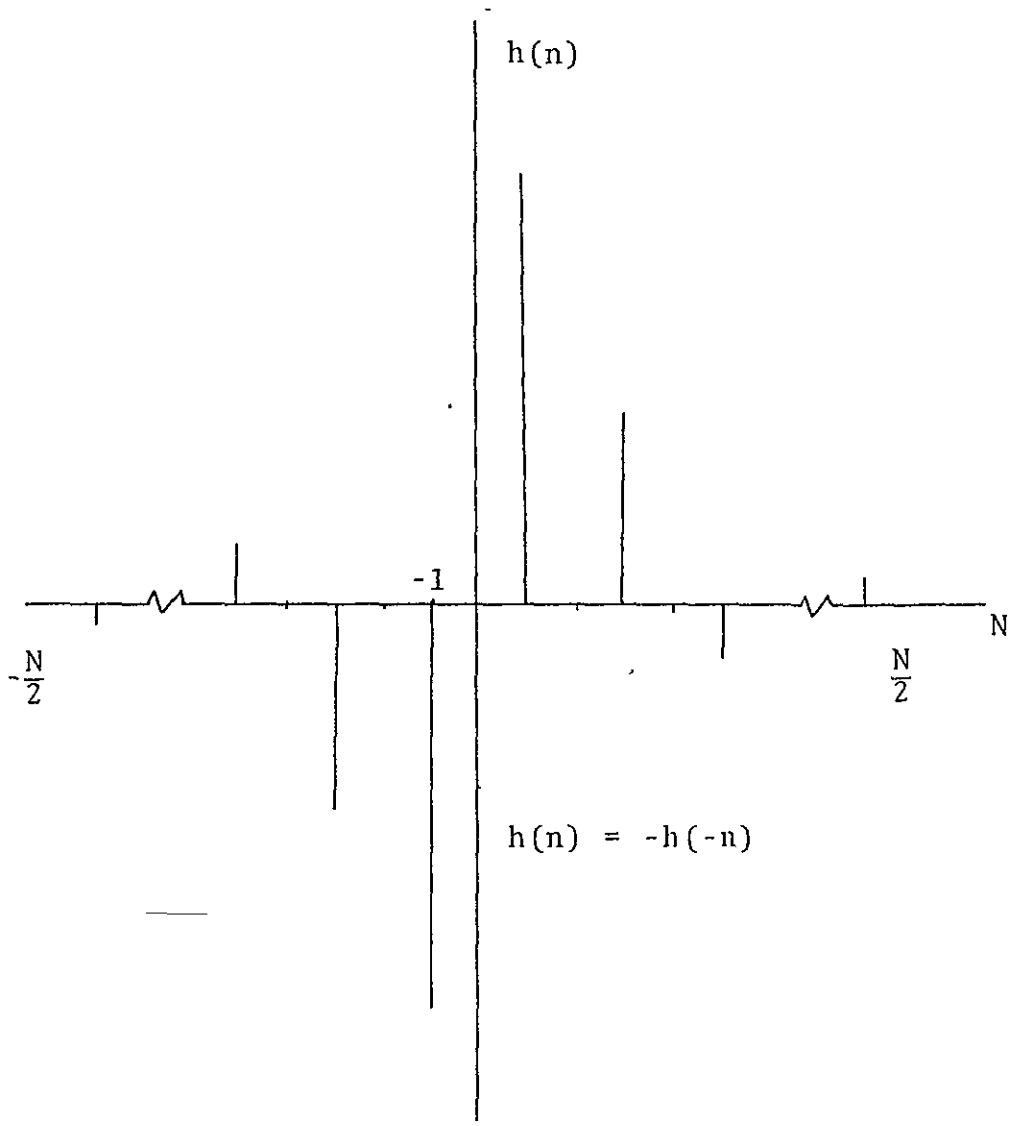

Figure 8. Typical Impulse Response of an FIR Hilbert Transformer.

Upper cutoff frequency = 0.45

Lower cutoff frequency = 0.05

Percent ripple in passband = 0.14%

To implement the filter, a cascade realization was used. The 38^{th} order (length 39) FIR filter is made up of four 8^{th} order filters, one 4^{th} order filter and one 2^{nd} order filter (see Figure 9). The coefficients used for the cascade implementation are:

	A(1)	A(2)
1^{st} 8^{th} order system	1.693	5.263
2^{nd} 8^{th} order system	-1.406	4.792
3^{rd} 8^{th} order system	4.296	7.634
4^{th} 8^{th} order system	-3.684	6.063
4^{th} order system	2.650	1.000
2^{nd} order system	0.000	-1.000
Gain constant	0.00128	

By passing the quadrature channel through this Hilbert transformer and delaying the inphase channel will cause the spectrum of the quadrature channel signal to be phase shifted by + 90° for positive frequencies and - 90° for negative frequencies with respect to the delayed inphase channel. Fore data can be obtained by adding the resultant signals of both channels. Aft data can be obtained by

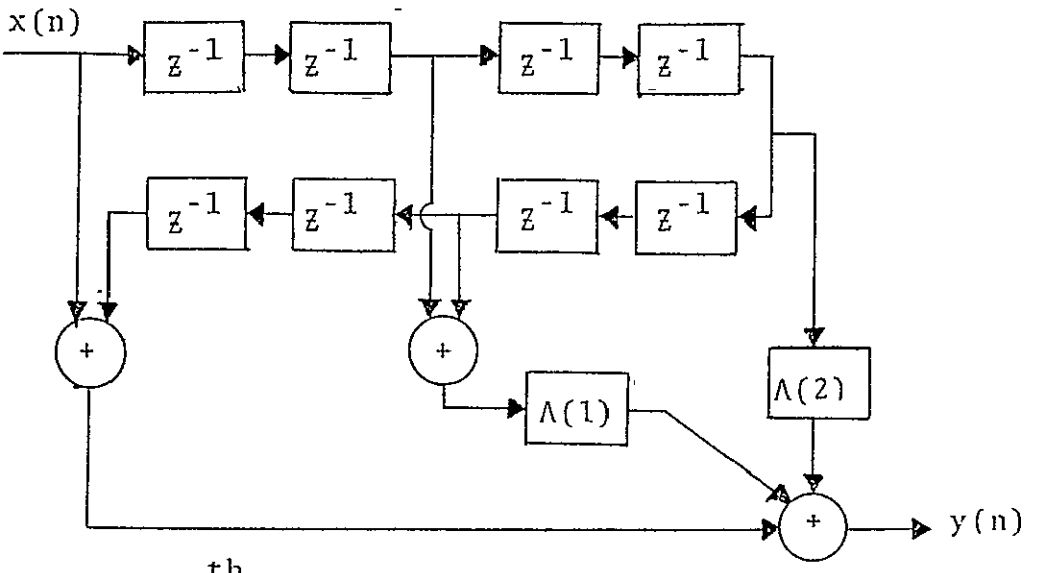

8^{th} Order Realization

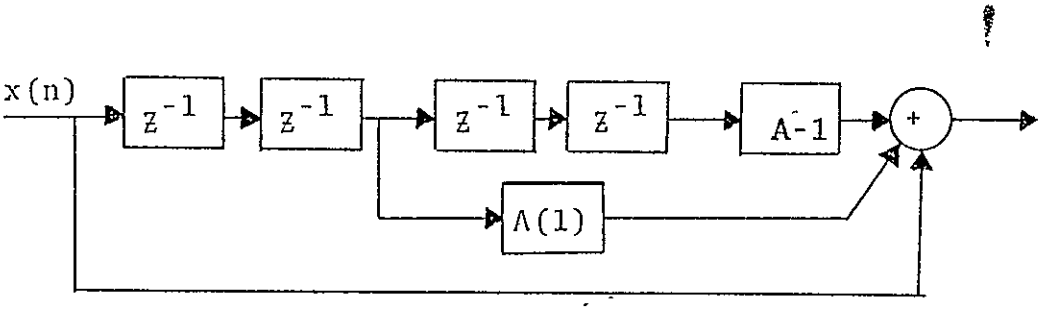

4^{th} Order Realization

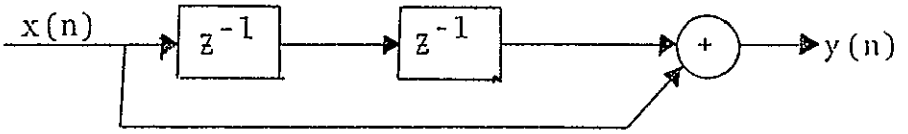

2^{nd} Order Realization

Figure 9. Realizations of 8^{th}, 4^{th}, and 2^{nd} Order Filters used to Implement FIR Hilbert Transformer.

subtracting the two resultant signals or by passing the inphase channel through the Hilbert transformer and delaying the quadrature channel, then adding the resultant signals.

Filter Design Parameters

The center frequency of the bandpass filter is determined by the Doppler shift of the radar signal and is a function of the velocity of the aircraft and the look angle. The Doppler frequency, corrected for drift angle, is described by

$$f_o = \frac{2V\sin\Theta\cos\phi}{\lambda}$$

The along track resolution of the cell viewed by the radar is a function of the velocity of the aircraft and of the bandwidth of the Doppler filter. In Figure 10 is shown the makeup of the ground cell.

The area viewed by the radar as modified by the Doppler filter is defined to be ΔX. The distance traveled by the aircraft in T seconds is ΔL so that the total length of the cell, L, is

$$L = \Delta X + \Delta L.$$

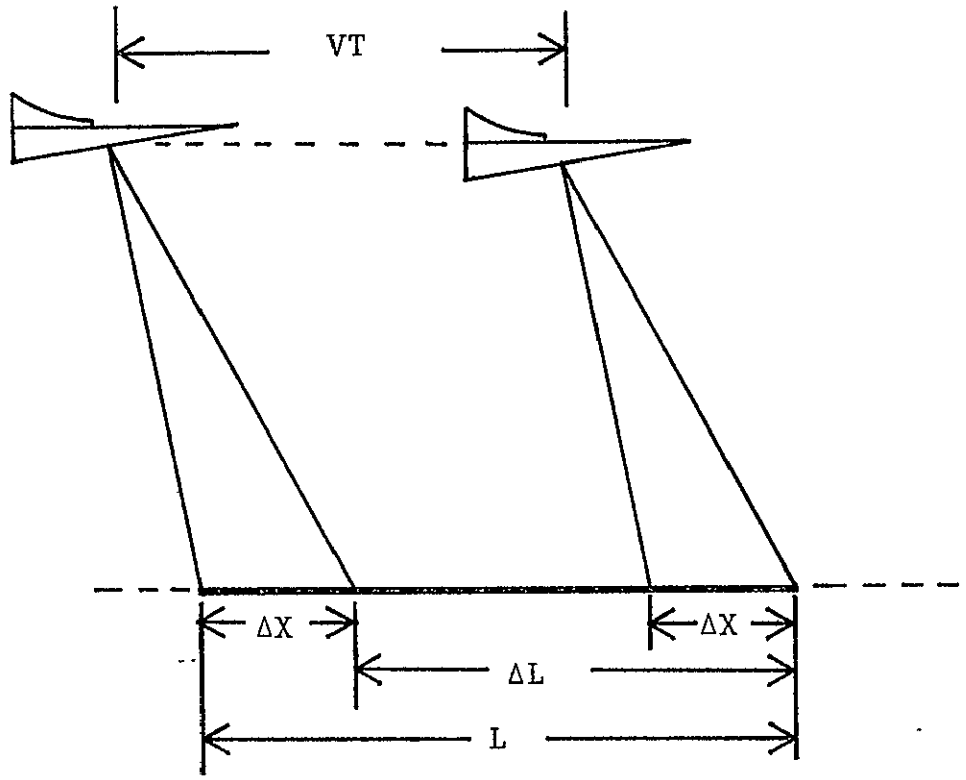

Figure 10. Illustration of components of grand cell length.
(L = ΔX + VT)

It can be shown that the change in Doppler frequency per change in along track distance is

$$\frac{\Delta f}{\Delta x} = \frac{2V\cos^3\Theta}{\lambda h}$$

The bandwidth of the filter can be determined as

$$\Delta f = \frac{2V\cos^3\Theta}{\lambda h} \Delta X,$$

which is

$$\Delta f = \frac{2V\cos^3\Theta}{\lambda h} (L-\Delta L), \text{ and}$$

$$\Delta f = \frac{2V\cos^3\Theta}{\lambda h} (L-VT).$$

The time for a single cell T is determined by the number of points, N, which are sampled in the analog-to-digital conversion process required for processing the analog radar data and by the rate at which the points are converted, f_s. Thus,

$$\Delta f = \frac{2V\cos^3\Theta}{\lambda h} (L-\frac{VN}{f_s}).$$

The center frequency for the filter design is then f_d, and the upper and lower cutoff frequencies are

$$f_d = f_d - \frac{\Delta f}{2} \quad \text{and,}$$

$$f_u = f_d + \frac{\Delta f}{2} \ .$$

Filter Design and Implementation

To obtain radar return as a function of angle, the power return must be measured for each angle of interest. Since the energy is encoded by the Doppler shift from the radar transmitter frequency, a bandpass filter centered at the Doppler frequency corresponding to the angle of interest will select the component of the return corresponding to a specific angle. In the software package, the filter function is accomplished by a digital filter implementation. The particular filter implemented is determined from a Butterworth filter design which is transformed into a discrete implementation.

The Butterworth filter provides a bandpass characteristic which is maximally flat. The M poles of the continuous frequency filter are determined by the relationship

$$s_k = e^{j\pi(1/2 + (2k-1)/2M)} \qquad k = 1, 2, 3, \ldots, M$$

and the transfer function is

$$H(s) = \frac{k_o}{\prod_{k=1}^{N} (s - s_k)}$$

This design provides a low-pass characteristic with a cutoff frequency of $\Omega = 1$. The transformation of this design to one which has a bandpass characteristic can be accomplished by replacing s with

$$s = \frac{s^2 + \Omega_1 \Omega_u}{s(\Omega_u - \Omega_1)}$$

where Ω_1, Ω_u are the cutoff frequencies of the filter. Applying this transformation for a single pole $\frac{1}{s - s_k}$, yields a general expression for the calculation of multiple poles.

$$\frac{1}{s - s_k} = \frac{1}{\frac{s^2 + \Omega_1 \Omega_u}{s(\Omega_u - \Omega_1)} + s_k}$$

Substituting $\omega_1 = \Omega_u - \Omega_1$ and $\omega_2^2 = \Omega_1 \Omega_u$ yields

$$\frac{1}{s - s_k} = \frac{1}{\frac{s + \omega_2}{s\omega_1} - s_k} = \frac{s\omega_1}{s^2 - s s_k \omega_1 + \omega_2^2}$$

Solving for the new poles s_1 and s_2, by application of the quadratic equation,

$$s_{1,2} = \frac{\omega_1 s_k \pm \sqrt{(\omega_1 s_k)^2 - 4\omega_2^2}}{2}$$

and the single pole Butterworth filter with a pole at s_k is transformed into a bandpass filter with poles s_1 and s_2 and a system function zero at $s = 0$. Thus,

$$\frac{1}{s-s_k} = \frac{s\omega_1}{(s-s_1)(s-s_2)}$$

The bandpass continuous frequency filter is transformed into a discrete frequency filter through the bilinear transform

$$s = \frac{2(1-z^{-1})}{T(1+z^{-1})}$$

Thus,

$$\frac{1}{s-s_1} = \frac{1}{\frac{2(1-z^{-1})}{T(1+z^{-1})} - s_1}$$

Manipulating, the fraction becomes

$$H(z) = \frac{T(1+z^{-1})}{(2+s_1T)\left(\frac{2-s_1T}{2+s_1T} - z^{-1}\right)}.$$

with a zero at $z^{-1} = -1$, and a pole at

$$z^{-1} = \frac{1-s_1T/2}{1+s_1T/2}$$

The zero at $s = 0$ becomes a zero at $z^{-1} = 1$, and a zero at $z^{-1} = -1$.

One difficulty with the bilinear transform is the nonlinear relationship which exists between the continuous frequency domain $s = j\Omega$ and the discrete frequency domain $z = e^{j\omega T}$. The correct discrete frequency will be obtained if the analog filter is designed such that

$$\Omega = \frac{2}{T}\tan\left(\frac{\omega T}{2}\right)$$

The filter design process is clear at this point. A Butterworth low-pass filter is designed. This filter is transformed to a bandpass characteristic with upper and lower cutoff frequencies

$$\Omega_u = \frac{2}{T}\tan\frac{\omega_u T}{2} \quad \text{and}$$

$$\Omega_1 = \frac{2}{T}\tan\left(\frac{\omega_1 T}{2}\right),$$

where ω_u and ω_l are the actual upper and lower cutoff frequencies desired. The poles and zeros of the discrete frequency domain filter are determined and the filter function H(z) is specified. To develop the direct form of the filter function

$$H(z) = \frac{P(z)}{A(z)}$$

the poles and zeros of the function are expanded into polynomials of z. The function H(z) is also evaluated at the center frequency and normalized for unity gain. The coefficients of the normalized filter are necessary for computing the implementation form selected.

The implementation of the digital filter is based on a design by Grey and Markel [9]. This implementation was selected for its adaptability to fixed point arithmetic and its stability and roundoff error performance, particularly in the presence of clustered poles. A computer program for computing the filter coefficients is presented in Markel and Grey [10]. The filter is an implementation of the equations

$$x_m^+(n) = c_m x_{m+1}^+ - k_m x_m^-(n)$$

$$x_{m+1}^-(n+1) = k_m x_{m+1}^-(n) + c_m x_m^-(n), \text{ and}$$

$$y_n = \sum_{m=0}^{N} v_m x_m^-(n+1)$$

with the input

$$x_n^+ = x_n(n)$$

and the constant

$$x_o^-(n+1) = x_o^+(n)$$

The signal flow diagram is shown in Figure 11. The input required to the coefficient calculation software is the direct form coefficient of H(z) where the denomination polynomial has been normalized, that is, $a_o = 1$.

$$H(z) = \frac{\sum_{i=0}^{N} p_i z^{-i}}{\sum_{i=0}^{N} a_i z^{-i}}$$

Area Calculation

A critical parameter in the calculation of scattering cross section is the area of the target resolution cell viewed by the radar system. As previously discussed, the target cell is limited by the Doppler contours corresponding to the bandpass edges of the spectral sampling filter and by the limits imposed by the antenna pattern. These cell boundaries change as a function of aircraft altitude and velocity as well as aircraft attitude parameters of roll and drift. Pitch does not affect the area definition.

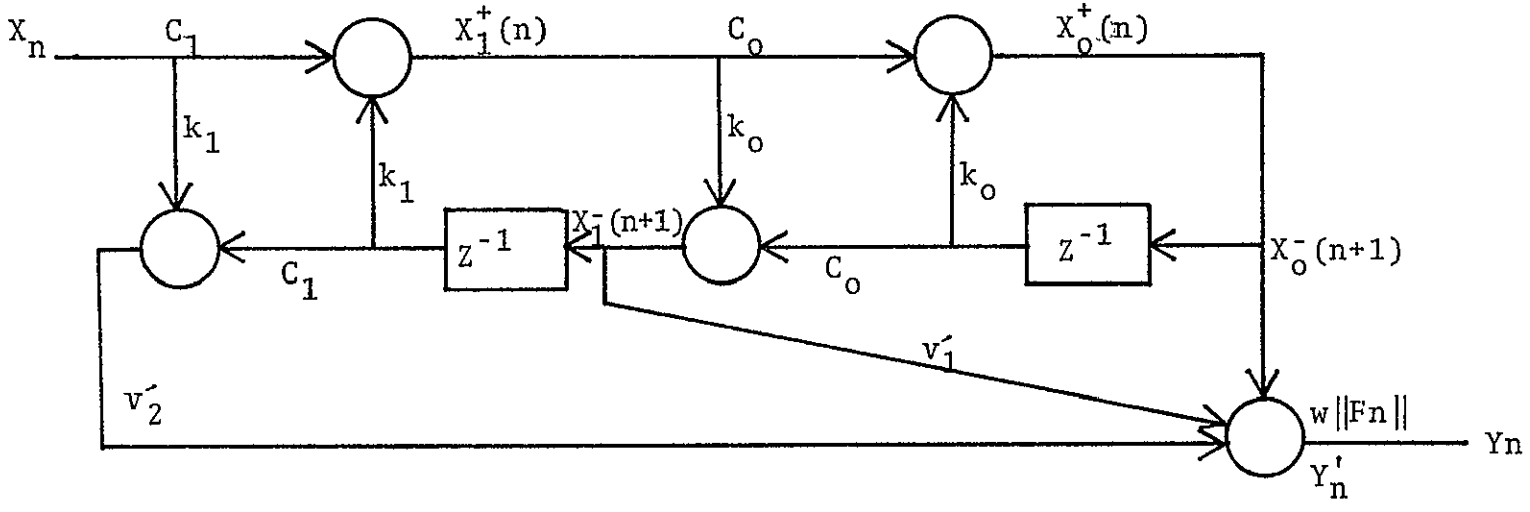

Figure 11. Filter signal flow graph.

The most exact method for calculating the target area is to perform a numerical integration over the cell boundaries; however, this is unreasonable in light of real-time processing constraints. When certain approximations are applied to the problem, a closed-form solution for calculation of area is obtained. An approximate area is determined by obtaining the width of the terrain cell at the nominal look angle, as determined by the beamwidth of the antenna pattern, and multiplying this by the length of the cell as determined by the intersection of the Doppler contours associated with the band edges of the spectral sampling filter. Equations for each of these curves are developed in [7] and the resulting area term is defined as

$$A = \frac{w'(y_2 - y_1)}{\cos\theta}$$

where

$$w' = \frac{2h\tan\beta/2}{\cos\phi\cos 4}$$

$$y_i = \frac{h\cos\phi}{1-k_i\cos^2\phi} \left| \tan\phi\tan\psi \pm \sqrt{\tan^2\psi(k_i-1) + k_i\cos^2\phi - 1} \right|$$

$$k_i = \left(\frac{2v}{f_i\lambda}\right)^2 \qquad i = 1, 2$$

$$f_1 = f_d - \frac{\Delta f}{2}$$

$$f_2 = f_d + \frac{\Delta f}{2}$$

and

$$f_d = \frac{2v\sin\theta\cos(\alpha + \phi)}{\lambda}$$

In these equations,

h = aircraft altitude

v = aircraft velocity

θ = look angle measured from aircraft nadir

ϕ = aircraft drift

ψ = aircraft roll

β = antenna across track beamwidth

$\alpha = \sin^{-1}(\tan\psi/\tan\phi)$

Δf = bandwidth of spectrum sampling filter

λ = wavelength of transmitted energy.

Coefficient Alignment Procedure

Alignment of the scattering coefficients from a single target is a major processing requirement. A processing algorithm has been developed which makes the alignment of computed coefficients a straightforward procedure. For each digitized record, coefficients are calculated from different terrain cells as determined by their particular angle of incidence. The sequence number of the cell immediately below the aircraft provides a convenient cell index. This index is used as the pointer to an array in which the values of the scattering coefficients and certain aircraft parameters are stored which relate to each target cell. Cell alignment is

accomplished by saving a computed scattering coefficient in the appropriate array position and reading out all the coefficients and aircraft parameters for a specific cell when all of its data have been acquired.

In Figure 12 is shown a diagram of the cell acquisition sequence. Each ground cell is referenced by a sequence number which is the pointer into the array where values associated with that target cell are saved. This array is shown in Figure 13. Note that all of the scattering coefficient values for the fore angles (σ°_0 - σ°_3) have been acquired for the ith target cell.

During the next acquisition cycle, the aircraft advances along the ground track by one target cell, and the index i is increased by one. In other words, the nadir point of the aircraft is at cell i + 1. The radar acquires cell i + 4 at the largest angle and σ°_3 for the i + 4^{th} cell is computed. Similarly, for the i + 3^{rd} target cell, σ°_2 is computed; for the i + 2^{nd} target, σ°_1 is computed; and σ°_0 for the i + 1^{st} cell is computed. These coefficient values are saved in the alignment array corresponding with the index of the target cell and the particular angle associated with the coefficient. The array thus fills with each new acquisition, and as the aircraft overflies the ground cell, associated flight parameters are also saved.

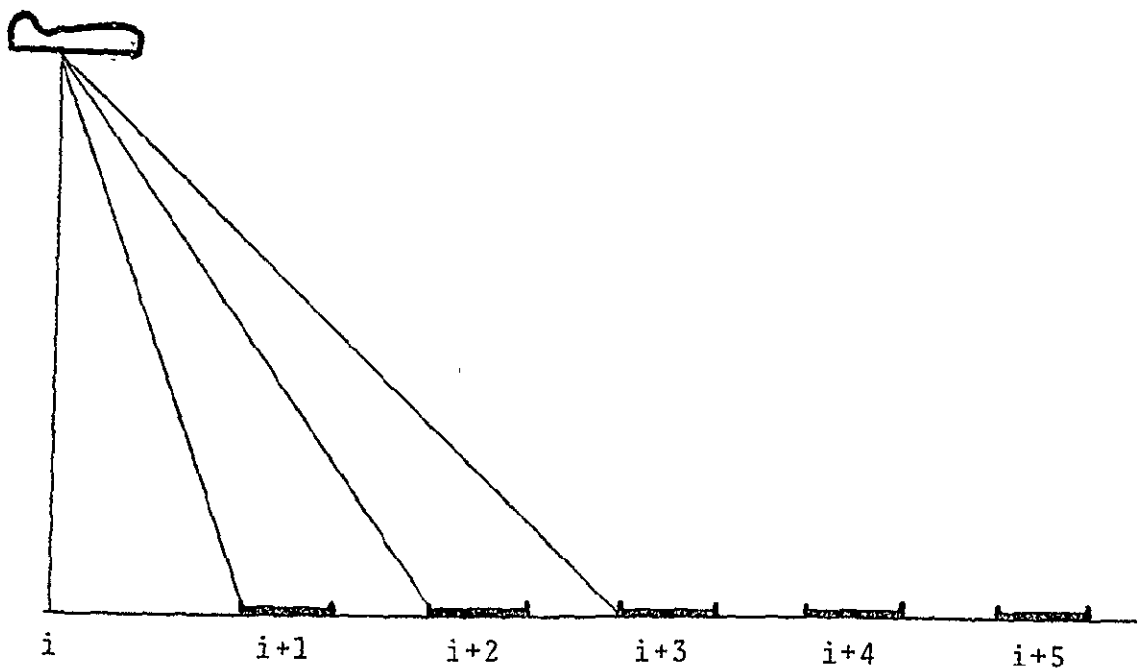

Figure 12. Cell Acquisition Sequence

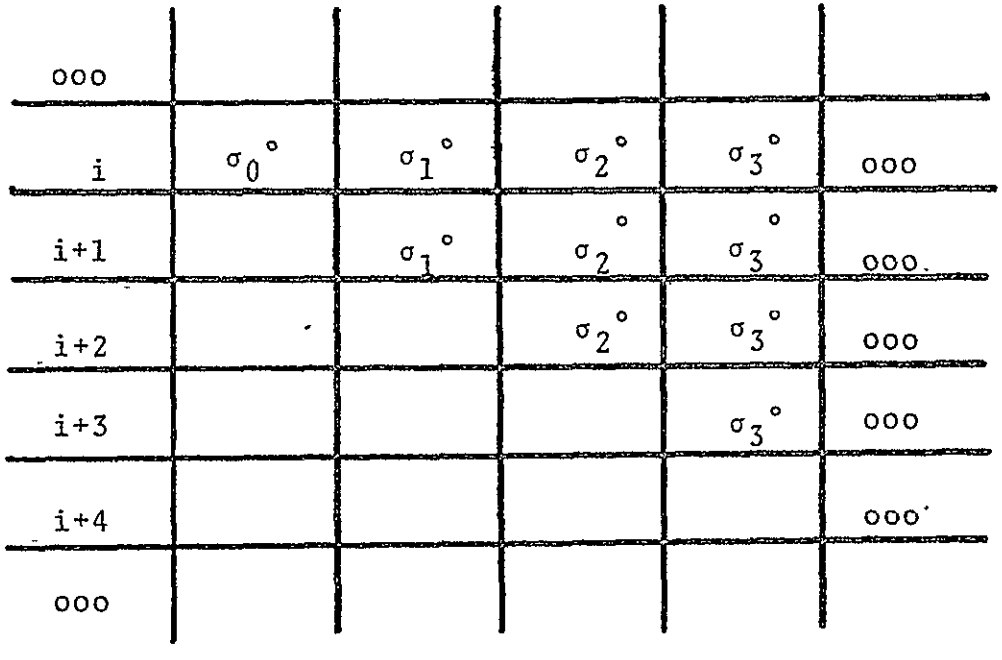

Figure 13. Coefficient Alignment Array

At the time of overflight, all the information about the target cell has been acquired for the forward look direction. If this is the total information required, then the aligned scattering coefficients for this target cell can be output along with the associated flight parameters at that point in time. Should the array postion position be continually reserved for a single cell, then as additional cells are acquired, the array size grows without bound. However, after the data are output, there is no further need to save their position in the alignment array.

Modulo arithmetic is implemented in the alignment algorithm for the index pointer into the array. If the array is of a fixed size large enough to accommodate all target cells which are viewed by the radar at a single instant, and the pointer to the array is computed modulo that number or larger, then as a data set is output for a particular target cell, this array position is assigned to a newly acquired target cell. In this manner, the array is of a fixed and, thus, bounded size, and an efficient utilization of storage memory is accomplished.

The accommodation of aft data is a simple extension of the procedure outlined and requires an

array which is twice as large. The minimum size of the accumulation array for fore and aft data is given by the formula

$$N = \frac{2h\tan 60°}{vT}$$

where

N = the number of indexed vectors

h = aircraft altitude in meters

v = aircraft velocity in meters/second, and

T = length of the acquisition cycle (sec).

Scattering coefficients which have an angle causing them to fall between the discrete target cell positions are assigned to the nearest target cell. Consequently, the average misalignment of scattering coefficients is not greater than half the target cell seperation distance.

Output Products

There are three basic output products from the scatterometer processing package. These are formatted in two punched card sets and a printed record of the processing. The printed record of the processing records mission identification parameters, average flight parameters input and configuration parameters to document the constants used in processing. Additionally, parameters resulting

from the digital filter designs are printed. As the data are processed, aircraft flight parameters, calibration values and calculated scattering coefficients at each angle are printed for each record. This provides the information required for the calculation of the scattering coefficients.

The aircraft parameters, calibration values and calculated coefficients are also provided in the punched card output. Should there be a discrepancy in alignment or flight parameters input, the coefficient can be readjusted without having to reprocess the entire data set. Also provided as part of the punched output are cards which contain the fully processed and aligned scattering coefficients with a time identification and a card sequence number. It is this punched card output which is processed by other reformatting programs to provide time history graphs of scattering coefficients and tabulated results. Examples of these output products are shown in Figures 14-15.

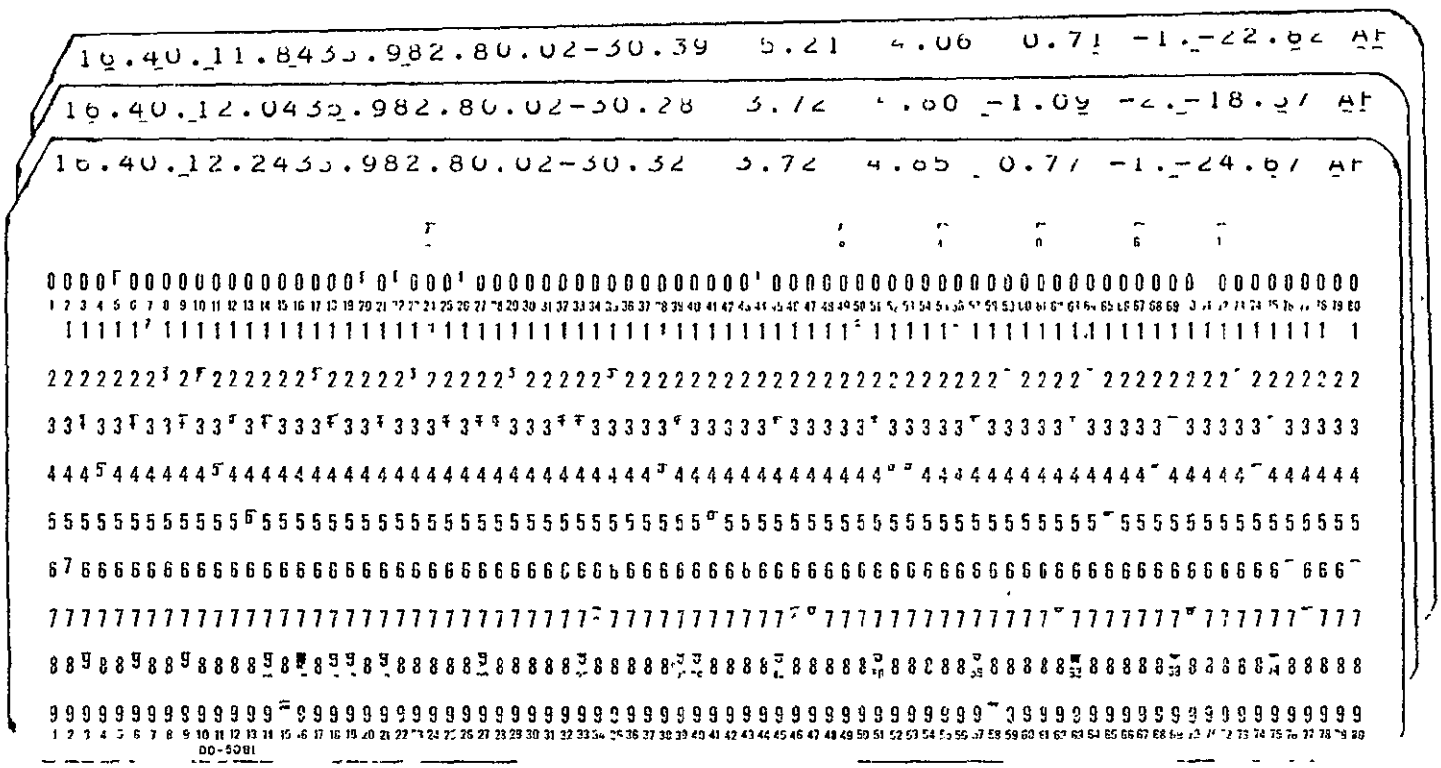

Figure 14. Non-aligned Punched Output.

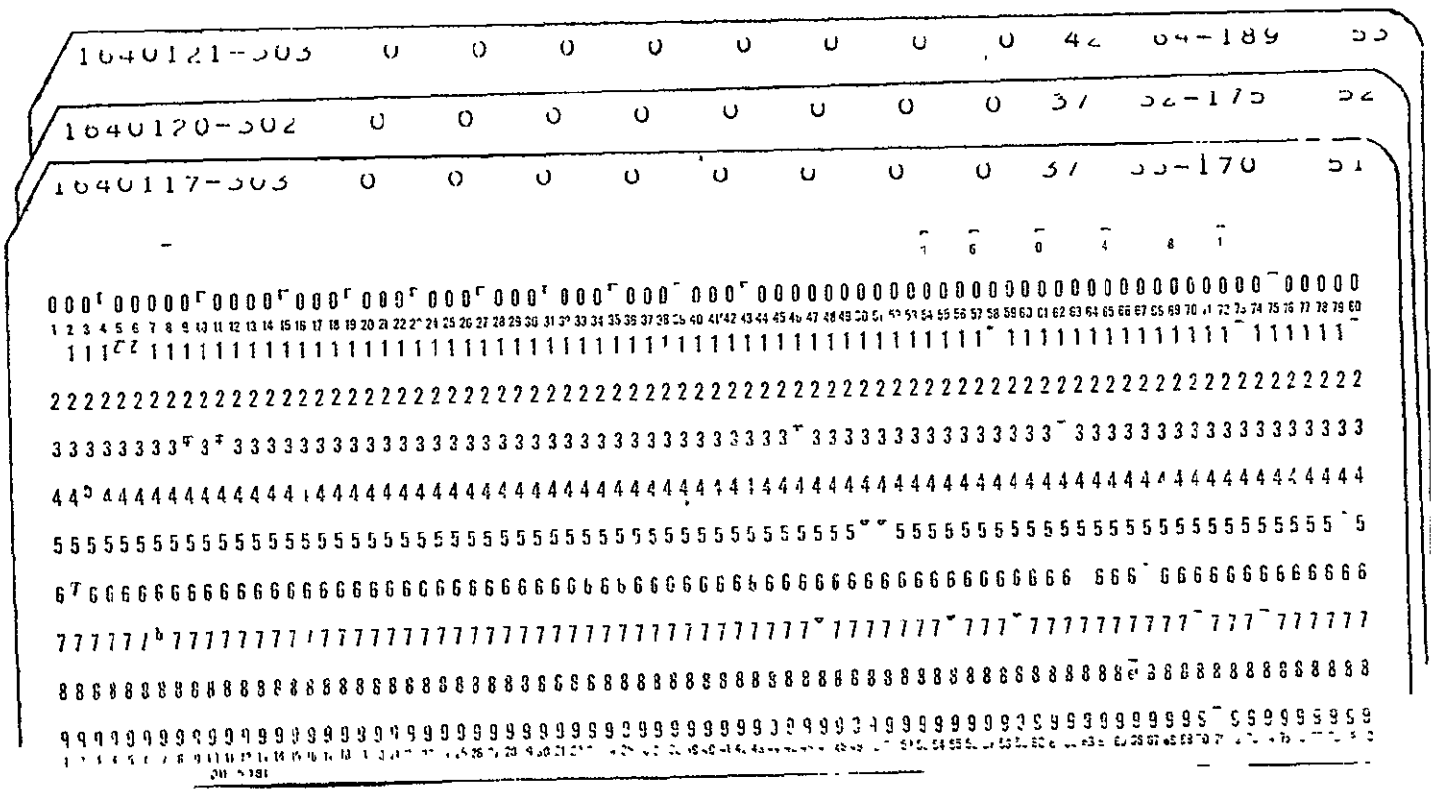

Figure 15. Aligned Punched Output.

Operation

There are several steps required for the processing of scatterometer data. The first is to convert the radar data from raw analog form into a digital data format on a computer magnetic tape for processing by the SCATPAC program. This is accomplished at the Remote Sensing Center by using a TI980 minicomputer system augmented with an analog-to-digital converter and an ADAS decommutating interface.

Radar data are converted two channel pairs at a time, and the converted data with appended aircraft parameters from the ADAS system are recorded on digital magnetic tape. In this procedure each polarization of each radar set is converted at one time.

The start time for conversion and data alignment is assured by recording ADAS time information for each digitized data record. Normally the 13.3 GHz signals are converted at a rate of 25,000Hz; the 1.6 GHz signals are converted at a 5000Hz rate; and the 400 MHz signals are converted at a 2500Hz rate. These rates are sufficient to fully recover the radar signals and the associated calibration signals. Normally 1024 points per data channel are converted with twelve-bit, bi-polar accuracy. The data thus recorded are processed by the software package on the Texas A&M University Amdhal 460V/6 computer.

Tables 1 through 5 describe the information required on each of the five data cards input to the processing software. The input of these parameters provides considerable flexibility in the processing of scatterometer data as angles, cell length and other parameter can be chosen at run time.

TABLE I

Job Control Execution Card

General Format:

//STEP___ EXEC SCAT, PFREG=___, TAPE=___, FILE=___

Definition of Parameters:

STEP___ specifies the STEP number in the over-all job; e.g., STEP 1, STEP 2, etc.

PFREQ=___ defines the specific polarization and frequency combination to process in the respective step; e.g., PFREQ=

VV 133 (13.3 GHz, Vertical/Like polarized)
HH 160 (1.6 GHz, Horizontal/Like polarized)
HV 160 (1.6 GHz, Horizontal/Cross polarized)
VV 400 (400 MHz, Vertical/Like polarized)
VH 400 (400 MHz, Vertical/Cross polarized)
HH 400 (400 MHz, Horizontal/Like polarized)
HV 400 (400 MHz, Horizontal/Cross polarized)

TAPE=___ specifies the CCT label number

FILE=___ specifies the CCT file number to be used

TABLE 2

//SYSIN DD * Card Number 1

Columns	Data Content	Format (FORTRAN)
1-10	Mission Nbr.	10A1
11-20	Site Nbr.	10A1
21-30	Date (of Mission)	10A1
31-40	Line Nbr.	10A1
41-50	Run Nbr.	10A1
51-80	Comments	30A1

TABLE 3

//SYSIN DD * Card Number 2

Columns	Data Content	Format (FORTRAN)
1-5	Points Digitized	I5
6-10	Look Angle (Fore = 1, Aft = -1, F+A = ϕ)	I5
11-15	Number of Angles ($\leq$8)	I5
16-20	First Angle Value	F5.0
21-25	Second Angle Value	F5.0
26-30	Third Angle Value	F5.0
31-35	Fourth Angle Value	F5.0
36-40	Fifth Angle Value	F5.0
41-45	Sixth Angle Value	F5.0
46-50	Seventh Angle Value	F5.0
51-55	Eighth Angle Value	F5.0

TABLE 4

//SYSIN DD * Card Number 3

Columns	Data Content	Format (FORTRAN)
1-2	Hours, Start Time	F2.0
3-4	Minutes, Start Time	F2.0
5-7	Seconds, Start Time	F3.1
8-10	---	
11-15	Seconds to be Processed	F5.1
16-20	Velocity (knots)	F5.1
21-25	Altitude (feet)	F5.1
26-30	Drift (degrees)	F5.1
31-35	Roll (degrees)	F5.1
36-40	Pitch (degrees)	F5.1

TABLE 5

//SYSIN DD * Card Number 4

Columns	Data Content	Format (FORTRAN)
1-5	Configuration (13.3 = 1, 1.6 = 2, 400 = 3)	I5
6-10	Cell Length (meters)	F5.0
11-15	Digitization Rate (H3)	F5.0
16-20	Channel 1 Gain (db)	F5.1
21-25	Channel 2 Gain (db)	F5.1
26-30	Calibration Constant (db)	F5.1
31-35	Cable Loss (2 way, db)	F5.1
36-40	Avg. Time Interval (sec.)	F5.1
41-45	Calib. Filter Bandwidth	F5.1

REFERENCES

[1] R. G. Reeves, Editor-in-Chief, Manual of Remote Sensing, American Society of Photogrammetry, 1975.

[2] M. I. Skolnik, Ed., Radar Handbook, McGraw-Hill Book Company, 1970.

[3] M. W. Long, "Radar Reflectivity of Land and Sea," Lexington Books, 1975.

[4] T. F. Bush and F. T. Ulaby, "Radar Return from a Continous Vegetation Canopy," I.E.E.E. Transactions On Antennas and Propagation, Vol. AP-24, pp. 269-275.

[5] J. W. Rouse, Jr., H. C. MacDonald, and W. P. Waite, "Geoscience Applications of Radar Sensors," I.E.E.E. Transactions on Geoscience Electronics, Vol. GE-7, pp. 2-19, January 1969.

[6] G. A. Bradley, "Remote Sensing of Ocean Winds using a Radar Scatterometer," Remote Sensing Laboratory Technical Report 177-22, September 1971.

[7] J. A. Schell, et. al. "An Airborne Radar Scatterometer Signal Processing System," Progress Report RSC-3182-1, Remote Sensing Center, Texas A&M University, May 1975.

[8] L. R. Rebiner and B. Gold, "Theory and Application of Digital Signal Processing", p. 136-140, Prentice-Hall, 1975.

[9] Markel, John D. and Gray, A. H., Jr.; I.E.E.E. Trans Accoust Speech Signal Process, Vol. ASSP-23n, 5 October 1975, pp. 473-486.

[10] Gray, A. H., Jr. and Markel, J. D.; I.E.E.E. Trans Accoust Speech Signal Process, Vol. ASSPn, 5 October 1975, pp. 486-494.